Thermosensitive release systems for image guided local drug delivery

Merel van Elk

The printing of this thesis was financially supported by:

Utrecht Institute for Pharmaceutical Sciences, Utrecht, The Netherlands

Avanti Polar Lipids

Bracco Imaging Europe B.V.

Lipoid GmbH

Sysmex Nederland B.V.

Greiner Bio-One

Printed by Proefschriftmaken.nl || Uitgeverij BOXPress

ISBN: 978-94-6295-355-0

This research was supported by Center for Translational Molecular Medicine (CTMM),HIFU-CHEM project (#030-301).

Thermosensitive release systems for image guided local drug delivery

Thermosensitieve formuleringen voor beeldgestuurde lokale geneesmiddelafgifte

(met een samenvatting in het Nederlands)

Proefschrift

ter verkrijging van de graad van doctor aan de Universiteit Utrecht
op gezag van de rector magnificus, prof.dr. G.J. van der Zwaan,
ingevolge het besluit van het college voor
promoties in het openbaar te verdedigen
op maandag 21 september 2015 des ochtends te 10.30 uur

door

Merel van Elk

geboren op 1 juni 1986 te Nijmegen

Promotoren:	Prof. dr. W.E. Hennink Prof. dr. G. Storm
Copromotoren:	Dr. T. Vermonden Dr. J.F.W. Nijsen

Contents

Chapter 1 **7**
Introduction

Chapter 2 **25**
Triggered release of doxorubicin from temperature sensitive poly(*N*-(2-hydroxypropyl)-methacrylamide mono/dilactate) grafted liposomes

Chapter 3 **43**
Safety evaluation of temperature-sensitive poly(*N*-(2-hydroxypropyl) methacrylamide mono/dilactate) grafted liposomes

Chapter 4 **65**
Modulating the stability and drug release characteristics of temperature-sensitive liposomes through PEGylation

Chapter 5 **77**
Alginate microgels loaded with temperature sensitive liposomes for magnetic resonance imageable drug release and microgel visualization

Chapter 6 **97**
Alginate microspheres containing temperature sensitive liposomes (TSL) for MR-guided embolization and triggered release of doxorubicin in vivo

Chapter 7 **117**
Summary and perspectives

Appendices
Nederlandse samenvatting **128**
Curriculum Vitae **133**
List of publication **135**
Acknowledgements **137**

1

Introduction

Cancer

Cancer is a major public health problem worldwide even though the cancer death rates have been continuously declining over the past 2 decades due to the improvement in chemotherapy, radiotherapy and surgical techniques. Overall, the risk of dying from cancer decreased by 22% between 1991 and 2011 [1,2]. Nevertheless, several types of cancer are hard to treat and also, the number of cancer patients increases yearly due to aging, growth of the population and the adoption of cancer associated lifestyle choices (e.g. smoking, physical inactivity and unhealthy diets) [1,3]. It is expected that 1.7 million new cancer cases will be diagnosed in the United States in 2015 [2]. Therefore, new treatment modalities are needed.

Chemotherapy

Cancer patients are often treated with chemotherapeutic drugs, radiotherapy and/or surgical resection. Chemotherapeutics impair cell mitosis and thereby target fast dividing cells like cancer cells [4]. The disadvantages of many chemotherapeutic drugs are their poor pharmacokinetics, low stability, low aqueous solubility and non-specific distribution throughout the body. Therefore, a high dose of these drugs needs to be administered to achieve therapeutic drug levels, leading to various adverse effects because also other fast dividing, healthy cells are affected. Examples of adverse effects of chemotherapeutic drugs are neuropathy, nausea, general discomfort, myelosuppression (suppression of the bone marrow's production of blood cells and platelets), alopecia (hair loss), nephrotoxicity and cardiotoxicity [5-7]. These adverse events often limit the dose and duration of the administered drugs. Another major problem is that cancer cells can become resistant towards chemotherapeutic drugs [8,9].

Liposomes

Nanosized drug delivery systems like liposomes have been developed for the encapsulation of chemotherapeutic drugs to improve the therapeutic efficacy and to reduce adverse events.

Liposomes are unilamellar or multilamellar vesicles, which were first described in the 1960s by Bangham [10,11]. Liposomes consist mainly of phospholipids, which spontaneously form a lipid bilayer surrounding an aqueous core when dispersed in water via non covalent interactions. Hydrophilic drugs can be encapsulated in the aqueous core of the liposomes while hydrophobic drugs can be solubilized in the lipid bilayer (Fig. 1).

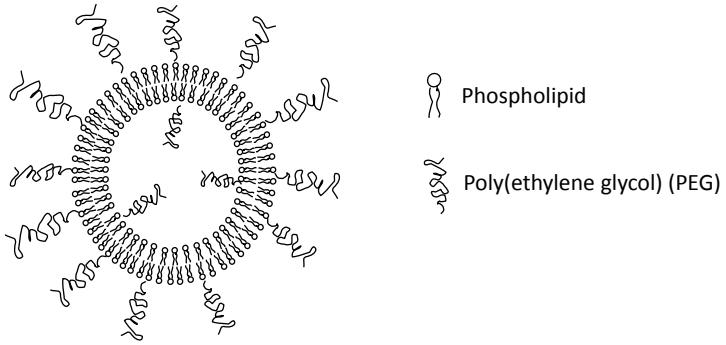

Figure 1. Schematic representation of a PEGylated liposome.

Liposomes of the first generation are rapidly cleared from the systemic circulation by macrophages of the reticuloendothelial system (RES) [12,13]; approximately 50-80% of the liposomes are removed from the circulation within 15-30 minutes after administration. The circulation half-life of liposomes was significantly improved by coupling poly(ethylene glycol) on their surface ('PEGylation'). The reason for this improved half-life is that poly(ethylene glycol) is a hydrophilic polymer, which forms a steric barrier around the liposomes reducing the recognition by cells from the RES [14-17]. This improved circulation time allowed liposome accumulation in tumors via the enhanced permeability and retention effect (EPR) [18-20]. Liposomes can extravasate from the blood vessels when the vasculature is discontinuous, which is the case in various tumors. New blood vessels are formed rapidly in tumor tissues due to the high demand of oxygen and nutrients, and therefore these blood vessels are immature and often leaky [21]. Furthermore, there is a lack of lymphatic drainage in tumor tissue reducing the clearance of liposomes from the tumor [22,23]. So far, the discovery and development of liposomes have resulted in the approval of several liposomal formulations for the treatment of cancer (Doxil®/Caelyx®, DaunoXome®, Myocet® and Marqibo®, Table 1) [24,25].

Table 1. Overview of marketed liposomal formulations for cancer treatment [24,25]

Product	Drug	Indication
Doxil®/Caelyx®	Doxorubicin	Kaposi's sarcoma Ovarian cancer Breast cancer Multiple myeloma
DaunoXome®	Daunorubicin	Kaposi's sarcoma
Myocet®	Doxorubicin	Breast cancer
Marqibo®	Vincristine	Acute lymphoblastic leukemia

The efficacy of these liposomal formulations depends on their passive accumulation in tumors via the EPR effect. However, the actual accumulation of the liposomes in the tumor is less than 10% of the administered dose and the majority of the liposomes is still taken up by macrophages present in liver and spleen [26]. Moreover, the EPR effect is very heterogeneous and varies between tumor types, from patient to patient and even varies within the tumor [19,27]. Furthermore, these liposomes are designed such that they exhibit a high stability in the blood circulation to prevent premature release of the drug before arrival at the tumor site. Because of this high stability, the release of these liposomes is slow and uncontrolled resulting in a relatively low free drug concentration in the tumor and as a consequence, cytotoxic free drug concentrations are not always reached in the tumor [28].

To increase the antitumor-activity of liposomal formulations, a higher concentration of free drug should be obtained in the tumor [29,30]. Triggerable liposomal drug release systems have great opportunities to increase and control the drug concentration in the tumor. Several methods of triggered release have been described in literature (e.g. pH, light and ultrasound) but so far heat is the most intensively studied trigger for drug release (Fig. 2).

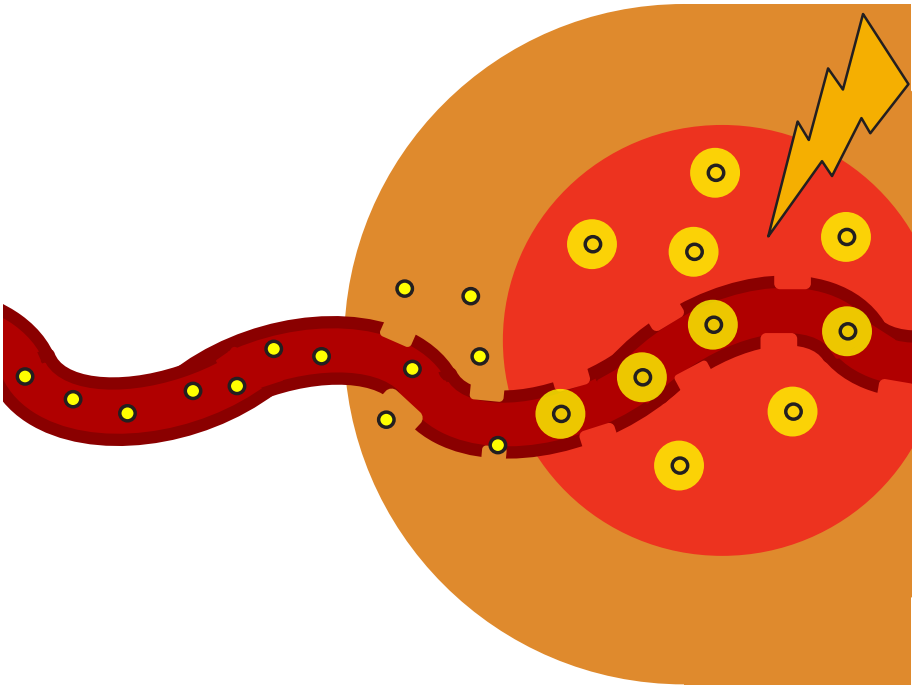

Figure 2. Drug release from temperature sensitive liposomes in a tumor during mild hyperthermia. Liposomes pass through the preheated tumor vasculature after intravenous administration. Subsequently, the release from the liposomes present in the vasculature and the tumor tissue is triggered due to the mild hyperthermia treatment.

Hyperthermia and temperature sensitive liposomes

The goal of temperature triggered drug release is to achieve high drug concentrations in the tumor upon mild hyperthermia, independent of the EPR effect. Therefore, the release from temperature sensitive liposomes should be ultrafast to facilitate a complete content release faster than the transit of the liposomes through the vasculature of the tumor. It has been reported that chemotherapeutic drugs and hyperthermia act synergistically, leading to an enhanced cytotoxic effect of the drug [29,31,32]. The temperature threshold for mild hyperthermia lies around 43 °C because higher temperatures induce vascular occlusion and hemorrhage, resulting in a decreased blood flow, followed by a decreased drug delivery. Besides, a temperature in the whole tumor above 43 °C is difficult to achieve clinically [29,33-35]. In this chapter, different temperature sensitive liposomes reported in literature will be shortly described and discussed (Table 2).

Traditional temperature sensitive liposomes (TTSL)

Traditional temperature sensitive liposomes (TTSL) were first introduced by Yatvin in 1978. These liposomes consisted of 1,2-dipalmitoyl-*sn*-glycero-3-phosphocholine (DPPC) and 1,2-distearoyl-*sn*-glycero-3-phosphocholine (DSPC) in a molar ratio of 3:1 and released neomycin (an antibiotic) at a temperature of 43-45 °C, which induced effective killing of E. Coli bacteria [36,37]. The drug was released from these TSL at temperatures above the melting phase transition temperature (T_m) of the lipid bilayer. At the T_m, the lipids undergo a phase transition from a solid gel phase to a liquid crystalline phase. Upon heating, grain boundaries are formed between domains in the solid phase and domains in the liquid phase, leading to membrane permeability and subsequent drug release. The permeability of the lipid bilayer is largest at the T_m since solid and gel domains coexist at this temperature.

Low temperature sensitive liposomes (LTSL)

TTSL do not meet the optimal release requirements since the release rate is too slow and the temperature at which the release occurs is too high (43-45 °C) for clinical applications [29,34,35,38].

Low temperature sensitive liposomes (LTSL) were developed by Anyarambhatla and Needham to increase the release rate and simultaneously decrease the release temperature [39,40]. DPPC was chosen as the main component of the LTSL since this phospholipid has a T_m of ~ 41 °C, which is ideal for the application of mild hyperthermia in the clinic. MSPC (1-stearoyl-2-hydroxy-*sn*-glycero-3-phosphocholine), a mono chain lysolipid, which is able to form micelles, was added to the LTSL formulation to induce fast release of the content during mild hyperthermia. At the phase transition temperature of the liposomes, the grain boundaries start to melt. The lipid mobility increases and the lysolipids accumulate in the grain boundaries forming pores which in turn induces fast release of the content [41-45] (Fig. 3).

LTSL contain 1,2-distearoyl-*sn*-glycero-3-phosphoethanolamine-*N*-[amino(polyethylene glycol)-2000] (DSPE-PEG2.000) not only to increase the half-life of the liposomes but it was also shown that DSPE-PEG2.000 stabilizes the formed pores induced by the lysolipids [46]. LTSL showed an ultrafast release rate of 80% doxorubicin (DOX) release in 20 seconds at 42 °C [40,47]. A complete tumor regression was obtained with LTSL in combination with mild hyperthermia (42 °C for 1 hour) in a xenograft mouse model. The reduction in tumor growth in mice treated with LTSL in combination with mild hyperthermia was more effective than the

Table 2. Overview of temperature sensitive liposomes, under development for the treatment of cancer

Liposome	Lipid composition	Drug	T_m/CP	Release	Animal model
TTSL [36]	DPPC:DPSC 3:1	Neomycin		44.5 °C (maximum release rate)	
LTSL [39,40]	DPPC:MSPC:DSPE-PEG 90:10:4	Doxorubicin	~41 °C	>20% at 37 °C in 15 min 80% at 42°C in 20 sec	FaDu/mice
HaT [51,52]	DPPC:Brij78 96:4	Doxorubicin	41 °C	10-20% at 37 °C in 30 min > 90% at 40-42 °C in 2.5 min	EMT-6/mice
$DPPG_2$ [59,64]	DPPC:DSPC:$DPPG_2$ 50:20:30	Doxorubicin	~42 °C	11% at 37 °C in 3 hours >95% at 42 °C in 2 min	BN175/rat (gemcitabine)
EOEOVE [81,82]	EPC:chol:poly(EOEOVE):PEG-PE 50:45:4:2	Doxorubicin	40.5 °C	<10% at 37 °C in 30 min ~90% at 45 °C in 1 min	CT26/mice

free drug, TTSL and non-temperature sensitive liposomes in combination with mild hyperthermia [39,40,47,48].
However, also shortcomings of LTSL have been reported. Approximately ~70% of the lysolipid desorbs from the LTSL within 1 hour after *in vivo* administration, which could hamper the maximal release *in vivo* from the LTSL [42,44]. Moreover, LTSL release > 20% of DOX at 37 °C within 15 minutes when incubated in serum rich medium, which limits the amount of DOX delivered to the tumor tissue and induces exposure of healthy tissue to DOX [49,50].

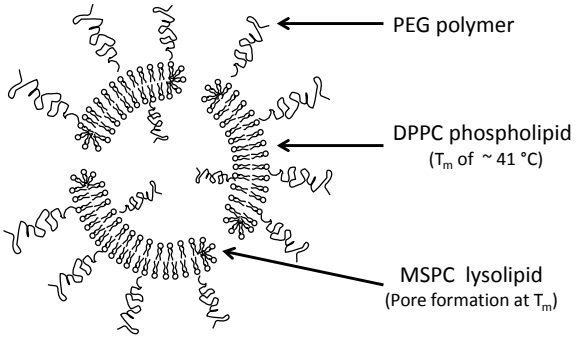

Figure 3. Schematic representation of a temperature sensitive liposome containing lysolipids. Lysolipids can form stable pores at the phase transition temperature of the liposome, inducing drug release.

Hyperthermia-activated cytotoxic liposomes (HaT)
Hyperthermia-activated cytotoxic liposomes (HaT, DPPC:Brij78 in a molar ratio of 96:4) were developed to simplify the LTSL formulation since Brij78 (Fig. 4) is a PEGylated single chain surfactant, which can replace MSPC (single chain lysolipid) and DSPE-PEG2.000 in the LTSL formulation [51,52]. A 100% DOX release was achieved from this HaT formulation within 3 minutes at 40-42 °C [52]. The HaT formulation showed a faster DOX release rate at 40 and 41 °C compared to LTSL while the stability in serum at 37 °C and the circulation half-life (0.5 hour) were similar for these two formulations [51,53]. The DOX delivery to a heated tumor (43 °C) was 1.4 fold increased when HaT was compared to LTSL, resulting in a significant enhanced tumor regression for the HaT formulation in BALB/C mice bearing EMT-6 tumors [51]. Oxaliplatin (OXA) and gemcitabine (GEM) were passively loaded into HaT (HaT-OXA or HaT-GEM) and showed a temperature triggered release profile. Only 17% of the administered HaT-OXA remained in the circulation 1 hour after injection and no improvement of OXA delivery from HaT-OXA was observed in the heated tumor compared to free administered OXA. For the HaT-GEM, 82% of the administered dose remained in the blood circulation for 1 hour and a 25 fold increase in drug deposition in the tumor was observed when HaT-GEM was delivered to a heated tumor compared to the free drug resulting in a complete tumor regression after a single dose of HaT-GEM. A significant shorter circulation time and antitumor efficacy were obtained by HaT-OXA in comparison with HaT-GEM. Presumably, OXA interacts with the phospholipids in the lipid bilayer, inducing a conformational change in the liposomal membrane, which results in an increased liver uptake and therefore an enhanced clearance from the blood

circulation. Therefore, less OXA is delivered to the tumor and no improvement in antitumor activity is observed [54].

The HaT formulation was further optimized by loading DOX with a Cu^{2+} gradient and post insertion of additional Brij78 (HaTII). The serum stability improved significantly at 37 °C with an enhanced drug release rate at 41-42 °C compared to LTSL. Compared to LTSL, the HaTII formulation showed a 2 times longer circulation time and a 2 fold increase in drug disposition in a heated EMT-6 tumor of a BALB/C mice resulting in an enhanced antitumor efficacy with complete growth inhibition [55].

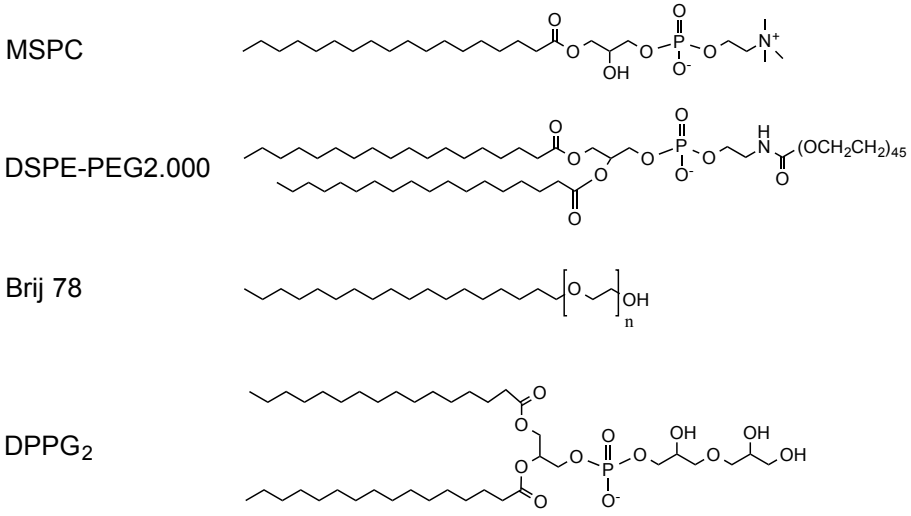

Figure 4. Chemical structures of MSPC (1-stearoyl-2-hydroxy-*sn*-glycero-3-phosphocholine), DSPE-PEG2.000 (1,2-distearoyl-*sn*-glycero-3-phosphoethanolamine-*N*-[amino(polyethylene glycol)-2000]), Brij 78 and $DPPG_2$ (1,2-dipalmitoyl-*sn*-glycero-3-phosphoglyceroglycerol).

$DPPG_2$ temperature sensitive liposomes

Liposomes composed of DPPC, DSPC and 1,2-dipalmitoyl-*sn*-glycero-3-phosphoglyceroglycerol ($DPPG_2$) have been developed to improve the liposomal stability in blood and to increase the circulation half-life. $DPPG_2$ is a synthetic phospholipid (Fig. 4) that is expected to prolong the circulation time since this phospholipid has a hydrophilic glycerol chain, which extends from the liposomes and therefore likely forms a steric barrier around the liposomes, comparable to PEG [56]. $DPPG_2$ could be incorporated into liposomes to a significantly higher extent (70%) compared to DSPE-PEG2.000 since $DPPG_2$ is not able to form micelles at high concentrations [56,57]. The circulation time ($t_{1/2}$) of $DPPG_2$-TSL was prolonged to 9.6 hours in hamsters and 5.0 hours in rats [56] compared to less than 1 hour for LTSL in rats and mice [51,58]. DOX was quantitatively released from $DPPG_2$-TSL at 42 °C and showed an improved stability in serum at 37 °C compared to LTSL with only 11% DOX release in 3 hours at 37 °C [59-61]. The size of liposomes can influence the release kinetics since the membrane curvature increases for smaller liposomes, resulting in a looser packaging of the phospholipids which, increases the membrane permeability. The release kinetics of $DPPG_2$-TSL were less affected by the size of the liposomes compared to LTSL [62]. Hexadecylphosphocholine (HePC) was

incorporated into $DPPG_2$-TSL since HePC is structurally related to MSPC (lysolipid in LTSL) and therefore its presence increased the release rate of $DPPG_2$-TSL to > 80% release within 10 seconds in serum [63].
A pharmacokinetic study in rats revealed that the half-life of gemcitabine was extended from 0.07 hour to 2.59 hours by encapsulation into $DPPG_2$-TSL. The tumor growth of a BN175 tumor in the hind leg of a Brown Norway rat was significantly suppressed by $DPPG_2$-TSL in combination with mild hyperthermia compared to gemcitabine in combination with mild hyperthermia or $DPPG_2$-TSL without mild hyperthermia [64].

LCST-polymer coated liposomes
Another technology to prepare temperature sensitive liposomes involves the modification of the liposomal surface with polymers displaying lower critical solution temperature (LCST) behavior. These polymers are water-soluble below the cloud point (CP) of the polymer, while above the CP, hydrogen bonds between water molecules and hydrogen bond forming groups of the polymer (e.g. amide bond) become weaker resulting in less hydrated polymer chains. Consequently, the polymers undergo a coil to globule transition, causing polymer precipitation. LCST polymers can be incorporated into liposomes by coupling the polymer to a hydrophobic moiety that solubilizes in the liposomal bilayer [65,66].

Poly(NIPAM) modified liposomes
Poly(*N*-isopropylacrylamide) (Poly(NIPAM)) is a temperature sensitive polymer with a CP of 32 °C and NIPAM based polymers have often been used as carriers for drug delivery [67-69]. NIPAM can be copolymerized with hydrophobic monomers which serve as an anchor for incorporation into liposomes. A copolymer of NIPAM and 1% octadecyl acrylate (ODA) was synthesized via free radical polymerization (poly(NIPAM-co-ODA)). Poly(NIPAM-co-ODA) had a CP of 27 °C, which is slightly lower than the CP of solely NIPAM due to the hydrophobic nature of the anchor units. A temperature triggered release of calcein or carboxyfluorescein (fluorescence markers) was observed when these polymers were coated onto DPPC or egg phosphocholine (EPC) liposomes even though this release was incomplete (< 70% after 5 minutes at 40 °C) [70]. An enhanced and complete calcein and DOX release was observed from 1,2-dioleoyl-*sn*-glycero-3-phosphoethanolamine (DOPE) liposomes coated with poly(NIPAM-co-ODA) [71,72]. DOPE itself does not self-assemble into liposomes but forms a nonbilayer structure (hexagonal H_{II}) [73,74]. However, liposomes containing DOPE can be prepared by stabilization with hydrated poly(NIPAM-co-ODA). Above the CP, the polymer becomes dehydrated and loses its stabilizing properties and thereby induces drug release by liposome aggregation and fusion [75].
The liposomes described above demonstrated that poly(NIPAM) is indeed able to trigger drug release from liposomes at increased temperatures but these liposomes are clinically not suitable due to the low release temperature (under physiological temperature). Therefore, NIPAM was copolymerized with *N,N*-didodecylacrylamide (NDDAM, anchor) and various amounts of the hydrophilic acrylamide (AAM) monomer. The CP of poly(NIPAM) increased from 28 to 34, 40 and 46 °C when copolymerized with 10% AAM, 20% AAM and 30% AAM, respectively. DOPE:EPC liposomes coated with poly(NIPAM-co-NDDAM-co-AAM) showed only a minimal

content release below the CP while an enhanced release was observed at temperatures above the polymer's CP. Liposomes coated with a polymer having a higher ratio of AAM and therefore a higher CP, had a higher release temperature, demonstrating that by adjusting the CP of the polymer the release could be tuned [76,77].
In another study, the influence of the position of the lipid anchor on the release kinetics was investigated. Copolymers with lipid anchors randomly distributed over the polymer chains were prepared by free radical polymerization of NIPAM, acryloylpyrrolidine (APr) and *N,N*-didodecylacrylamide (NDDAM lipid anchor) (poly(NIPAM-co-APr-co-NDDAM). Copolymers with a terminal anchor were obtained by free radical polymerization of NIPAM and APr and subsequent conjugation to *N,N*-didodecyl succinamic acid ($2C_{12}$) to obtain $2C_{12}$-poly(NIPAM-co-APr). Liposomes modified with a terminal anchor polymer ($2C_{12}$-poly(NIPAM-co-APr)) released the content more rapidly upon a small temperature change compared to liposomes coated with copolymers having random anchor units (poly(NIPAM-co-APr-co-NDDAM)). The polymer mobility might be more restricted when the lipid anchors are randomly distributed over the polymer chains compared to polymers with a terminal anchor. Therefore, terminal anchor polymers dehydrate more efficiently, inducing a more rapid content release [78].
Free radical polymerization is a polymerization method, which has limited control over the molecular weight and results in polymers with a relatively high polydispersity. Therefore, poly(NIPAM-co-propylacrylic acid) was synthesized by reversible addition-fragmentation chain transfer (RAFT) and yielded polymers with a M_n of 30 kDa, a CP of 42 °C (at pH 6.5) and a PDI of only 1.2. Liposomes modified with this polymer released 100% DOX at 42 °C within 5 minutes with a minimum release at 37 °C (<10% after 1 hour incubation). The release at 42 °C was faster from poly(NIPAM-co-propylacrylic acid) coated liposomes compared to TTSL. Unfortunately, the release kinetics from polymer coated liposomes from which the polymers were polymerized via free radical polymerization or RAFT were not compared [79].

Poly(EOEOVE) grafted liposomes
Besides RAFT, living cationic polymerization also provides a high level of control over the molecular weight of the synthesized polymers and generates polymers with a low polydispersity. Using this method, block-copolymers of (2-ethoxy)ethoxyethyl vinyl ether (EOEOVE, temperature sensitive component) and octadecyl vinyl ether (ODVE, anchor) were synthesized with various chain lengths. Polymers with a higher molecular weight showed a more enhanced release at a narrow temperature range near the CP than polymers with a lower molecular weight [80]. Presumably, a polymer with a longer chain length forms a larger dehydrated block above the CP, inducing a stronger interaction with the membrane and therefore induces a more enhanced release. Poly(EOEOVE-b-ODVE) with a CP of 40.5 °C released 90% DOX at 45 °C within 1 minute but was rather unstable at 37 °C (30% release in 30 minutes). The stability at 37 °C was improved by PEGylation (<10% DOX release in 30 minutes) while enhancing the release rate above the CP even further. So, PEGylation reduced the release below the CP of the polymer while PEGylation accelerated the release above the CP of the polymer. According to the authors, the partly dehydrated poly(EOEOVE-b-ODVE) might interact with PEG on the surface of the liposomes, weakening the interaction between EOEOVE and the liposomes. Furthermore,

PEGylation of the poly(EOEOVE-b-ODVE) modified liposomes increased the circulation time in mice while reducing the uptake by macrophages of the liver. The tumor growth was strongly suppressed after injection of these DOX loaded liposomes in combination with hyperthermia treatment while the tumor suppressive effect was less pronounced when only liposomes were administered without hyperthermia treatment [81]. The accumulation of these liposomes in the tumor could be monitored when gadolinium chelates were coated to the PEGylated liposomes [82]. Furthermore, Fe_3O_4 nanoparticles could be incorporated into the lipid bilayer of poly(EOEOVE-b-ODVE) modified liposomes via hydrophobic interactions. An alternating magnetic field was used to heat the Fe_3O_4 nanoparticles and induce the release of a fluorescent marker [83].

Elastin like peptide (ELP) coated liposomes

Fatty acid conjugated elastin like polypeptides (ELP) show LCST behavior and can be coated onto DOX loaded liposomes (ELP-liposomes). ELP-liposomes released > 95% of the content in 10 seconds at 42 °C while less than 20% was released within 30 minutes at 37 °C in serum. ELP-liposomes had a plasma half-life of 2.03 hour compared to a half-life of 0.92 hour for LTSL. A significant delay in tumor growth was achieved by ELP-liposomes in combination with high intensity focused ultrasound compared to LTSL after one intravenous injection [84]. A 7 fold increase in cellular uptake of $\alpha_v\beta_3$ overexpressing cells was observed when ELP-liposomes were coupled to a cRGD binding moiety, which resulted in a 5 times higher tumor accumulation compared to ELP-liposomes in mice. This implies that tumors can be targeted through the interaction between cRGD grafted onto liposomes and $\alpha_v\beta_3$ integrin receptors on tumor-associated endothelial cells or tumors [85].

Image guided drug delivery using temperature sensitive liposomes

Magnetic Resonance Imaging (MRI) is a medical imaging technique and has a wide range of applications in medical diagnosis, staging of disease and follow-up. Most MR images represent the relative response of hydrogen nuclei to absorbed radio frequency energy. However, the image contrast is not only a function of the hydrogen nuclei distribution, but it is also influenced by other physical factors including differences in the ability to re-emit the absorbed radio frequency signal (i.e. relaxation).

MRI contrast agents change these relaxation processes of hydrogen nuclei inside tissue and thereby change the inherent contrast of tissues on MR images. For MRI, the contrast agents used are generally based on either iron-oxide nanoparticles, providing negative contrast on T_2^*-weighted images, or gadolinium (Gd) complexes, providing positive contrast on T_1-weighted images.

Incorporation of Gd complexes in the hydrophilic core of TSL causes a decrease of T_1 relaxivity due to the shielding of the Gd complexes from the surrounding water by the liposomal membrane. However, when the liposomal membrane of TSL becomes more permeable to water molecules at the T_m of the lipid bilayer, the T_1 relaxivity increases markedly due to the more efficient water exchange between liposome interior and exterior (bulk water) and can be observed as a signal increase on T_1-weighted images. Manganese as well as gadolinium have been used as MRI contrast agents in TSL to measure the content release [49,53,60,86,87]. DOX can be loaded into TSL via a manganese gradient whereby stable DOX-manganese complexes are formed. Both

DOX and manganese are released simultaneously upon mild hyperthermia and therefore the release of manganese can be used to trace DOX release [88-91]. Gd complexes have also been used as tracers for drug release after co-encapsulation with the drug in TSL [50,58,92].

Drug eluting beads

An attractive alternative method for localized drug delivery of chemotherapeutics is via transarterial chemoembolization (TACE). During the TACE procedure, a catheter is positioned in the arterial supply of a tumor via which a chemotherapeutic drug is administered followed by embolic particles [93,94]. These embolic particles block the feeding vessels of the tumor and restrict nutrient and oxygen supply to the tumor cells. In addition, the blockage of the blood vessels by the embolic particles reduces the washout of the chemotherapeutic drug, which results in higher drug concentrations in the tumor area (i.e. increased efficacy) and reduced systemic exposure (i.e. less side effects) [94,95].

Recently, drug eluting beads (DEBs) that consist of embolic particles with sizes ranging from 70-150 µm to 500-700 µm, loaded with a chemotherapeutic drug, have been developed for TACE procedure. An attractive feature of these DEBs is that they can deliver the embolic particles and the chemotherapeutic drugs simultaneously [94,96,97]. One of the clinically used DEB formulations is based on crosslinked polyvinyl alcohol (PVA) modified with sulfonic acid groups to obtain negatively charged microspheres (DC beads®). A high drug concentration of positively charged cytostatics such as DOX and irinotecan can be achieved in these PVA DEBs via an ion exchange mechanism [97-99]. Clinical trials have shown that embolization with DEBs leads to a significant reduction in peak plasma concentrations and area under the curve of DOX [100,101] while increasing the antitumor efficacy compared to conventional TACE [102,103].

A drawback of these clinically used DEBs is, however, that they lack the ability to be visualized both during and after administration. Therefore, it is not possible to monitor the microsphere distribution in the tumor tissue, which is likely very important to predict the treatment efficacy. Furthermore, in preclinical and clinical studies it was shown that the beads that are currently used for chemoembolization display a sustained release profile leading to low drug concentrations in the tumor over long periods of time (weeks) [99,104,105]. In contrast, a triggered drug release is expected to result in higher drug concentrations in the tumor with a subsequently higher tumor regression (section 4-5).

Aim of this thesis

The research described in this thesis was performed as part of the HIFU-CHEM project (project of CTMM) that investigated new treatment options for liver and bone malignancies using MRI guided High Intensity Focused Ultrasound (HIFU) in combination with ThermoDox® (LTSL under development by the American company Celsion [106]). MRI guided HIFU in combination with ThermoDox® is a promising method providing a non-invasive option for the treatment of solid tumors [107].

Of the above described liposomes, the LTSL is the only formulation currently under clinical investigation. However, a limitation of this liposomal formulation is that it releases > 20% of DOX at 37 °C within 15 minutes in serum and likely also in blood, therefore limiting the amount of DOX delivered to the tumor tissue while exposing healthy tissue to DOX. Liposomes coated with copolymers of poly(NIPAM) are the most intensively studied LCST-polymer coated liposomes so far. Although much progress has been made in the recent years, the release profiles of these liposomes are not optimal and moreover, these polymers are not biodegradable. Therefore, there is a need for other temperature triggered drug delivery systems with more favorable release and biodegradation characteristics.

The research described in this thesis that in turn was part of a CTMM program, aims to develop new biodegradable temperature-sensitive drug delivery carriers that release their content fast at mild hyperthermia to achieve high drug concentrations in the tumor. Preferably, no leakage at 37 °C occurs since premature release of the drug before arrival at the tumor site limits the amount of drug delivered to the tumor tissue and induces exposure of healthy tissue to the drug. Therefore, this thesis focusses on the development of new thermosensitive liposomes for temperature triggered DOX release. Additionally, this thesis describes the development of alginate microspheres that combine embolization with on-demand triggered drug release and whereby the microspheres as well as the drug releasing process can be visualized using MRI.

In **Chapter 2**, the development of liposomes grafted with the temperature sensitive chol-pHPMAlac is described. The influence of the polymers molecular weight, copolymer composition and grafting density on the release characteristics was investigated. Multiple *in vitro* assays (cellular uptake and toxicity assays) were performed in **Chapter 3** to get insight into the interaction between chol-pHPMAlac grafted liposomes with blood cells and other cells with which the liposomes likely come in contact after intravenous administration. **Chapter 4** attempts to optimize the release kinetics of chol-pHPMAlac grafted liposomes by preventing liposome aggregation via PEGylation while maintaining the temperature sensitive release kinetics.
In **Chapter 5**, alginate microspheres loaded with temperature sensitive liposomes (TSL) were developed, which release their payload after mild hyperthermia. These TSL contained [Gd(HPDO3A)(H_2O)], a T_1 MRI contrast agent, for real time monitoring of the release while the alginate microspheres were crosslinked with barium ions and holmium ions (T_2^* MRI contrast agent) to allow microsphere visualization. Subsequently, a formulation containing DOX and [Gd(HPDO3A)(H_2O)] in TSL was developed, which was loaded in alginate microspheres crosslinked with barium ions and mixed with empty microspheres crosslinked with holmium ions. The feasibility of MRI visualization of the [Gd(HPDO3A)(H_2O)] release and holmium crosslinked microspheres was evaluated *in vivo* in **Chapter 6**.
Chapter 7 summarizes this thesis and discusses the described findings and conclusions.

References

1. Siegel RL, Ma J, Zou Z, Jemal A. Cancer statistics, 2014. CA Cancer J Clin 2014;64:9-29.
2. Siegel RL, Miller KD, Jemal A. Cancer statistics, 2015. CA Cancer J Clin 2015;65:5-29.
3. Jemal A, Bray F, Center MM, Ferlay J, Ward E, Forman D. Global cancer statistics. CA Cancer J Clin 2011;61:69-90.
4. Hanahan D, Weinberg RA. The hallmarks of cancer. Cell 2000;100:57-70.
5. Gharib M, Burnett A. Chemotherapy induced cardiotoxicity: current practice and prospects of prophylaxis. Eur J Hearth Fail 2002;4:235-242.
6. Crawford J, Dale DC, Lyman GH. Chemotherapy induced neutropenia. Cancer 2004;100:228-237.
7. Gale RP. Antineoplastic chemotherapy myelosuppression: mechanisms and new approaches. Exp Hematol 1985;13 Suppl 16:3-7.
8. Szakács G, Paterson JK, Ludwig JA, Booth-Genthe C, Gottesman MM. Targeting multidrug resistance in cancer. Nat Rev Drug Discov 2006;5:219-234.
9. Baguley BC. Multiple drug resistance mechanisms in cancer. Mol Biotechnol 2010;46:308-316.
10. Bangham A, Horne R. Negative staining of phospholipids and their structural modification by surface-active agents as observed in the electron microscope. J Mol Biol 1964;8:660-IN10.
11. Bangham A, Standish MM, Watkins J. Diffusion of univalent ions across the lamellae of swollen phospholipids. J Mol Biol 1965;13:238-IN27.
12. Beaumier PL, Hwang KJ. Effects of liposome size on the degradation of bovine brain sphingomyelin/cholesterol liposomes in the mouse liver. Biochim Biophys Acta 1983;731:23-30.
13. Gregoriadis G, Ryman BE. Fate of Protein Containing Liposomes Injected into Rats. Eur J Biochem 1972;24:485-491.
14. Lasic DD, Martin FJ, Gabizon A, Huang SK, Papahadjopoulos D. Sterically stabilized liposomes: a hypothesis on the molecular origin of the extended circulation times. Biochim Biophys Acta 1991;1070:187-192.
15. Allen TM, Hansen C, Martin F, Redemann C, Yau-Young A. Liposomes containing synthetic lipid derivatives of poly(ethylene glycol) show prolonged circulation half-lives in vivo. Biochim Biophys Acta 1991;1066:29-36.
16. Gabizon A, Catane R, Uziely B, Kaufman B, Safra T, Cohen R, et al. Prolonged circulation time and enhanced accumulation in malignant exudates of doxorubicin encapsulated in polyethylene-glycol coated liposomes. Cancer Res 1994;54:987-992.
17. Torchilin VP, Omelyanenko VG, Papisov MI, Bogdanov Jr. AA, Trubetskoy VS, Herron JN, et al. Poly(ethylene glycol) on the liposome surface: on the mechanism of polymer-coated liposome longevity. Biochim Biophys Acta 1994;1195:11-20.
18. Maeda H. Tumor-selective delivery of macromolecular drugs via the EPR effect: background and future prospects. Bioconjug Chem 2010;21:797-802.
19. Bae YH, Park K. Targeted drug delivery to tumors: Myths, reality and possibility. J Control Release 2011;153:198-205.
20. Lammers T, Kiessling F, Hennink WE, Storm G. Drug targeting to tumors: Principles, pitfalls and (pre-) clinical progress. J Control Release 2012;161:175-187.
21. Maeda H, Wu J, Sawa T, Matsumura Y, Hori K. Tumor vascular permeability and the EPR effect in macromolecular therapeutics: a review. J Control Release 2000;65:271-284.
22. Maeda H, Matsumura Y. Tumoritropic and lymphotropic principles of macromolecular drugs. Crit Rev Ther Drug Carrier Syst 1989;6:193-210.

23. Matsumura Y, Maeda H. A new concept for macromolecular therapeutics in cancer chemotherapy: mechanism of tumoritropic accumulation of proteins and the antitumor agent smancs. Cancer Res 1986;46:6387-6392.
24. Allen TM, Cullis PR. Liposomal drug delivery systems: From concept to clinical applications. Adv Drug Deliv Rev 2013;65:36-48.
25. Wicki A, Witzigmann D, Balasubramanian V, Huwyler J. Nanomedicine in cancer therapy: Challenges, opportunities, and clinical applications. J Control Release 2015;200:138-157.
26. Harrington KJ, Mohammadtaghi S, Uster PS, Glass D, Peters AM, Vile RG, et al. Effective targeting of solid tumors in patients with locally advanced cancers by radiolabeled pegylated liposomes. Clin Cancer Res 2001;7:243-254.
27. Jain RK, Stylianopoulos T. Delivering nanomedicine to solid tumors. Nat Rev Clin Oncol 2010;7:653-664.
28. Bandak S, Goren D, Horowitz A, Tzemach D, Gabizon A. Pharmacological studies of cisplatin encapsulated in long-circulating liposomes in mouse tumor models. Anticancer Drugs 1999;10:911-920.
29. Landon CD, Park JY, Needham D, Dewhirst MW. Nanoscale drug delivery and hyperthermia: The materials design and preclinical and clinical testing of low temperature-sensitive liposomes used in combination with mild hyperthermia in the treatment of local cancer. Open Nanomed J 2011;3:38-64.
30. Yarmolenko PS, Zhao Y, Landon C, Spasojevic I, Yuan F, Needham D, et al. Comparative effects of thermosensitive doxorubicin-containing liposomes and hyperthermia in human and murine tumours. Int J Hyperthermia 2010;26:485-498.
31. Hahn GM, Braun J, Har-Kedar I. Thermochemotherapy: synergism between hyperthermia (42-43 degrees) and adriamycin (of bleomycin) in mammalian cell inactivation. Proc Natl Acad Sci U S A 1975;72:937-940.
32. Herman TS. Temperature dependence of adriamycin, cis-diamminedichloroplatinum, bleomycin, and 1,3-bis(2-chloroethyl)-1-nitrosourea cytotoxicity in vitro. Cancer Res 1983;43:517-520.
33. Hildebrandt B, Wust P, Ahlers O, Dieing A, Sreenivasa G, Kerner T, et al. The cellular and molecular basis of hyperthermia. Crit Rev Oncol Hematol 2002;43:33-56.
34. Thrall DE, Prescott DM, Samulski TV, Dewhirst MW, Cline JM, Lee J, et al. Serious toxicity associated with annular microwave array induction of whole-body hyperthermia in normal dogs. Int J Hyperthermia 1992;8:23-32.
35. Dewhirst MW, Sim DA. The utility of thermal dose as a predictor of tumor and normal tissue responses to combined radiation and hyperthermia. Cancer Res 1984;44:4772-4780.
36. Yatvin MB, Weinstein JN, Dennis WH, Blumenthal R. Design of liposomes for enhanced local release of drugs by hyperthermia. Science 1978;202:1290-1293.
37. Yatvin MB, Muhlensiepen H, Porschen W, Weinstein JN, Feinendegen LE. Selective delivery of liposome-associated cis-dichlorodiammineplatinum(II) by heat and its influence on tumor drug uptake and growth. Cancer Res 1981;41:1602-1607.
38. Kong G, Dewhirst MW. Hyperthermia and liposomes. Int J Hyperthermia 1999;15:345-370.
39. Kong G, Anyarambhatla G, Petros WP, Braun RD, Colvin OM, Needham D, et al. Efficacy of liposomes and hyperthermia in a human tumor xenograft model: importance of triggered drug release. Cancer Res 2000;60:6950-6957.
40. Needham D, Anyarambhatla G, Kong G, Dewhirst MW. A new temperature-sensitive liposome for use with mild hyperthermia: characterization and testing in a human tumor xenograft model. Cancer Res 2000;60:1197-1201.
41. Winter ND, Murphy RK, O'Halloran TV, Schatz GC. Development and modeling of arsenic-trioxide-loaded thermosensitive liposomes for anticancer drug delivery. J Liposome Res 2011;21:106-115.

42. Sandstrom MC, Ickenstein LM, Mayer LD, Edwards K. Effects of lipid segregation and lysolipid dissociation on drug release from thermosensitive liposomes. J Control Release 2005;107:131-142.
43. Mills JK, Needham D. Lysolipid incorporation in dipalmitoylphosphatidylcholine bilayer membranes enhances the ion permeability and drug release rates at the membrane phase transition. Biochim Biophys Acta 2005;1716:77-96.
44. Banno B, Ickenstein LM, Chiu GN, Bally MB, Thewalt J, Brief E, et al. The functional roles of poly (ethylene glycol) lipid and lysolipid in the drug retention and release from lysolipid containing thermosensitive liposomes in vitro and in vivo. J Pharm Sci 2010;99:2295-2308.
45. Ickenstein LM, Arfvidsson MC, Needham D, Mayer LD, Edwards K. Disc formation in cholesterol-free liposomes during phase transition. Biochim Biophys Acta 2003;1614:135-138.
46. Needham D, Park J, Wright AM, Tong J. Materials characterization of the low temperature sensitive liposome (LTSL): effects of the lipid composition (lysolipid and DSPE–PEG2000) on the thermal transition and release of doxorubicin. Faraday Discuss 2013;161:515-534.
47. Anyarambhatla GR, Needham D. Enhancement of the phase transition permeability of DPPC liposomes by incorporation of MPPC: A new temperature-sensitive liposome for use with mild hyperthermia. J Liposome Res 1999;9:491-506.
48. Needham D, Dewhirst MW. The development and testing of a new temperature-sensitive drug delivery system for the treatment of solid tumors. Adv Drug Deliv Rev 2001;53:285-305.
49. Negussie AH, Yarmolenko PS, Partanen A, Ranjan A, Jacobs G, Woods D, et al. Formulation and characterisation of magnetic resonance imageable thermally sensitive liposomes for use with magnetic resonance-guided high intensity focused ultrasound. Int J Hyperthermia 2011;27:140-155.
50. de Smet M, Langereis S, van den Bosch S, Grull H. Temperature-sensitive liposomes for doxorubicin delivery under MRI guidance. J Control Release 2010;143:120-127.
51. Tagami T, Ernsting MJ, Li SD. Efficient tumor regression by a single and low dose treatment with a novel and enhanced formulation of thermosensitive liposomal doxorubicin. J Control Release 2011;152:303-309.
52. Tagami T, Ernsting MJ, Li SD. Optimization of a novel and improved thermosensitive liposome formulated with DPPC and a Brij surfactant using a robust in vitro system. J Control Release 2011;154:290-297.
53. Tagami T, Foltz WD, Ernsting MJ, Lee CM, Tannock IF, May JP, et al. MRI monitoring of intratumoral drug delivery and prediction of the therapeutic effect with a multifunctional thermosensitive liposome. Biomaterials 2011;32:6570-6578.
54. May JP, Ernsting MJ, Undzys E, Li S. Thermosensitive liposomes for the delivery of gemcitabine and oxaliplatin to tumors. Mol Pharm 2013;10:4499-4508.
55. Tagami T, May JP, Ernsting MJ, Li S. A thermosensitive liposome prepared with a Cu2+ gradient demonstrates improved pharmacokinetics, drug delivery and antitumor efficacy. J Control Release 2012;161:142-149.
56. Lindner LH, Eichhorn ME, Eibl H, Teichert N, Schmitt-Sody M, Issels RD, et al. Novel temperature-sensitive liposomes with prolonged circulation time. Clin Cancer Res 2004;10:2168-2178.
57. Ashok B, Arleth L, Hjelm RP, Rubinstein I, Önyüksel H. In vitro characterization of PEGylated phospholipid micelles for improved drug solubilization: effects of PEG chain length and PC incorporation. J Pharm Sci 2004;93:2476-2487.
58. de Smet M, Heijman E, Langereis S, Hijnen NM, Grull H. Magnetic resonance imaging of high intensity focused ultrasound mediated drug delivery from temperature-sensitive liposomes: an in vivo proof-of-concept study. J Control Release 2011;150:102-110.
59. Hossann M, Wiggenhorn M, Schwerdt A, Wachholz K, Teichert N, Eibl H, et al. In vitro stability and content release properties of phosphatidylglyceroglycerol containing thermosensitive liposomes. Biochim Biophys Acta 2007;1768:2491-2499.

60. Wang T, Hossann M, Reinl HM, Peller M, Eibl H, Reiser M, et al. In vitro characterization of phosphatidylglyceroglycerol-based thermosensitive liposomes with encapsulated 1H MR T1-shortening gadodiamide. Contrast Media Mol Imaging 2008;3:19-26.
61. Hossann M, Syunyaeva Z, Schmidt R, Zengerle A, Eibl H, Issels RD, et al. Proteins and cholesterol lipid vesicles are mediators of drug release from thermosensitive liposomes. J Control Release 2012;162:400-406.
62. Hossann M, Wang T, Wiggenhorn M, Schmidt R, Zengerle A, Winter G, et al. Size of thermosensitive liposomes influences content release. J Control Release 2010;147:436-443.
63. Lindner LH, Hossann M, Vogeser M, Teichert N, Wachholz K, Eibl H, et al. Dual role of hexadecylphosphocholine (miltefosine) in thermosensitive liposomes: active ingredient and mediator of drug release. J Control Release 2008;125:112-120.
64. Limmer S, Hahn J, Schmidt R, Wachholz K, Zengerle A, Lechner K, et al. Gemcitabine treatment of rat soft tissue sarcoma with phosphatidyldiglycerol-based thermosensitive liposomes. Pharm Res 2014;31:2276-2286.
65. Kono K. Thermosensitive polymer-modified liposomes. Adv Drug Deliv Rev 2001;53:307-319.
66. van Elk M, Deckers R, Oerlemans C, Shi Y, Storm G, Vermonden T, et al. Triggered release of doxorubicin from temperature-sensitive poly(N-(2-hydroxypropyl)-methacrylamide mono/dilactate) grafted liposomes. Biomacromolecules 2014;15:1002-1009.
67. Jalani G, Jung CW, Lee JS, Lim DW. Fabrication and characterization of anisotropic nanofiber scaffolds for advanced drug delivery systems. Int J Nanomedicine 2014;9:33.
68. Saleem Q, Zhang Z, Gradinaru CC, Macdonald PM. Liposome-coated hydrogel spheres: delivery vehicles with tandem release from distinct compartments. Langmuir 2013;29:14603-14612.
69. Peng J, Qi T, Liao J, Chu B, Yang Q, Li W, et al. Controlled release of cisplatin from pH-thermal dual responsive nanogels. Biomaterials 2013;34:8726-8740.
70. Kono K, Hayashi H, Takagishi T. Temperature-sensitive liposomes: liposomes bearing poly (N-isopropylacrylamide). J Control Release 1994;30:69-75.
71. Kono K, Henmi A, Yamashita H, Hayashi H, Takagishi T. Improvement of temperature-sensitivity of poly (N-isopropylacrylamide)-modified liposomes. J Control Release 1999;59:63-75.
72. Hayashi H, Kono K, Takagishi T. Temperature-controlled release property of phospholipid vesicles bearing a thermo-sensitive polymer. Biochim Biophys Acta 1996;1280:127-134.
73. Allen TM, Hong K, Papahadjopoulos D. Membrane contact, fusion, and hexagonal (HII) transitions in phosphatidylethanolamine liposomes. Biochemistry; 1990;29:2976-2985.
74. Ishida T, Kirchmeier MJ, Moase EH, Zalipsky S, Allen TM. Targeted delivery and triggered release of liposomal doxorubicin enhances cytotoxicity against human B lymphoma cells. Biochim Biophys Acta 2001;1515:144-158.
75. Hayashi H, Kono K, Takagishi T. Temperature-dependent associating property of liposomes modified with a thermosensitive polymer. Bioconjug Chem 1998;9:382-389.
76. Hayashi H, Kono K, Takagishi T. Temperature sensitization of liposomes using copolymers of N-isopropylacrylamide. Bioconjug Chem 1999;10:412-418.
77. Han HD, Shin BC, Choi HS. Doxorubicin-encapsulated thermosensitive liposomes modified with poly (N-isopropylacrylamide-co-acrylamide): drug release behavior and stability in the presence of serum. Eur J Pharm Biopharm 2006;62:110-116.
78. Kono K, Nakai R, Morimoto K, Takagishi T. Thermosensitive polymer-modified liposomes that release contents around physiological temperature. Biochim Biophys Acta 1999;1416:239-250.
79. Ta T, Convertine AJ, Reyes CR, Stayton PS, Porter TM. Thermosensitive liposomes modified with poly (N-isopropylacrylamide-co-propylacrylic acid) copolymers for triggered release of doxorubicin. Biomacromolecules 2010;11:1915-1920.

80. Kono K, Murakami T, Yoshida T, Haba Y, Kanaoka S, Takagishi T, et al. Temperature sensitization of liposomes by use of thermosensitive block copolymers synthesized by living cationic polymerization: effect of copolymer chain length. Bioconjug Chem 2005;16:1367-1374.
81. Kono K, Ozawa T, Yoshida T, Ozaki F, Ishizaka Y, Maruyama K, et al. Highly temperature-sensitive liposomes based on a thermosensitive block copolymer for tumor-specific chemotherapy. Biomaterials 2010;31:7096-7105.
82. Kono K, Nakashima S, Kokuryo D, Aoki I, Shimomoto H, Aoshima S, et al. Multi-functional liposomes having temperature-triggered release and magnetic resonance imaging for tumor-specific chemotherapy. Biomaterials 2011;32:1387-1395.
83. Katagiri K, Imai Y, Koumoto K, Kaiden T, Kono K, Aoshima S. Magnetoresponsive on-demand release of hybrid liposomes formed from Fe3O4 nanoparticles and thermosensitive block copolymers. Small 2011;7:1683-1689.
84. Park SM, Kim MS, Park S, Park ES, Choi K, Kim Y, et al. Novel temperature-triggered liposome with high stability: formulation, in vitro evaluation, and in vivo study combined with high-intensity focused ultrasound (HIFU). J Control Release 2013;170:373-379.
85. Kim MS, Lee D, Park K, Park S, Choi E, Park ES, et al. Temperature-triggered tumor-specific delivery of anticancer agents by cRGD-conjugated thermosensitive liposomes. Colloids Surf B Biointerfaces 2014;116:17-25.
86. Kokuryo D, Nakashima S, Ozaki F, Yuba E, Chuang K, Aoshima S, et al. Evaluation of thermo-triggered drug release in intramuscular-transplanted tumors using thermosensitive polymer-modified liposomes and MRI. Nanomedicine 2015;11:229-238.
87. Peller M, Schwerdt A, Hossann M, Reinl HM, Wang T, Sourbron S, et al. MR characterization of mild hyperthermia-induced gadodiamide release from thermosensitive liposomes in solid tumors. Invest Radiol 2008;43:877-892.
88. Yeo SY, de Smet M, Langereis S, Vander Elst L, Muller RN, Grüll H. Temperature-sensitive paramagnetic liposomes for image-guided drug delivery: Mn 2 versus [Gd (HPDO3A)(H 2 O)]. Biochim Biophys Acta 2014;1838:2807-2816.
89. Davis RM, Viglianti BL, Yarmolenko P, Park JY, Stauffer P, Needham D, et al. A method to convert MRI images of temperature change into images of absolute temperature in solid tumours. Int J Hyperthermia 2013;29:569-581.
90. Viglianti BL, Abraham SA, Michelich CR, Yarmolenko PS, MacFall JR, Bally MB, et al. In vivo monitoring of tissue pharmacokinetics of liposome/drug using MRI: illustration of targeted delivery. Magn Reson Med 2004;51:1153-1162.
91. Ponce AM, Viglianti BL, Yu D, Yarmolenko PS, Michelich CR, Woo J, et al. Magnetic resonance imaging of temperature-sensitive liposome release: drug dose painting and antitumor effects. J Natl Cancer Inst 2007;99:53-63.
92. Hossann M, Wang T, Syunyaeva Z, Wiggenhorn M, Zengerle A, Issels RD, et al. Non-ionic Gd-based MRI contrast agents are optimal for encapsulation into phosphatidyldiglycerol-based thermosensitive liposomes. J Control Release 2013;166:22-29.
93. Brown DB, Gould JE, Gervais DA, Goldberg SN, Murthy R, Millward SF, et al. Transcatheter therapy for hepatic malignancy: standardization of terminology and reporting criteria. J Vasc Interv Radiol 2009;20:S425-S434.
94. Lewandowski RJ, Geschwind J, Liapi E, Salem R. Transcatheter intraarterial therapies: Rationale and overview. Radiology 2011;259:641-657.
95. Lencioni R. Loco-regional treatment of hepatocellular carcinoma in the era of molecular targeted therapies. Oncology 2010;78:107-112.

96. Hong K, Khwaja A, Liapi E, Torbenson MS, Georgiades CS, Geschwind JFH. New intra-arterial drug delivery system for the treatment of liver cancer: Preclinical assessment in a rabbit model of liver cancer. Clin Cancer Res 2006;12:2563-2567.
97. Lewis AL, Dreher MR. Locoregional drug delivery using image-guided intra-arterial drug eluting bead therapy. J Control Release 2012;161:338-350.
98. Lewis AL, Gonzalez MV, Lloyd AW, Hall B, Tang YQ, Willis SL, et al. DC bead: In vitro characterization of a drug-delivery device for transarterial chemoembolization. J Vasc Interv Radiol 2006;17:335-342.
99. Lewis AL, Holden RR. DC Bead embolic drug-eluting bead: clinical application in the locoregional treatment of tumours. Expert Opin Drug Deliv 2011;8:153-169.
100. Poon RT, Tso WK, Pang RW, Ng KK, Woo R, Tai KS, et al. A phase I/II trial of chemoembolization for hepatocellular carcinoma using a novel intra-arterial drug-eluting bead. Clin Gastroenterol Hepatol 2007;5:1100-1108.
101. Varela M, Real MI, Burrel M, Forner A, Sala M, Brunet M, et al. Chemoembolization of hepatocellular carcinoma with drug eluting beads: efficacy and doxorubicin pharmacokinetics. J Hepatol 2007;46:474-481.
102. Dhanasekaran R, Kooby DA, Staley CA, Kauh JS, Khanna V, Kim HS. Comparison of conventional transarterial chemoembolization (TACE) and chemoembolization with doxorubicin drug eluting beads (DEB) for unresectable hepatocelluar carcinoma (HCC). J Surg Oncol 2010;101:476-480.
103. Nicolini D, Svegliati-Baroni G, Candelari R, Mincarelli C, Mandolesi A, Bearzi I, et al. Doxorubicin-eluting bead vs conventional transcatheter arterial chemoembolization for hepatocellular carcinoma before liver transplantation. World J Gastroenterol 2013;19:5622-5632.
104. Namur J, Citron SJ, Sellers MT, Dupuis MH, Wassef M, Manfait M, et al. Embolization of hepatocellular carcinoma with drug-eluting beads: Doxorubicin tissue concentration and distribution in patient liver explants. J Hepatol 2011;55:1332-1338.
105. Namur J, Wassef M, Millot J, Lewis AL, Manfait M, Laurent A. Drug-eluting beads for liver embolization: Concentration of doxorubicin in tissue and in beads in a pig model. J Vasc Interv Radiol 2010;21:259-267.
106. http://celsion.com/. ;accessed May 2015.
107.http://www.ctmm.nl/nl/downloadsnl-pdf/volledig-programma-artikel-pdf/full-article-on-project-hifu-chem. ;accessed May 2015.

2

Triggered release of doxorubicin from temperature sensitive poly(*N*-(2-hydroxypropyl)-methacrylamide mono/dilactate) grafted liposomes

Merel van Elk, Roel Deckers, Chris Oerlemans, Yang Shi,
Gert Storm, Tina Vermonden and Wim E. Hennink

Biomacromolecules. 2014;15(3):1002-9

Abtract

The objective of this study was to design temperature sensitive liposomes with tunable release characteristics that release their content at elevated temperature generated by high intensity focused ultrasound (HIFU) exposure. To this end, thermosensitive polymers of *N*-(2-hydroxypropyl)methacrylamide mono/dilactate of different molecular weights and composition with a cholesterol anchor (chol-pHPMAlac) were synthesized and grafted onto liposomes loaded with doxorubicin (DOX). The liposomes were incubated at different temperatures and their release kinetics were studied. A good correlation between the release-onset temperature of the liposomes and the cloud point (CP) of chol-pHPMAlac was found. However, release took place at significantly higher temperatures than the CP of chol-pHPMAlac, likely at the CP the dehydration and thus hydrophobicity is insufficient to penetrate and permeabilize the liposomal membrane. Liposomes grafted with chol-pHPMAlac with a CP of 11.5 °C released 89% DOX within 5 minutes at 42 °C while for the liposomes grafted with a polymer with CP of 25.0 °C, a temperature of 52 °C was needed to obtain the same extent of DOX release. At a fixed copolymer composition, an increase in molecular weight from 6.5 to 14.5 kDa decreased the temperature at which DOX was released with a release-onset temperature from 52 to 42 °C. Liposomes grafted with 5% chol-pHPMAlac exhibited a rapid release to a temperature increase while at a grafting density of 2 and 10%, the liposomes were less sensitive to an increase in temperature. Sequential release of DOX was obtained by mixing liposomes grafted with chol-pHPMAlac having different CP's. Chol-pHPMAlac grafted liposomes released DOX nearly quantitatively after pulsed wave HIFU.

In conclusion, the release of DOX from liposomes grafted with thermosensitive polymers of *N*-(2-hydroxypropyl)methacrylamide mono/dilactate can be tuned by the characteristics and the grafting density of chol-pHPMAlac, making these liposomes attractive for local drug delivery using hyperthermia.

Introduction

Nanosized drug delivery systems are developed to improve the therapeutic efficacy and/or to reduce unwanted side effects of existing drugs as well as drug candidates. These delivery systems accumulate in the tumor after intravenous injection via the enhanced permeability and retention (EPR) effect [1-3]. Liposomes are the most intensively studied drug delivery systems [4-7] and a number of studies showed that encapsulation of doxorubicin (DOX) in liposomes resulted in an increased therapeutic index particularly due to significantly reduced cardio toxicity and other unwanted side effects [8,9]. Triggerable liposomal drug release systems have great opportunities to increase and control the drug concentrations in the tumor. Examples of triggers are pH [10,11], light [12,13] and ultrasound [14,15] but so far heat is the most intensively studied trigger for drug release [16,17]. Hyperthermia is known to increase the blood flow and permeability of blood vessels, resulting in a more extensive liposome extravasation at the target site and thus higher drug concentrations at the site of action [18-21]. High intensity focused ultrasound (HIFU) is an attractive modality to locally increase the temperature in e.g. a tumor, because the ultrasound field penetrates deeply into tissue (~10 cm) and can be focused in a small spot (~1 mm). It has been shown that temperature sensitive liposomes release their content upon exposure to HIFU *in vitro* as well as *in vivo* [22-25], due to enhanced permeability of the lipid bilayer when phospholipids pass their gel-to-liquid phase transition temperature (T_m) [26,27]. Particularly, the incorporation of a lysolipid in the bilayer of liposomes improved the temperature sensitive release significantly [28-30]. Lysolipids form pores in the lipid bilayer when crossing the T_m of the lipid bilayer [31-33] resulting in a complete DOX release within seconds at 42 °C [34]. A drawback of this system is however the high leakage at 37 °C in the circulation (20% release in 15 minutes at 37 °C) [34,35], which is associated with a high risk of toxicity towards healthy tissue. Another temperature sensitive liposome with 1,2-dipalmitoyl-*sn*-glycero-3-phosphoglyceroglycerol (DPPGOG) [36-38] had a better stability in the circulation while remaining temperature sensitive. Liposomes containing Brij 78 showed even faster release kinetics compared to the liposomes containing lysolipids [39-41].

An alternative approach to render liposomes temperature sensitive is by grafting thermosensitive polymers on their surfaces [42-45]. These polymers display lower critical solution temperature (LCST) behavior meaning that they are soluble in an aqueous solution at a low temperature but dehydrate and aggregate when the polymers are heated above the cloud point (CP). When these temperature sensitive polymers are grafted on the liposome surface and become dehydrated above their CP, they will interact with the lipid bilayer possibly inducing aggregation and destabilization, resulting in release of an entrapped compound (Fig. 1). Poly(*N*-isopropylacrylamide) (pNIPAM) displays LCST behavior around 32 °C [46] and the CP of this polymer can be modulated by copolymerization with other monomers [44]. PNIPAM and its copolymers have been grafted onto liposomes which were used to trigger release of entrapped DOX [43,44,47]. Also, poly(2-(2-ethoxy)ethoxyethyl vinyl ether) grafted onto the surface of liposomes induced temperature triggered DOX release [45,48,49]. The liposomes described so far have a fixed release temperature due to the composition of the lipids and the properties of the polymer. In this study, we develop temperature sensitive liposomes of which the release temperature is tunable.

N-(2-hydroxypropyl)methacrylamide mono/dilactate polymers are used for the design of drug delivery systems e.g. micelles and hydrogels [50-53]. It was previously reported that grafting of these polymers on liposomes resulted in temperature triggered release of calcein [54].

Polymers of *N*-(2-hydroxypropyl)methacrylamide mono/dilactate were synthesized with a cholesterol anchor (chol-pHPMAlac), which facilitates incorporation in the liposomal bilayer [54]. In this study, temperature sensitive properties of the liposomes were tailored by varying the copolymer composition (resulting in variation of the CP), molecular weight and grafting density of chol-pHPMAlac. Finally, we showed that HIFU-induced temperature increase can be used to trigger DOX release from chol-pHPMAlac grafted liposomes.

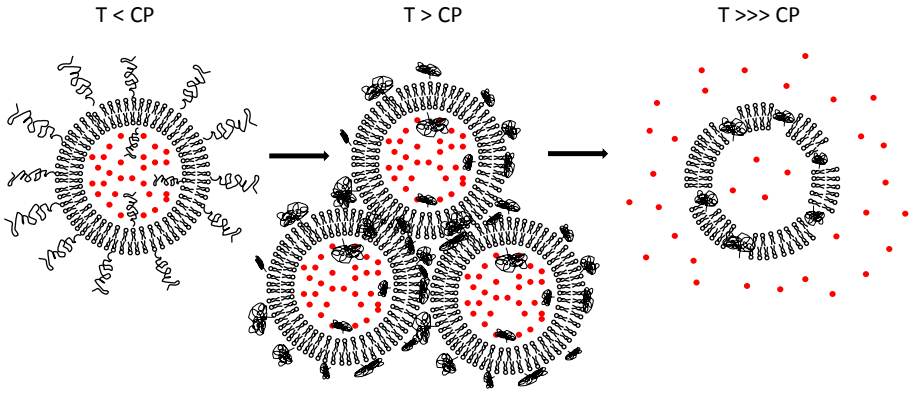

Fig. 1. Schematic representation of heat triggered DOX release from liposomes grafted with polymers displaying LCST behavior.

Materials and methods

Materials

Thiocholesterol and *N,N*,-azobisisobutyronitrile (AIBN) were purchased from Sigma-Aldrich Chemie BV, Zwijndrecht, the Netherlands. 1,4-Dioxane was purchased from Biosolve Chemie, Valkenswaard, The Netherlands. 1,2-Dioleoyl-*sn*-glycero-3-phosphoethanolamine (DOPE) and 1,2-distearoyl-*sn*-glycero-3-phosphoethanolamine-*N*-[amino(polyethylene glycol)-2000] (DSPE-PEG2.000) were purchased from Avanti Polar Lipids, Alabaster, USA. Egg phosphocholine (EPC) was purchased from Lipoid GmbH, Ludwigshafen, Germany. Doxorubicin-HCl was purchased from Guanyu bio-technology Co., LTD, Xi'an, China.

Synthesis of HPMA mono/dilactate polymers with cholesterol anchor

2-Hydroxypropyl methacrylamide (HPMA), HPMAmono and dilactate were synthesized as described previously [55]. HPMA mono/dilactate polymers with a cholesterol anchor (chol-pHPMAlac) were synthesized according to a previously reported method [54]. In brief, HPMA mono/dilactate was dissolved in distilled 1,4-dioxane at a concentration of 100 mg/mL with monomer ratios varying from 35:65 to 80:20 (HPMA mono/HPMA dilactate, mol/mol). *N,N*-Azobisisobutyronitrile (AIBN) was used as initiator at a ratio of 500:1 (monomer/AIBN, mol/mol). The molar ratio of thiocholesterol (chain transfer agent) was varied from 20:1 to 125:1 (monomer/chain transfer agent). Three nitrogen/vacuum cycles were applied to remove oxygen and the polymerization reaction was performed for 24 hours at 70 °C. Polymers were precipitated in diethyl ether and the supernatant was discarded after centrifugation. The polymers were stored in the freezer until further use.

Polymer characterization

The copolymer composition of chol-pHPMAlac was determined by ^{1}H NMR (Gemini 300 MHz spectrometer) in $(CD_3)_2SO$. The ratio of HPMAmonolactate/HPMAdilactate (ML/DL) was determined from the integral of the peak at 5.0 ppm (CO-C*H*(CH_3)-O) divided by the integral of the peaks at 4.1 and 4.2 ppm (CO-C*H*(CH_3)-OH).

The cloud point (CP) of chol-pHPMAlac was determined by light scattering at 650 nm. Chol-pHPMAlac was dissolved at 5 mg/mL in 120 mM ammonium acetate (pH 5.0). Samples were heated from 0 till 70 °C with a rate of 1 °C /min. The CP was taken as the onset of increasing scattering intensity [55,56].

The number average molecular weight (M_n), weight average molecular weight (M_w) and thus the dispersity (Đ) were measured with GPC using a Plgel 5 µm MIXED-D column and PEGs with narrow molecular weights as standards. DMF containing 10 mM LiCl was used as eluent at an elution rate of 0.7 mL/min. The column temperature was 40 °C [56].

Liposome preparation

Two different liposomal formulations were prepared: temperature sensitive-polymer coated liposomes composed of DOPE, EPC and chol-pHPMAlac (in molar ratios of 70:25:2-10) and a control formulation, which consisted of DOPE, EPC and DSPE-PEG2.000 (molar ratio of 70:25:5). The phospholipids and chol-pHPMAlac were dissolved in 5 mL chloroform (12 µmol phospholipid/mL). A lipid film was formed after evaporation of chloroform under reduced pressure and the remaining

traces of chloroform were removed overnight under a nitrogen flow. The lipid film was subsequently hydrated in 4 mL 240 mM ammonium sulfate buffer (pH 5.4) at a concentration of 15 μmol phospholipid/mL. The liposomal dispersion was extruded through two 200 nm filters (2 times) and two 100 nm filters (8 times). The extruded liposomes were dialyzed against 20 mM HEPES buffer pH 7.4 also containing 8 g NaCl/L and 292 mg EDTA/L. The liposomes were loaded with 1 mL (5 mg/mL) doxorubicin (DOX) for 4 hours at 4 °C [57,58]. Free DOX and free chol-pHPMAlac were removed by ultracentrifugation (125.000 g for 45 minutes at 4 °C) of the liposome dispersion. The liposomes were resuspended in 2 mL 20 mM HEPES buffer pH 7.4 (2.5 mg/mL DOX) and stored at 4 °C.

Liposome characterization

The DOX concentration was determined after disruption of the liposomes with Triton X-100 [17] using fluorescence measurements (excitation wavelength 485 nm, emission wavelength 600 nm). The concentration of phospholipids in the liposomal dispersion was measured using the phosphate assay of Rouser [59]. The size of the liposomes and the polydispersity index were measured with dynamic light scattering (DLS) (Malvern CGS-3 multiangle goniometer). This technique was also used to determine the aggregation temperature of the liposomes. Samples were heated from 5 to 50 °C with a rate of 1 °C/min and measurements were performed every minute.

The grafting density of chol-pHPMAlac on liposomes was determined by ^{1}H NMR. The free chol-pHPMAlac was separated from the liposomes by ultracentrifugation at 125.000 g for 45 minutes at 4 °C. Liposomes were freeze-dried and dissolved in $CDCl_3$ [60]. The amount of liposome associated chol-pHPMAlac was calculated by comparing the phospholipid peaks (5.2 and 5.3 ppm) with the chol-pHPMAlac peak (5.0 ppm, (CO-C*H*(CH_3)-O)) before and after ultracentrifugation.

The release of DOX was measured by the change in fluorescence intensity in time (excitation wavelength 468 nm, emission wavelength 558 nm). DOX-loaded liposomes (1 μL) were added to preheated 20 mM HEPES buffer at pH 7.4 (2 mL) of 25, 37, 42, 47, 52 and 57 °C and the fluorescence intensity was measured in time. Triton X-100 (10%, 20 μL) was added at the end of the experiment to destroy remaining liposomes to determine the total amount of DOX present. The percentage DOX release was calculated using the following equation: $(I_t-I_0)/(I_{TX}-I_0)$ x 100 in which I_t is the fluorescence intensity at time t, I_0 the intensity at the start of the experiment and I_{TX} the fluorescence intensity after addition of Triton X-100.

High intensity focused ultrasound (HIFU) triggered release

Liposomes were exposed to pulsed wave HIFU (PW-HIFU) using a home-built HIFU system equipped with a single element transducer with an external radius aperture of 120 mm and a focal length of 80 mm. An AG 1006 amplifier/generator generated a sinusoidal signal of 1.4 MHz. The liposome dispersion (1 mL, in an Eppendorf tube) was placed in the sample holder which was located in the focal point of the transducer. The HIFU transducer plus sample holder were submerged in degassed water at 35 °C. Liposomes were exposed to PW-HIFU (PRF = 1 kHz, DC = 20%) during 2, 5, 10, 15 and 30 minutes with an acoustic power of 20 W. These ultrasound settings allowed for heating of the sample over longer duration with a maximum temperature of 53 °C. The temperature in the Eppendorf tube was measured after different exposure times in order to avoid interference of the thermometer in the ultrasound field.

Results and discussion

Polymer synthesis and characterization

Poly(HPMAmono/HPMAdilactate)'s with a cholesterol anchor and of different compositions and molecular weights were synthesized via free radical polymerization using thiocholesterol as chain transfer agent (CTA) (Fig. 2).

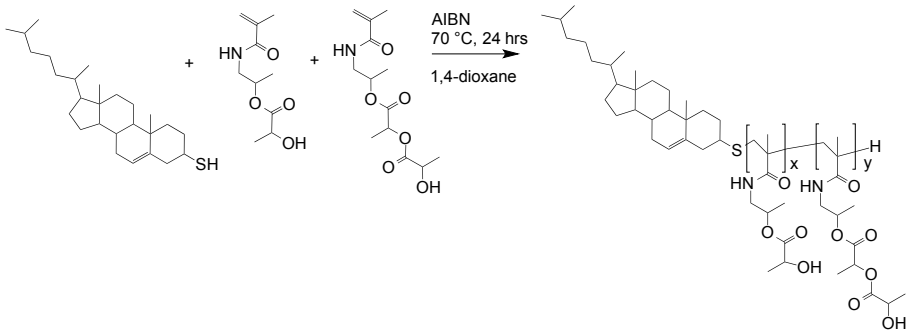

Fig. 2. Synthesis of poly(*N*-(2-hydroxypropyl)methacrylamide mono/dilactate with a cholesterol anchor (chol-pHPMAlac).

The characteristics of the synthesized polymers are summarized in table 1.

Table 1. Characteristics of chol-pHPMAlac

Monomer feed ratio (monolactate:dilactate) (mol/mol)	CTA:Monomer (mol/mol)	Copolymer composition[a] (monolactate:dilactate) (mol/mol)	Yield (%)	M_n [b] (kDa)	M_w [b] (kDa)	CP[c] (°C)
35:65	1:50	30:70	50	10.5	16.5	11.5
50:50	1:20	44:56	39	6.5	10.5	20.0
50:50	1:50	44:56	52	10.0	17.0	19.0
50:50	1:125	41:59	70	14.5	27.0	17.5
65:35	1:50	54:46	69	11.0	19.0	25.0
80:20	1:50	67:33	74	11.0	20.5	32.0

[a] Determined by ^{1}H NMR

[b] Determined by GPC

[c] Determined by light scattering at 650 nm

The yield of different chol-pHPMAlac polymers varied between 40-75%. Four polymers with different compositions ranging from 35:65 to 80:20 (monolactate/dilactate, (ML/DL)) were synthesized. The percentage of HPMAdilactate in the copolymers was slightly higher than in the feed, which is in line with previous studies of pHPMAlac polymers [56]. The M_n of the synthesized polymer could not be determined via the end group - polymer ratio since the methyl protons of cholesterol as well as pHPMAlac display a peak at 0.7 ppm in the ^{1}H NMR spectrum (Fig. 3). The CPs of different chol-pHPMAlac polymers ranged from 11.5 °C for the polymer with the highest content of HPMAdilactate to 32.0 °C for the polymer with the lowest

HPMAdilactate content. This observation is in line with previous experiments and can be explained by the higher hydrophilicity of HPMAmonolactate over HPMAdilactate [56]. The CP of chol-pHPMAlac is lower than the CP of the same polymer without cholesterol anchor (19 and 34 °C respectively) likely due to the hydrophobic nature of cholesterol [54]. Chol-pHPMAlac synthesized with a fixed monomer/CTA ratio of 50:1 and a varying monomer ratio had a M_n of 10 – 11 kDa with a dispersity (Đ) of 1.6 – 1.7.

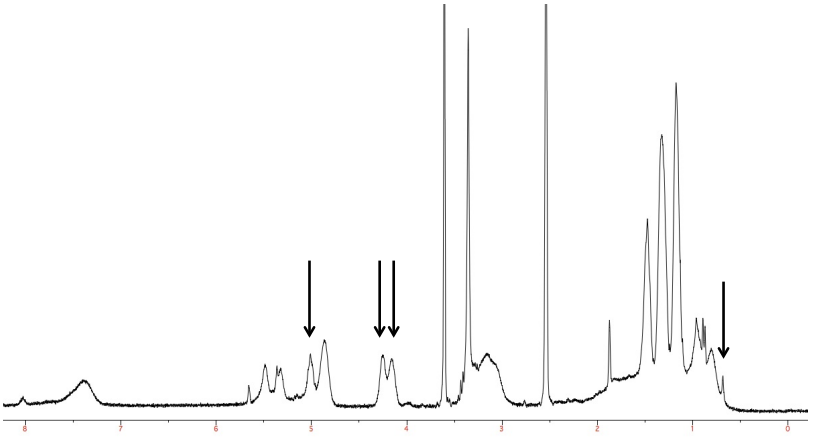

Fig. 3. ^{1}H NMR spectrum of chol-pHPMAlac (50:50 ML/DL, CTA:monomer ratio 1:20) in $(CD_3)_2SO$. The copolymer composition was determined from the integral of the peak at 5.0 ppm (CO-C*H*(CH_3)-O) divided by the integral of the peaks at 4.1 and 4.2 ppm (CO-C*H*(CH_3)-OH). The cholesterol anchor displays a peak at 0.7 ppm.

Three polymers with different molecular weights and a fixed copolymer composition (50:50, monolactate/dilactate in the feed) were synthesized by varying the ratio between the monomers and CTA from 20:1 to 125:1. The molecular weight decreased with increasing amount CTA in the reaction mix from 14.5 to 6.5 kDa, in agreement with expectations [61-63]. Upon decreasing the M_n of the polymers, the signal of cholesterol at 0.7 ppm became more distinct in the ^{1}H NMR spectrum. Chol-pHPMAlac with a molecular weight of 14.5 kDa had a slightly lower CP of 17.5 °C compared to the CP of chol-pHPMAlac with molecular weights of 6.5 and 10.0 kDa (20.0 and 19.0 °C respectively) which can be ascribed to the slightly higher HPMAdilactate content of this polymer as well as its higher molecular weight compared to the smaller polymers since the CP decreases with an increase in molecular weight [64,65].

Liposome characterization

Liposomes grafted with chol-pHPMAlac and DSPE-PEG2.000 were prepared and loaded with DOX using an ammonium sulfate gradient. Non-coated liposomes (DOPE:EPC, 70:25) aggregated during preparation since they form a nonbilayer structure (hexagonal H_{II}) [66,67] and were excluded from further experiments. The DOX encapsulation efficiency was > 95% for all formulations, which was also observed previously for the loading of DOX with a pH gradient [57,58]. The size of the liposomes varied between 100 and 150 nm with a PDI of ~ 0.1. NMR analysis showed that 50% of the added chol-pHPMAlac was grafted on the liposome surface, likely because not all the polymers have a cholesterol anchor [63].

Temperature triggered release of doxorubicin

A formulation of DOPE and EPC stabilized with DSPE-PEG2.000, a non-temperature sensitive polymer, was prepared, and as expected, did not show detectable release of DOX at temperatures from 25 - 52 °C in 30 minutes.

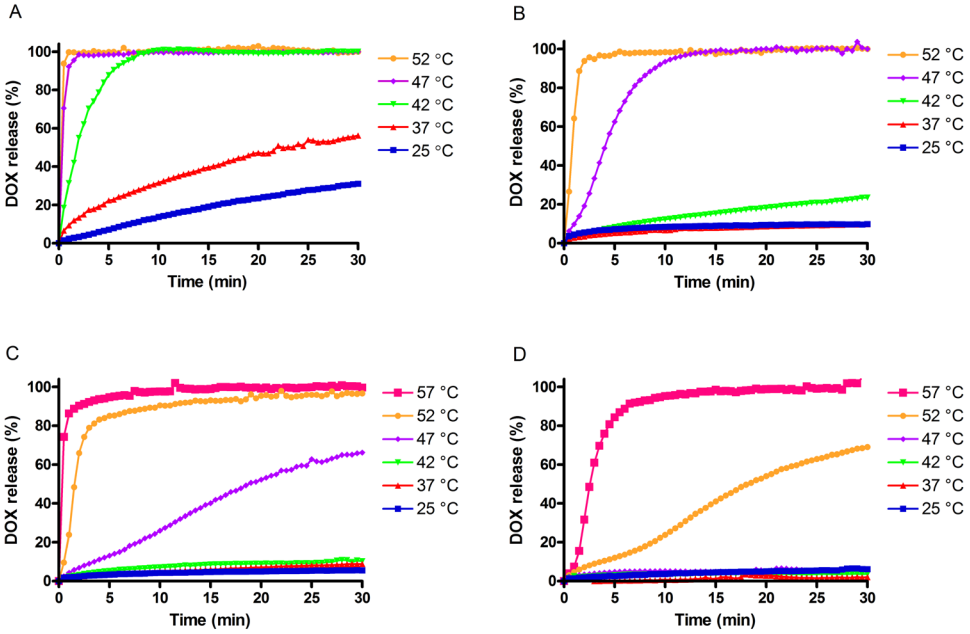

Fig. 4. Temperature triggered release of DOX from DOPE:EPC (70:25) liposomes coated with 5% chol-pHPMAlac having different CPs. (A) 11.5, (B) 19.0, (C) 25.0 and (D) 32.0 °C. The liposomes were dispersed in 20 mM HEPES pH 7.4.

Fig. 4 shows the DOX release profiles of liposomes grafted with chol-pHPMAlac with CPs ranging from 11.5 to 32.0 °C. The liposomes grafted with chol-pHPMAlac with a CP of 11.5 °C released 31 % of their DOX loading at 25 °C in 30 minutes, while complete release took place at 42 °C within 10 minutes (Fig. 4A).

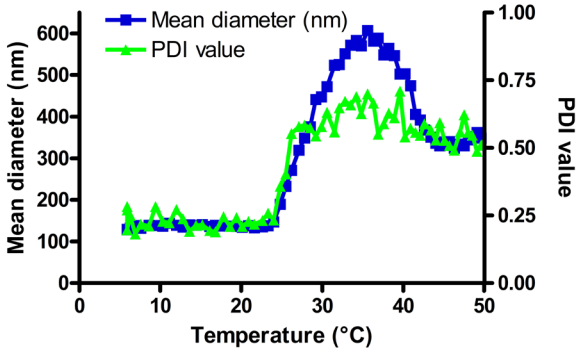

Fig. 5. Mean diameter and polydispersity index (PDI) of DOPE:EPC (molar ratio 70:25) liposomes coated with 5% chol-pHPMAlac with a CP of 11.5 °C and a M_n of 10.5 kDa upon incubation from 5 to 50 °C with a heating rate of 1 °C/min.

As can be seen in Fig. 5, liposomes grafted with chol-pHPMAlac (35:65, ML/DL) were stable till 25 °C as evidenced from a small particle size and low PDI. Above this temperature, the particle size and PDI increased significantly demonstrating that the particles aggregated. Chol-pHPMAlac dehydrates above the CP making the surface of the liposomes more hydrophobic, which in turn results in aggregation. The liposomes grafted with chol-pHPMAlac with a CP of 19.0 °C released less than 10% of the loading in 30 minutes at 37 °C, while complete release was observed in 10 minutes at 47 °C. The liposomes grafted with chol-pHPMAlac with a CP of 25.0 °C released ~ 70% of the loading within 30 minutes at 47 °C while the formulation with a CP of 32.0 °C was stable at this temperature but released 70% in 30 minutes at 52 °C (Fig. 4). Figure 6 summarizes the release of DOX from liposomes grafted with chol-pHPMAlac of different copolymer compositions after 5 minutes. The different formulations showed similar release profiles that only differ in onset temperature. The release-onset temperature followed the expected trend since an increase in CP resulted in an increase in release temperature. Remarkably, the release-onset temperature of the liposomes is about 20 °C higher than the CP of the polymer that is grafted on the surface. Apparently, the dehydration of the thermosensitive polymers is a gradual process, which starts at the CP. DOX present in the aqueous core of the liposomes is released approximately 20 °C above the CP, suggesting that the polymers will become sufficiently hydrophobic to penetrate into the lipid bilayer at this temperature. The gradual process of dehydration was shown previously for pHPMAlac polymers upon a temperature increase of hydrogels containing thermosensitive poly(*N*-(2-hydroxypropyl) methacrylamide lactate) A-blocks and a hydrophilic poly(ethylene glycol) B-block [68].

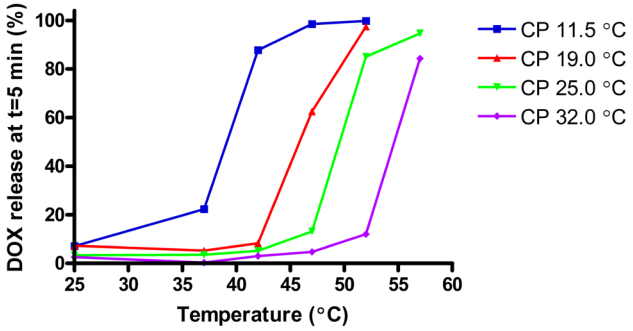

Fig. 6. DOX release after 5 minutes incubation in 20 mM HEPES of pH 7.4 at different temperatures from DOPE:EPC (70:25) liposomes coated with chol-pHPMAlac with CPs of 11.5 to 32.0 °C.

Liposomes were grafted with chol-pHPMAlac of different molecular weights to examine the influence of polymer chain length on the release kinetics. Chol-pHPMAlac (50:50 ML/DL) with a varying M_n of 6.5 to 14.5 kDa displayed a CP of 20.0 to 17.5 °C respectively (Table 1). All formulations showed only a minor amount of DOX release at 37 °C (Fig. 7). This figure also shows that liposomes coated with chol-pHPMAlac with a M_n of 6.5 kDa released 10% of the loading at 47 °C for 5 minutes, whereas at 52 °C this formulation released over 50% of its content in 5 minutes. Grafting liposomes with chol-pHPMAlac with a M_n of 10.0 kDa resulted

in a formulation that showed only a minor release at 42 °C but it showed complete release at 52 °C within 5 minutes. Liposomes grafted with chol-pHPMAlac with a M_n of 14.5 kDa had the lowest release-onset temperature and showed quantitative release of DOX in 5 minutes at 47 °C. Although a slight difference in CP was observed for these polymers, it is unlikely that this small difference in CP (2.5 °C) can explain the significant difference in release-onset temperature of these liposomes (~10 °C). Hence, the results indicate that upon dehydration, longer polymer chains more effectively destabilize the lipid bilayer, leading to release at lower temperatures.

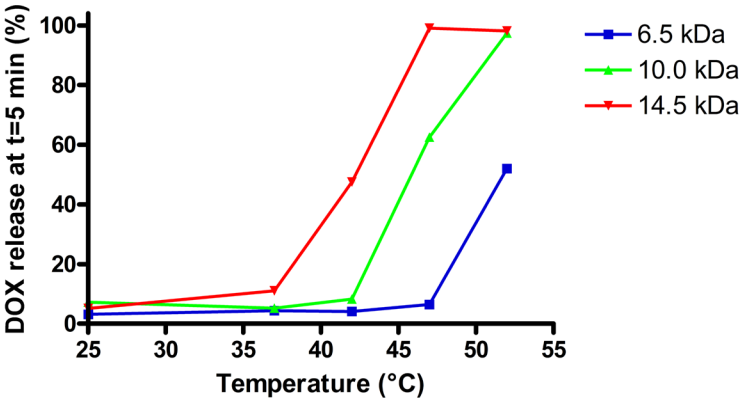

Fig. 7. DOX release from DOPE:EPC (70:25) liposomes coated with chol-pHPMAlac with M_n ranging from 6.5 - 14.5 kDa in 20 mM HEPES buffer pH 7.4.

Different amounts of chol-pHPMAlac with a fixed M_n of 10.0 kDa and a fixed copolymer composition (50:50, ML/DL, CP of polymer 19.0 °C) were grafted on the liposomal surface to evaluate the effect of polymer grafting density on the release kinetics at elevated temperatures. Liposomes with a grafting density of 2% showed already a moderate release at 25 °C and a substantial release of 33% in 5 minutes at 37 °C (Fig. 8). As mentioned DOPE:EPC liposomes without chol-pHPMAlac grafting were not stable and aggregated during preparation [66,67]. Likely this low polymer grafting density was not sufficient to stabilize the liposomes with this lipid composition. Liposomes grafted with 10% chol-pHPMAlac released 30% of the loading in 30 minutes at 37 °C and no steep increase in release was found upon increasing temperature (Fig. 8). Apparently, the grafting density of 10% is too high to obtain triggerable liposomes since no sharp increase in release was observed upon increasing the temperature. The most stable formulation at 37 °C (less than 10% release during 30 minutes incubation) with a fast release at 47 °C (> 90% during 10 minutes incubation) were liposomes grafted with 5% chol-pHPMAlac (50:50, ML/DL, 10.0 kDa).

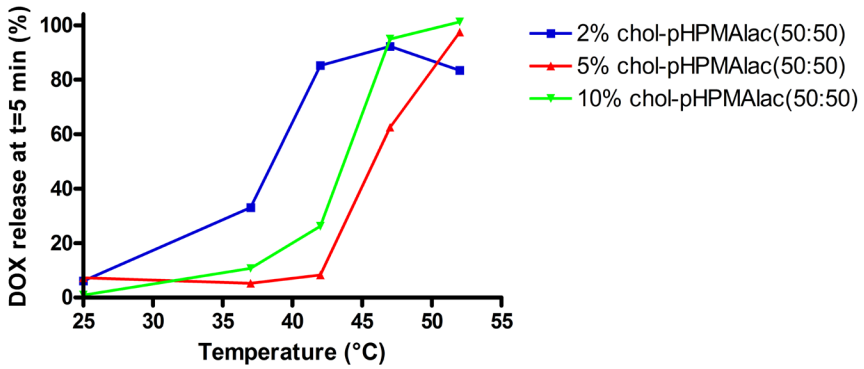

Fig. 8. DOX release from DOPE:EPC(70:25) liposomes with different grafting densities of chol-pHPMAlac (2, 5 and 10% in the feed ratio) in 20 mM HEPES pH 7.4.

To obtain a sequential DOX release upon heating, a liposomal mixture was prepared containing equal amounts of liposomes grafted with chol-pHPMAlac(50:50, ML/DL) and liposomes grafted with chol-pHPMAlac(80:20, ML/DL) in a 1:1 ratio (Fig. 4). This mixture was incubated first at 37 °C for 30 minutes followed by incubation for 30 minutes at 47 °C and finally for 30 minutes at 57 °C. Figure 9 shows that this mixture of liposomes released <10% in 30 minutes at 37 °C. After 30 minutes incubation at 47 °C, approximately 50% of the DOX was released corresponding to the full content release of the liposome grafted with chol-pHPMAlac(50:50, ML/DL) (Fig. 4B). When the sample was subsequently heated to 57 °C the total content was released within 3 minutes indicating that the liposomes grafted with chol-pHPMAlac(80:20, ML/DL) also released their content (Fig. 4D).

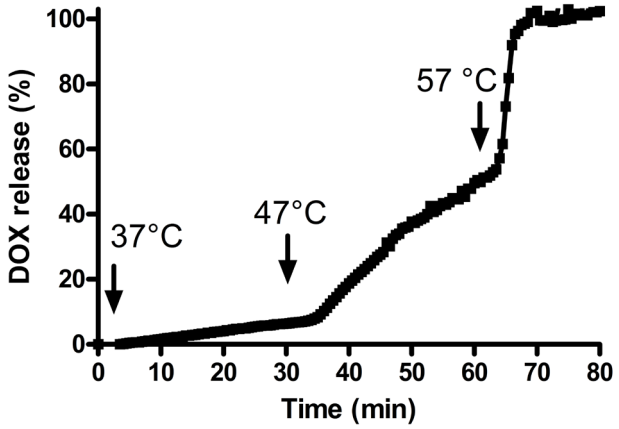

Fig. 9. DOX release from a 1:1 mixture of DOPE:EPC:chol-pHPMA(50:50, ML/DL) (CP: 19.0 °C, M_n: 10.0 kDa) with DOPE:EPC:chol-pHPMA(80:20, ML/DL) (CP: 32.0 °C, M_n: 11.0 kDa) in 20 mM HEPES pH 7.4. The release was measured for 30 minutes at 37 °C followed by incubation for 30 minutes at 47 and 57 °C, respectively.

To investigate the effect of a HIFU-induced temperature increase on the release of temperature sensitive liposomes, the above described DOX loaded liposomes grafted with 5% chol-pHPMAlac(50:50, ML/DL, 10 kDa) were exposed to pulsed wave-HIFU (PW-HIFU) of 20 W and a duty cycle of 20%. This exposure resulted in a temperature increase from 35 °C to 51 °C within 2 minutes, with a final temperature of 53 °C reached after 4 minutes exposure, after which the temperature remained constant during the experimental time frame. Fig 10 shows the DOX release from this liposome formulation as a function of HIFU exposure (0-30 minutes at 20W). When liposomes were exposed to HIFU, a maximum release of 69% was obtained after 5 minutes exposure and 83% release after 30 minutes. Since an increase in temperature to 53 °C was measured upon HIFU exposure, the DOX release of the liposomes can most likely be ascribed to the increase in temperature, although a mechanical effect cannot be excluded [22]. The liposomes that were not exposed to HIFU showed less than 20% release after 30 minutes incubation at 35 °C indicating that the DOX release is induced by the PW-HIFU and resulting heat exposure.

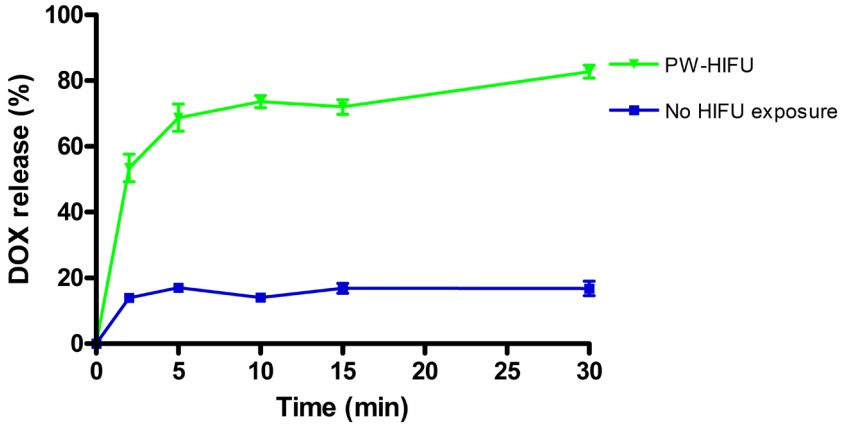

Fig. 10 DOX release from liposomes grafted with chol-pHPMAlac with a CP of 19.0 °C and a M_n of 10.0 kDa after exposure to PW-HIFU with an acoustic power of 20 W and a duty cycle of 20%. Control samples were not exposed to HIFU.

Conclusion

Thermosensitive HPMAmono/dilactate polymers with a cholesterol anchor and of different composition and molecular weight were grafted on the surface of liposomes to tune the release of doxorubicin by a temperature trigger. A straightforward relation between the cloud point (CP) of the polymers and the release-onset was found. A lower CP of the thermosensitive polymers resulted in a formulation that released their content at lower temperatures. The release of entrapped doxorubicin can also be tuned by varying the molecular weight of chol-pHPMAlac's and grafting density. The onset temperature of the release increased with decreasing molecular weight of the chol-pHPMAlac. Chol-pHPMAlac with a CP of 19.0 °C and a M_n of 10.0 kDa had the most attractive release characteristics since this formulation was stable at body temperature but released its content nearly quantitatively within 10 minutes during hyperthermia (47 °C).

Acknowledgement
Dr. Sander Langereis and prof. Dr. Holger Gruell from Philips Research Eindhoven are kindly acknowledged for their valuable input and discussions. This research was performed within the framework of CTMM, the Center for Translational Molecular Medicine (www.ctmm.nl), project HIFU-CHEM (grant 030-301).

References

1. Maeda H. Tumor-selective delivery of macromolecular drugs via the EPR effect: background and future prospects. Bioconjug Chem 2010;21:797-802.
2. Maeda H, Wu J, Sawa T, Matsumura Y, Hori K. Tumor vascular permeability and the EPR effect in macromolecular therapeutics: a review. J Control Release 2000;65:271-284.
3. Barenholz Y. Doxil(R)--the first FDA-approved nano-drug: lessons learned. J Control Release 2012;160:117-134.
4. Lammers T, Kiessling F, Hennink WE, Storm G. Drug targeting to tumors: principles, pitfalls and (pre-) clinical progress. J Control Release 2012;161:175-187.
5. Torchilin VP. Targeted pharmaceutical nanocarriers for cancer therapy and imaging. AAPS J 2007;9:E128-47.
6. Torchilin VP. Recent advances with liposomes as pharmaceutical carriers. Nat Rev Drug Discov 2005;4:145-160.
7. Svenson S. Clinical translation of nanomedicines. Curr Opin Solid State Mater Sci 2012;16:287-294.
8. O'Brien ME, Wigler N, Inbar M, Rosso R, Grischke E, Santoro A, et al. Reduced cardiotoxicity and comparable efficacy in a phase III trial of pegylated liposomal doxorubicin HCl (CAELYX/Doxil) versus conventional doxorubicin for first-line treatment of metastatic breast cancer. Ann Oncol 2004;15:440-449.
9. Harris L, Batist G, Belt R, Rovira D, Navari R, Azarnia N, et al. Liposome-encapsulated doxorubicin compared with conventional doxorubicin in a randomized multicenter trial as first-line therapy of metastatic breast carcinoma. Cancer 2002;94:25-36.
10. Lu T, Wang Z, Ma Y, Zhang Y, Chen T. Influence of polymer size, liposomal composition, surface charge, and temperature on the permeability of pH-sensitive liposomes containing lipid-anchored poly(2-ethylacrylic acid). Int J Nanomedicine 2012;7:4917-4926.
11. Banerjee S, Sen K, Pal TK, Guha SK. Poly(styrene-co-maleic acid)-based pH-sensitive liposomes mediate cytosolic delivery of drugs for enhanced cancer chemotherapy. Int J Pharm 2012;436:786-797.
12. Paasonen L, Laaksonen T, Johans C, Yliperttula M, Kontturi K, Urtti A. Gold nanoparticles enable selective light-induced contents release from liposomes. J Control Release 2007;122:86-93.
13. Mueller A, Bondurant B, O'Brien DF. Visible-Light-Stimulated Destabilization of PEG-Liposomes. Macromolecules 2000;33:4799-4804.
14. Evjen TJ, Nilssen EA, Barnert S, Schubert R, Brandl M, Fossheim SL. Ultrasound-mediated destabilization and drug release from liposomes comprising dioleoylphosphatidylethanolamine. Eur J Pharm Sci 2011;42:380-386.
15. Yan F, Li L, Deng Z, Jin Q, Chen J, Yang W, et al. Paclitaxel-liposome-microbubble complexes as ultrasound-triggered therapeutic drug delivery carriers. J Control Release 2013;166:246-255.
16. Gaber MH, Hong K, Huang SK, Papahadjopoulos D. Thermosensitive sterically stabilized liposomes: formulation and in vitro studies on mechanism of doxorubicin release by bovine serum and human plasma. Pharm Res 1995;12:1407-1416.
17. de Smet M, Langereis S, van den Bosch S, Grull H. Temperature-sensitive liposomes for doxorubicin delivery under MRI guidance. J Control Release 2010;143:120-127.

18. Karino T, Koga S, Maeta M. Experimental studies of the effects of local hyperthermia on blood flow, oxygen pressure and pH in tumors. Jpn J Surg 1988;18:276-283.
19. Gaber MH, Wu NZ, Hong K, Huang SK, Dewhirst MW, Papahadjopoulos D. Thermosensitive liposomes: extravasation and release of contents in tumor microvascular networks. Int J Radiat Oncol Biol Phys 1996;36:1177-1187.
20. Matteucci ML, Anyarambhatla G, Rosner G, Azuma C, Fisher PE, Dewhirst MW, et al. Hyperthermia increases accumulation of technetium-99m-labeled liposomes in feline sarcomas. Clin Cancer Res 2000;6:3748-3755.
21. Kong G, Braun RD, Dewhirst MW. Characterization of the effect of hyperthermia on nanoparticle extravasation from tumor vasculature. Cancer Res 2001;61:3027-3032.
22. Oerlemans C, Deckers R, Storm G, Hennink WE, Nijsen JF. Evidence for a new mechanism behind HIFU-triggered release from liposomes. J Control Release 2013;168:327-333.
23. de Smet M, Heijman E, Langereis S, Hijnen NM, Grull H. Magnetic resonance imaging of high intensity focused ultrasound mediated drug delivery from temperature-sensitive liposomes: an in vivo proof-of-concept study. J Control Release 2011;150:102-110.
24. Grull H, Langereis S. Hyperthermia-triggered drug delivery from temperature-sensitive liposomes using MRI-guided high intensity focused ultrasound. J Control Release 2012;161:317-327.
25. Deckers R, Paradissis A, Oerlemans C, Talelli M, Storm G, Hennink WE, et al. New insights into the HIFU-triggered release from polymeric micelles. Langmuir 2013;29:9483-9490.
26. Yatvin MB, Weinstein JN, Dennis WH, Blumenthal R. Design of liposomes for enhanced local release of drugs by hyperthermia. Science 1978;202:1290-1293.
27. Yatvin MB, Muhlensiepen H, Porschen W, Weinstein JN, Feinendegen LE. Selective delivery of liposome-associated cis-dichlorodiammineplatinum(II) by heat and its influence on tumor drug uptake and growth. Cancer Res 1981;41:1602-1607.
28. Anyarambhatla GR, Needham D. Enhancement of the phase transition permeability of DPPC liposomes by incorporation of MPPC: A new temperature-sensitive liposome for use with mild hyperthermia. J Liposome Res 1999;9:491-506.
29. Needham D, Anyarambhatla G, Kong G, Dewhirst MW. A new temperature-sensitive liposome for use with mild hyperthermia: characterization and testing in a human tumor xenograft model. Cancer Res 2000;60:1197-1201.
30. Kong G, Anyarambhatla G, Petros WP, Braun RD, Colvin OM, Needham D, et al. Efficacy of liposomes and hyperthermia in a human tumor xenograft model: importance of triggered drug release. Cancer Res 2000;60:6950-6957.
31. Mills JK, Needham D. Lysolipid incorporation in dipalmitoylphosphatidylcholine bilayer membranes enhances the ion permeability and drug release rates at the membrane phase transition. Biochim Biophys Acta 2005;1716:77-96.
32. Sandstrom MC, Ickenstein LM, Mayer LD, Edwards K. Effects of lipid segregation and lysolipid dissociation on drug release from thermosensitive liposomes. J Control Release 2005;107:131-142.
33. Winter ND, Murphy RK, O'Halloran TV, Schatz GC. Development and modeling of arsenic-trioxide-loaded thermosensitive liposomes for anticancer drug delivery. J Liposome Res 2011;21:106-115.
34. Negussie AH, Yarmolenko PS, Partanen A, Ranjan A, Jacobs G, Woods D, et al. Formulation and characterisation of magnetic resonance imageable thermally sensitive liposomes for use with magnetic resonance-guided high intensity focused ultrasound. Int J Hyperthermia 2011;27:140-155.
35. Mills JK, Needham D. The materials engineering of temperature-sensitive liposomes. Methods Enzymol 2004;387:82-113.
36. Lindner LH, Eichhorn ME, Eibl H, Teichert N, Schmitt-Sody M, Issels RD, et al. Novel temperature-sensitive liposomes with prolonged circulation time. Clin Cancer Res 2004;10:2168-2178.

37. Hossann M, Wiggenhorn M, Schwerdt A, Wachholz K, Teichert N, Eibl H, et al. In vitro stability and content release properties of phosphatidylglyceroglycerol containing thermosensitive liposomes. Biochim Biophys Acta 2007;1768:2491-2499.
38. Lindner LH, Hossann M, Vogeser M, Teichert N, Wachholz K, Eibl H, et al. Dual role of hexadecylphosphocholine (miltefosine) in thermosensitive liposomes: active ingredient and mediator of drug release. J Control Release 2008;125:112-120.
39. Tagami T, Ernsting MJ, Li SD. Efficient tumor regression by a single and low dose treatment with a novel and enhanced formulation of thermosensitive liposomal doxorubicin. J Control Release 2011;152:303-309.
40. Tagami T, Ernsting MJ, Li SD. Optimization of a novel and improved thermosensitive liposome formulated with DPPC and a Brij surfactant using a robust in vitro system. J Control Release 2011;154:290-297.
41. Tagami T, Foltz WD, Ernsting MJ, Lee CM, Tannock IF, May JP, et al. MRI monitoring of intratumoral drug delivery and prediction of the therapeutic effect with a multifunctional thermosensitive liposome. Biomaterials 2011;32:6570-6578.
42. Kono K. Thermosensitive polymer-modified liposomes. Adv Drug Deliv Rev 2001;53:307-319.
43. Kono K, Nakai R, Morimoto K, Takagishi T. Thermosensitive polymer-modified liposomes that release contents around physiological temperature. Biochim Biophys Acta 1999;1416:239-250.
44. Kono K, Henmi A, Yamashita H, Hayashi H, Takagishi T. Improvement of temperature-sensitivity of poly(N-isopropylacrylamide)-modified liposomes. J Control Release 1999;59:63-75.
45. Kono K, Ozawa T, Yoshida T, Ozaki F, Ishizaka Y, Maruyama K, et al. Highly temperature-sensitive liposomes based on a thermosensitive block copolymer for tumor-specific chemotherapy. Biomaterials 2010;31:7096-7105.
46. Kono K, Hayashi H, Takagishi T. Temperature-sensitive liposomes: liposomes bearing poly (N-isopropylacrylamide). J Control Release 1994;30:69-75.
47. Hayashi H, Kono K, Takagishi T. Temperature sensitization of liposomes using copolymers of N-isopropylacrylamide. Bioconjug Chem 1999;10:412-418.
48. Kono K, Murakami T, Yoshida T, Haba Y, Kanaoka S, Takagishi T, et al. Temperature sensitization of liposomes by use of thermosensitive block copolymers synthesized by living cationic polymerization: effect of copolymer chain length. Bioconjug Chem 2005;16:1367-1374.
49. Kono K, Nakashima S, Kokuryo D, Aoki I, Shimomoto H, Aoshima S, et al. Multi-functional liposomes having temperature-triggered release and magnetic resonance imaging for tumor-specific chemotherapy. Biomaterials 2011;32:1387-1395.
50. Shi Y, van Steenbergen MJ, Teunissen EA, Novo L, Gradmann S, Baldus M, et al. Pi-Pi stacking increases the stability and loading capacity of thermosensitive polymeric micelles for chemotherapeutic drugs. Biomacromolecules 2013;14:1826-1837.
51. Talelli M, Oliveira S, Rijcken CJ, Pieters EH, Etrych T, Ulbrich K, et al. Intrinsically active nanobody-modified polymeric micelles for tumor-targeted combination therapy. Biomaterials 2013;34:1255-1260.
52. Vermonden T, Jena SS, Barriet D, Censi R, van der Gucht J, Hennink WE, et al. Macromolecular diffusion in self-assembling biodegradable thermosensitive hydrogels. Macromolecules 2010;43:782-789.
53. Censi R, Vermonden T, Deschout H, Braeckmans K, di Martino P, De Smedt SC, et al. Photopolymerized thermosensitive poly(HPMAlactate)-PEG-based hydrogels: effect of network design on mechanical properties, degradation, and release behavior. Biomacromolecules 2010;11:2143-2151.
54. Paasonen L, Romberg B, Storm G, Yliperttula M, Urtti A, Hennink WE. Temperature-sensitive poly(N-(2-hydroxypropyl)methacrylamide mono/dilactate)-coated liposomes for triggered contents release. Bioconjug Chem 2007;18:2131-2136.

55. Neradovic D, van Steenbergen MJ, Vansteelant L, Meijer YJ, van Nostrum CF, Hennink WE. Degradation mechanism and kinetics of thermosensitive polyacrylamides containing lactic acid side chains. Macromolecules 2003;36:7491-7498.
56. Soga O, van Nostrum CF, Hennink WE. Poly(N-(2-hydroxypropyl) methacrylamide mono/di lactate): a new class of biodegradable polymers with tuneable thermosensitivity. Biomacromolecules 2004;5:818-821.
57. Mayer LD, Bally MB, Cullis PR. Uptake of adriamycin into large unilamellar vesicles in response to a pH gradient. Biochim Biophys Acta 1986;857:123-126.
58. Mayer LD, Tai LC, Bally MB, Mitilenes GN, Ginsberg RS, Cullis PR. Characterization of liposomal systems containing doxorubicin entrapped in response to pH gradients. Biochim Biophys Acta 1990;1025:143-151.
59. Rouser G, Fkeischer S, Yamamoto A. Two dimensional then layer chromatographic separation of polar lipids and determination of phospholipids by phosphorus analysis of spots. Lipids 1970;5:494-496.
60. Romberg B, Kettenes-van den, de Vringer T, Storm G, Hennink WE. 1H NMR spectroscopy as a tool for determining the composition of poly(hydroxyethyl-L-asparagine)-coated liposomes. Bioconjug Chem 2006;17:860-864.
61. Jansen J, Ghaffar A, van der Horst, T. N., Mihov G, van der Wal S, Feijen J, et al. Controlling the kinetic chain length of the crosslinks in photo-polymerized biodegradable networks. J Mater Sci Mater Med 2013;24:877-888.
62. Henríquez C, Bueno C, Lissi EA, Encinas MV. Thiols as chain transfer agents in free radical polymerization in aqueous solution. Polymer 2003;44:5559-5561.
63. Valdebenito A, Encinas MV. Thiophenols as chain transfer agents in the polymerization of vinyl monomers. Polymer 2005;46:10658-10662.
64. de Graaf AJ, Azevedo Prospero dos, Santos, II, Pieters EH, Rijkers DT, van Nostrum CF, Vermonden T, et al. A micelle-shedding thermosensitive hydrogel as sustained release formulation. J Control Release 2012;162:582-590.
65. de Graaf AJ, Boere KW, Kemmink J, Fokkink RG, van Nostrum CF, Rijkers DT, et al. Looped structure of flowerlike micelles revealed by 1H NMR relaxometry and light scattering. Langmuir 2011;27:9843-9848.
66. Ishida T, Kirchmeier MJ, Moase EH, Zalipsky S, Allen TM. Targeted delivery and triggered release of liposomal doxorubicin enhances cytotoxicity against human B lymphoma cells. Biochim Biophys Acta 2001;1515:144-158.
67. Allen TM, Hong K, Papahadjopoulos D. Membrane contact, fusion, and hexagonal (HII) transitions in phosphatidylethanolamine liposomes. Biochemistry; 1990;29:2976-2985.
68. Vermonden T, Besseling NAM, van Steenbergen MJ, Hennink WE. Rheological studies of thermosensitive triblock copolymer hydrogels. Langmuir 2006;22:10180-10184.

3

Safety evaluation of temperature-sensitive poly(*N*-(2-hydroxypropyl) methacrylamide mono/dilactate) grafted liposomes

Abstract

Background: Liposomes grafted with chol-pHPMAlac have been developed for temperature-triggered release of doxorubicin (DOX) in solid tumors. These liposomes release DOX completely during mild hyperthermia.
Aim: Liposomes can interact with blood proteins and various types of cells (e.g. endothelial cells, platelets and macrophages) after intravenous administration which can limit the deposition of the liposomes at the target site. Secondly, interaction of liposomes with blood platelets might result in platelet activation resulting in the formation of thrombi, which can occlude blood vessels. Therefore, it is important to get insight into the interaction between chol-pHPMAlac-grafted liposomes with cells and in particularly blood cells that come in contact with the liposomes after intravenous administration. The aim of this research is therefore to investigate DOX release kinetics as a function of temperature and composition, stability, *in vitro* uptake and cytotoxicity for cancer cells and somatic cells, and platelet activating potential of the liposomes.
Methods: DOX release was determined spectrofluorometrically. Liposome stability was determined in buffer and serum by nanoparticle tracking analysis. Association with/uptake by and toxicity of empty liposomes for AML-12, HepG2 (hepatocytes), RAW 264.7 (macrophages), and HUVEC (endothelial) cells was assayed *in vitro*. Platelet activation was determined by analysis of P-selectin expression and fibrinogen binding.
Results: DOPE:EPC liposomes (diameter = 135 nm) grafted with 5% chol-pHPMAlac (cloud point (CP) = 16 °C; M_n = 8.5 kDa) released less than 10% DOX at 37 °C in 30 minutes whereas complete release took place at 47 °C or higher in 10 minutes. The size of these liposomes remained stable in buffer and serum during 24 hours at 37 °C. Fluorescently labeled chol-pHPMAlac-liposomes without DOX loading exhibited poor association with/uptake by the used cells, were not cytotoxic, and did not activate platelets in buffer as well as in whole blood.
Conclusions: Overall, these results suggest that chol-pHPMAlac-grafted liposomes are not expected to be rapidly cleared from the circulation and most likely do not produce thromboembolic complications after injection. Therefore these liposomes are good candidates for temperature triggered DOX delivery to tumor stroma.

Introduction

Cancer is one of the most common causes of death in both economically developed countries and developing countries [1]. Worldwide, liver cancer is the fifth most frequently diagnosed cancer in men and the second most frequent cause of cancer death [1]. Nowadays, surgical resection is the primary curative therapy for patients with liver cancer. Unfortunately, only 20-35% of the patients are eligible for partial resection or liver transplantation and the recurrence rate is high [2-4]. Additionally, systemic chemotherapy is mostly ineffective for these patients because only low drug concentrations are obtained in the tumor, while the treatment results in severe adverse events and patient morbidity [5].

Nanosized drug delivery systems have been developed to improve the therapeutic efficacy and/or to reduce unwanted side effects of chemotherapeutic drugs. These delivery systems accumulate in tumors after intravenous injection via the enhanced permeability and retention (EPR) effect [6-8]. Liposomes are well-known examples of nanosized drug delivery systems, which can encapsulate e.g. cytostatic drugs in high concentrations [9-12]. However, liposomes are designed to exhibit a high stability in the circulation in order to prevent premature release of the drug before arrival at the tumor. Therefore, the release of these liposomes is slow and uncontrolled resulting in a relatively low free drug concentration in the tumor and as a consequence, cytotoxic free drug concentrations are not always reached in the tumor [13,14]. In order to increase the drug concentration in the tumor, liposomes have been developed that are capable of releasing drugs in response to a specific stimulus at the target site. Particularly, temperature triggered liposomal drug release systems have shown great opportunities to modulate and increase tumor drug concentrations. Hyperthermia is known to increase the blood flow and permeability of blood vessels [15], resulting in a more extensive liposome extravasation at the target site and thus higher drug concentrations at the site of action [16,17]. Thereby, it has been reported that chemotherapeutic drugs have a synergetic interaction with hyperthermia, leading to a stronger cytotoxic effect of the chemotherapeutic drug [13,18,19]. Temperature sensitive liposomes (TSL) have been shown to release their drug content rapidly at elevated temperatures [20-22]. Several studies have shown that rapid intravascular release of DOX from TSL leads to high intravascular drug concentrations, which subsequently enhances the drug penetration into the tumor tissue [13,20,23,24]. This approach led to a 20-30 times higher drug deposition in the tumor tissue compared to free drug administration and as a result improves antitumor efficacy [23,25].

Temperature sensitive *N*-(2-hydroxypropyl)methacrylamide mono/dilactate polymers show lower critical solution temperature (LCST) behavior meaning that they are soluble in an aqueous solution at a low temperature but dehydrate and aggregate when the polymers are heated above their cloud point (CP). Polymers of *N*-(2-hydroxypropyl)methacrylamide mono/dilactate were synthesized with a cholesterol anchor (chol-pHPMAlac) to facilitate their incorporation into liposomes and these liposomes grafted with chol-pHPMAlac released DOX quantitatively after mild hyperthermia [26]. However, the release profile of TSL is not the only factor determining the success of a formulation in a clinical setting. Liposomes can interact with blood proteins and various types of cells (e.g. endothelial cells, platelets and macrophages) after intravenous administration which can limit the deposition of the liposomes at the target

site. Secondly, interaction of liposomes with blood platelets might result in platelet activation resulting in the formation of thrombi, which can occlude blood vessels. Therefore, it is important to get insight into the interaction between chol-pHPMAlac-grafted liposomes with cells and in particularly blood cells that come in contact with the liposomes after intravenous administration.

The aim of this study was therefore to investigate DOX release kinetics as a function of temperature and composition, stability, *in vitro* cell association/uptake and cytotoxicity for cancer cells and somatic cells, and platelet activating potential of the liposomes.

Materials and methods

Materials

Thiocholesterol, *N,N*,-azobisisobutyronitrile (AIBN), Triton X-100 (TX-100), formaldehyde, sodium dodecyl sulfate (SDS), Dulbecco's modified eagle's medium (high glucose), fetal bovine serum, and antibiotic antimycotic solution (100x) were purchased from Sigma-Aldrich (St. Louis, MO). 1,2-Dioleoyl-*sn*-glycero-3-phosphoethanolamine (DOPE), 1,2-dipalmitoyl-*sn*-glycero-3-phosphocholine (DPPC), 3β-[*N*-(N',N'-dimethylaminoethane)-carbimoyl]cholesterol (DC-cholesterol), and L-α-phosphatidylethanolamine-*N*-(lissamine rhodamine B sulfonyl) (Rho-PE) were purchased from Avanti Polar Lipids (Alabaster, AL). Egg phosphocholine (EPC) and 1,2-distearoyl-*sn*-glycero-3-phosphoethanolamine-*N*-[amino(polyethylene glycol)] (DSPE-PEG, average polymer mass of 2,000 Da) were obtained from Lipoid (Ludwigshafen, Germany). Doxorubicin-HCl was obtained from Guanyu Bio-technology (Xi'an, China). EGM-2 kit + EBM medium and Human Umbilical Vein Endothelial cells (HUVECs) were purchased from Lonza (Basel, Switserland). RAW 264.7 and HepG2 cells were obtained from ATCC (Manassas, VA). AML-12 cells were a gift from R. Houtkooper (Academical medical center, Amsterdam). Lipofectamine 2000 was purchased from Invitrogen/Life Technologies (Carlsbad, CA). APC-conjugated mouse anti-human CD42b antibodies (clone HIP1) and PE-conjugated mouse anti-human P-selectin antibodies (clone AK-4) were obtained from BD Biosciences (Franklin Lakes, NJ). Polyclonal FITC-conjugated rabbit anti-human fibrinogen antibodies were purchased from Dako (Glostrup, Denmark). Thrombin receptor activator peptide 6 (TRAP-6) was obtained from Bachem (Bubendorf, Switzerland). 1,4-Dioxane was purchased from Biosolve (Valkenswaard, the Netherlands). All other chemicals were of analytical grade. Cell culture flasks, 96 well plates, cell scrapers, tubes and pipettes were purchased from Greiner Bio-One (Alphen aan den Rijn, The Netherlands).

Synthesis of HPMA mono/dilactate polymers with cholesterol anchor

2-Hydroxypropyl methacrylamide (HPMA), HPMA monolactate and HPMA dilactate were synthesized as described previously [27]. HPMA mono/dilactate polymers with a cholesterol anchor (chol-pHPMAlac) were synthesized according to a previously reported method [26,28]. Briefly, HPMA monolactate/dilactate (~8 mmol) were dissolved in distilled 1,4-dioxane at a concentration of 100 mg/mL and at monolactate:dilactate molar ratios of 50:50 or 100:0. The presence of dilactate in the polymer synthesized with HPMA monolactate only, can be explained by a dilactate contamination in the starting compounds, evidenced by ^{1}H-NMR measurements. AIBN was used as initiator at a molar ratio of 500:1 (monomer/AIBN). The molar ratio of thiocholesterol (chain transfer agent) and the HPMA monomers was 1:50. Three nitrogen/vacuum cycles were applied to remove oxygen and the polymerization reaction was performed for 24 hours at 70 °C. The obtained polymers were precipitated in diethyl ether and the supernatant was discarded after centrifugation (3,000 x g, 15 minutes at 4 °C). The polymers were dried overnight in a vacuum oven at 25 °C and stored at -20 °C until further use.

Polymer characterization

The copolymer composition of chol-pHPMAlac was determined by ^{1}H-NMR (Gemini 300 MHz spectrometer, Varian, Palo Alto, CA) in $(CD_3)_2SO$. The ratio of

HPMA monolactate/HPMA dilactate (ML/DL) was determined from the integral of the peak at 5.0 ppm (CO-C*H*(CH_3)-O) divided by the integral of the peaks at 4.1 and 4.2 ppm (CO-C*H*(CH_3)-OH).
The cloud point (CP) of chol-pHPMAlac was determined by light scattering at 650 nm (model UV-2450, Shimadzu Scientific Instruments, Kyoto, Japan). Chol-pHPMAlac was dissolved at 5 mg/mL in 120 mM ammonium acetate buffer, pH = 5.0. Samples were heated from 0 − 70 °C at a rate of 1 °C /min. The CP was defined as the temperature at which an increase in light scattering occurred.
The number average molecular weight (M_n) and weight average molecular weight (M_w) of chol-pHPMAlac were measured using gel permeation chromatography (GPC) using a refractive index detector, a Plgel 5 µm MIXED-D column, and PEGs with narrow molecular weights as standards. DMF containing 10 mM LiCl was used as eluent at an elution rate of 1.0 mL/min. The column temperature was maintained at 65 °C.

Preparation of doxorubicin-loaded liposomes
Three different liposomal formulations were prepared: temperature-sensitive polymer-coated liposomes composed of DOPE:EPC:chol-pHPMAlac(43-57) (70:25:5 molar ratio) and non-temperature sensitive formulations consisting of DOPE:EPC:chol-pHPMAlac(82-18) and DOPE:EPC:DSPE-PEG2000 (70:25:5). The phospholipids and chol-pHPMAlac were dissolved in 5 mL chloroform (15 µmol phospholipid/mL). A lipid film was formed after evaporation of chloroform under reduced pressure and the remaining traces of chloroform were removed overnight under a nitrogen flow. The lipid film was subsequently hydrated with 5 mL of 240 mM ammonium sulfate buffer (pH = 5.4) to a concentration of 15 µmol phospholipid/mL. The liposomal dispersion was extruded 2x through two 200-nm filters (GE water & process technologies, Trevose, PA) and 8x through two 100-nm filters (LIPEX extruder, Northern Lipids Inc, Burnaby, Canada). The extruded liposomes were dialyzed against 20 mM HEPES buffer, pH = 7.4, containing 8 g NaCl/L. The liposomes (3 mL) were loaded with doxorubicin (DOX, 5mg/mL, 1.5 mL) for 4 hours at 4 °C to obtain
self-quenching DOX concentrations in the liposomes [26]. Free DOX and free chol-pHPMAlac were removed by ultracentrifugation (125,000 x g for 45 minutes at 4 °C). The liposome-containing pellet was resuspended in 3 mL of 20 mM HEPES buffer, pH = 7.4, and stored at 4 °C in the dark.

Preparation of fluorescent liposomes for cell association studies
Empty liposomes labeled with Rho-PE (DOPE:EPC:chol-pHPMAlac(43-57)/chol-pHPMAlac(82-18)/DSPE-PEG2000:Rho-PE, 70:25:5:0.1) were prepared as described in section 2.4 with some modifications. The lipid film was hydrated with 5 mL phosphate buffered saline (PBS), and after extrusion the unbound chol-pHPMAlac was removed by ultracentrifugation (125,000 x g for 45 minutes at 4 °C). The liposomes were resuspended in 5 mL PBS and stored at 4 °C. Cationic liposomes consisting of DPPC:DC-cholesterol:cholesterol:Rho-PE, 70:25:5:0.1 (referred to as DC-cholesterol liposomes) were prepared as described by Broekgaarden *et al* [29] as a control formulation for the cellular association/uptake assays.

Liposome characterization
The size and the polydispersity index were measured with dynamic light scattering (DLS; CGS-3 multiangle goniometer, Malvern Instruments, Malvern, PA). Intensity correlation functions were measured using a wavelength of 632.8 nm, a scattering

angle of 90°, and unimodal analysis. The size of the liposomes was also determined by nanoparticle tracking analysis (NTA) using a NanoSight LM10SH with a 532-nm laser and an EMCDD camera (Malvern Instruments). Liposomes were incubated in PBS or fetal bovine serum (FBS) at 37 °C for 1 or 24 hours, after which the liposomes were diluted in PBS and measured for 60 seconds with a threshold of 4. The captured videos were analyzed with NTA 3.0 image analysis software (Malvern Instruments). The zeta potential (ζ potential) was determined in 20 mM HEPES buffer, pH = 7.4, by laser Doppler electrophoresis using a Zetasizer Nano-Z (Malvern Instruments).
The total DOX concentration was determined after solubilization of the liposomes with TX-100 (0.1% final concentration) [26] using fluorescence spectroscopy (λex = 485 nm ± 5 , λem = 600 ± 5 nm, FLUOstar Optima, BMG Labtech, Ortenberg, Germany). Concentrations were extrapolated from the linear fit function of the DOX standard curve.
The time-based release of DOX was measured by the change in fluorescence intensity in time (λex = 468 ± 5 nm, λem = 558 ± 5 nm, Fluorolog, Horiba Scientific, Edison, NJ). DOX-loaded liposomes (1 µL, 15 mM phospholipids) were added to 20 mM HEPES buffer (pH = 7.4, 1.6 mL) preheated to 37, 42, 47, 52 or 57 °C and the fluorescence intensity was measured in time. TX-100 (10%, 16 µL) was added at the end of the experiment to solubilize the liposomes to determine the total amount of DOX present. The percentage DOX release was calculated using the following equation: $(I_t - I_0) / (I_{TX} - I_0) \times 100\%$ in which I_t is the fluorescence intensity at time t, I_0 the intensity at the start of the experiment, and I_{TX} the fluorescence intensity after addition of TX-100.

Cell lines and culture conditions
Human umbilical vein endothelial cells (HUVECs) were cultured in EGM 2 plus EBM medium. Murine RAW 264.7 macrophages were cultured in DMEM high glucose medium. Mouse AML-12 hepatocytes and human hepatocellular carcinoma HepG2 cells were cultured in William's E medium supplemented with 10% L-glutamine. The culture media were supplemented with 10% FBS, penicillin (100 IU/mL), streptomycin (100 µg/mL), and amphotericin B (0.25 µg/mL, unless indicated otherwise). Cells were cultured at standard conditions (37 °C, 5% CO2, humidified atmosphere).

Cell association assays
For cell association studies, HUVECs, AML-12, HepG2, and RAW 264.7 cells were seeded in 96-wells plates at a density of 4.2×10^4 cells/well (90 µL, near confluence for HUVECs, HepG2, and RAW 264.7 cells, 60% confluence for AML-12 cells). After 4 hours, the cells were incubated with 10 µL prediluted Rho-labeled liposomes (section 2.5, 0-150 µM final phospholipid concentration which are clinically relevant) for 30 minutes or 24 hours at standard culture conditions. Cells were washed 2x with PBS and lysed with 20% methanol and 0.1% SDS in PBS. The fluorescence intensity of Rho was measured at λ_{ex} = 550 ± 5 nm, λ_{em} = 600 ± 5 nm (FLUOstar Optima, BMG Labtech, Ortenberg, Germany). Relative fluorescence intensities were plotted versus the concentration of the liposomes. Moreover, liposome uptake by/association with cells was visualized by fluorescence- and phase contrast microscopy (BZ-9000, Plan Fluor 20× objective, Keyence, Osaka, Japan). Cells were cultured and incubated with Rho-liposomes as described above, washed 2x with PBS after 30 minutes incubation, and imaged (Texas Red filter set, λ_{ex} = 562 ± 20 nm, λ_{em} = 624 ± 20 nm).

Cell viability assay

Cell viability was determined with the MTS assay (CellTiter 96, Promega, Madison, WI) following incubation with liposomes or lipofectamine (positive control). HUVECs, AML-12, HepG2, and RAW 264.7 cells were seeded in 96-wells plates at a density of 2×10^4 cells/well (100 µL). After 24-hour incubation (confluence of ~70%), the medium was refreshed (90 µL/well) and 10 µL of the liposomal suspension or PBS (control) was added to a final phospholipid concentration ranging from 0 – 150 µM. Cells were incubated with the liposomes for 24 hours. Hydrogen peroxide (H_2O_2, 10 µL, 30%) was added to several control wells to induce cell death. Subsequently, the medium was refreshed and 20 µL of CellTiter 96 was added per well. The plates were incubated at standard conditions for 4 hours after which absorbance was measured at 492 nm with a reference absorbance at 620 nm. The cell viability was calculated using the following equation: $(I_{sample} - I_{H2O2}) / (I_{PBS} - I_{H2O2}) \times 100\%$ in which I_{sample} is the absorbance of the sample incubated with liposomes, I_{H2O2} the absorbance after adding hydrogen peroxide, and I_{PBS} the absorbance of the cells incubated with PBS.

Liposome-induced platelet activation assays

Liposome-induced platelet activation was evaluated for isolated platelets and platelets in whole blood. Blood was withdrawn from healthy volunteers into citrate anticoagulation tubes. Platelets were isolated according to a previously described method [30,31]. Blood was centrifuged at 160 x g for 15 minutes at room temperature (RT) to obtain platelet rich plasma (PRP). Acid citrate dextrose (2.5% w/v trisodium citrate, 1.5% w/v citric acid, and 2% w/v D-glucose) was added to the PRP in a 1:10 ratio (v/v) to lower the pH to 6.5. PRP was centrifuged at 400 x g for 15 minutes at RT and the platelet pellet was resuspended in HEPES-buffered Tyrode's solution (HT; 145 mM NaCl, 5 mM KCL, 0.5 mM Na_2HPO_4, 1 mM $MgSO_4$, 5.55 mM D-glucose, and 10 mM HEPES, pH = 6.5). Prostacyclin was added at a final concentration of 10 ng/mL to inhibit platelet activation. The platelet suspension was centrifuged at 400 x g for 15 minutes at RT and the pellet was resuspended in HT buffer (pH = 7.3) to a concentration of 2×10^5 platelets/µL. The liposomes (150 µM final phospholipid concentration) were mixed with APC-anti-GP1B (25:1), FITC-anti-fibrinogen (25:1), and PE-anti-P-selectin (12.5:1). Thrombin receptor activator peptide 6 (TRAP-6, strong platelet activator [31]) was used as a positive control (208 µM final concentration). The mixtures were incubated at 37 °C for 30 minutes prior to use, after which 10 µL of isolated platelets or whole blood was added and incubated for 20 minutes at RT. The incubation was stopped by adding 700 µL fixation buffer (4% w/v formaldehyde and 137 mM NaCl in Milli-Q) to the samples. The fluorescence intensity of APC-anti-GP1B, FITC-anti-fibrinogen, and PE-anti-P-selectin was measured by flow cytometry (FACS Canto II apparatus, BD Bioscience, Franklin Lakes, NJ). Ten thousand events were collected in the platelet gate and data (mean fluorescence intensity, MFI) were analyzed with BD FACSDiva software (BD Bioscience, Franklin Lakes, NJ).

Statistical analysis

Statistical analysis was performed with the software GraphPad 4. A two-way ANOVA was performed followed by a Bonferroni posttest for statistical analysis of the liposome diameters after incubation in buffer and serum. A one-way ANOVA was performed followed by a Tukey test for statistical analysis of the liposomal association with/uptake by various celltypes.

Results and discussion

Polymer characterization

Chol-pHPMAlac(43-57) with a low CP (16 °C) was synthesized since we have shown previously that liposomes grafted with this polymer release their content at mild hyperthermia [26]. Chol-pHPMAlac(82-18) with a high CP (42 °C) was prepared as a control because liposomes grafted with this polymer are not expected to release their content at mild hyperthermia. The characteristics of the synthesized polymers are shown in Table 1.

Table 1. Characteristics of chol-pHPMAlac

Copolymer composition[a] (monolactate:dilactate) (mol/mol)	Yield	M_n[b] (kDa)	M_w[b] (kDa)	PDI[b]	CP[c]
43:57	64%	8.5	12.5	1.5	16 °C
82:18	84%	9.0	14.0	1.6	42 °C

[a] Determined by ^{1}H-NMR
[b] Determined by GPC
[c] Determined by light scattering at 650 nm

Liposome characterization and doxorubicin release characteristics

Liposomes were grafted with chol-pHPMAlac(43-57), chol-pHPMAlac(82-18), or DSPE-PEG2000 (non-temperature sensitive polymer) and the liposome characteristics are shown in Table 2. The size of liposomes grafted with chol-pHPMAlac(82-18) and DSPE-PEG2000 remained unchanged at 37 °C when heated from 10 to 60 °C at a heating rate of 1 °C/min, as evidenced by the unaltered particle size and PDI. Liposomes grafted with chol-pHPMAlac(43-57) aggregated at 37 °C as both size and the PDI increased ~ 5- and ~ 6-fold, respectively, at this temperature.
Chol-pHPMAlac(43-57) starts to dehydrate above its CP (16 °C), which renders the surface of the liposomes hydrophobic, that in turn results in aggregation.

Table 2. Characteristics of DOPE:EPC liposomes (molar ratio 70:25) grafted with 5 mol% temperature sensitive or non-temperature sensitive polymer.

	Chol-pHPMAlac(43-57)	Chol-pHPMAlac(82-18)	DSPE-PEG2000
Size (PBS)[a]	135 ± 1 nm	136 ± 1 nm	135 ± 3 nm
PDI (PBS)[a]	0.06 ± 0.01	0.08 ± 0.03	0.09 ± 0.08
Size (PDI) at 37 °C (PBS)[a]	656 nm (0.61)	135 nm (0.09)	138 nm (0.08)
ζ potential (20 mM HEPES, pH 7.4)[b]	-5 ± 4 mV	-4 ± 2 mV	-7 ± 1 mV
ζ potential (20 mM HEPES, pH7.4 + 0.8% NaCl)[b]	-0.3 ± 1.0 mV	1 ± 2 mV	-1 ± 2 mV

[a] Determined by DLS (at 37 °C measured during a heating run from 10 − 60 °C at a heating rate of 1 °C/min)
[b] Determined by laser Doppler electrophoresis

Liposomes grafted with chol-pHPMAlac(43-57) released less than 10% of DOX during 30-minute incubation at 37 °C. Conversely, at 42 °C DOX released at a rate of 1% per minute, whereas complete DOX release occurred within 10 minutes at temperatures of ≥ 47 °C (Figure 1A) showing that the release rate increased at higher temperatures. In line with expectations, liposomes consisting of DOPE (T_m = -16 °C [32]) and EPC grafted with chol-pHPMAlac(82-18) or DSPE-PEG2000 did not release DOX during 30-minute incubation at 37 − 57 °C (Figure 1B and C).

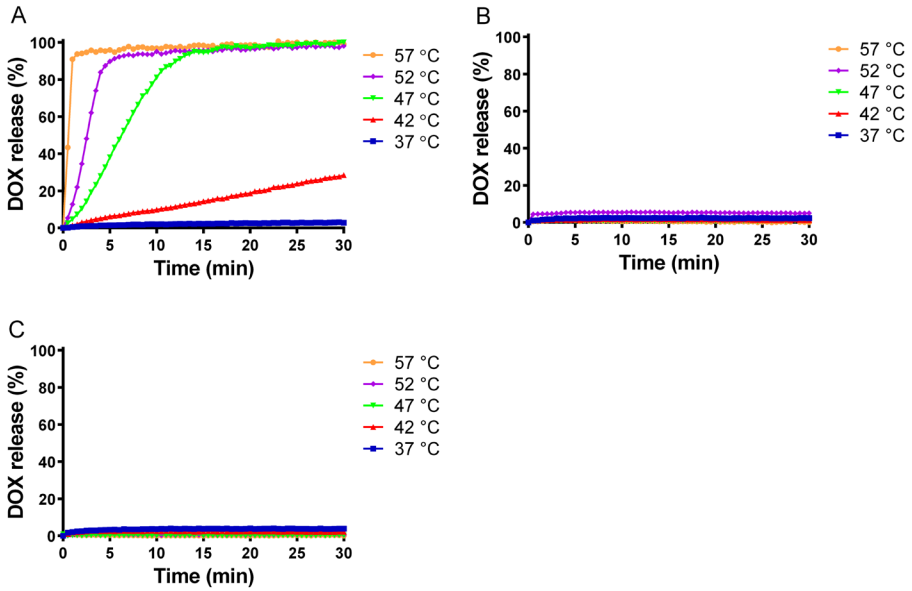

Figure 1. Temperature-triggered release of DOX from DOPE:EPC (70:25) liposomes grafted with 5% chol-pHPMAlac(43-57) (A), chol-pHPMAlac(82-18) (B), or DSPE-PEG2000 (C). Release was measured in a buffer composed of 20 mM HEPES, 0.8% NaCl, pH = 7.4 since DOX-loaded liposomes were prepared in this physiologically compatible buffer.

Liposome stability in buffer and serum

The stability of the liposomal formulations was evaluated in PBS and FBS at 37 °C during 1- and 24-hour incubation (i.e., quasi-physiological conditions) using NTA (Figure 2). No significant change in size was observed for all the liposomal formulations, demonstrating that the liposomes retained their integrity in a proteinaceous environment and did not aggregate. PEG is a hydrophilic polymer and forms a steric barrier around the liposomes that increases the colloidal stability of liposomes and reduces adsorption of proteins on their surface [33-36]. Chol-pHPMAlac is also hydrophilic at temperatures below the CP and is therefore expected to form a hydrophilic shell around the liposomes similar as PEG. Interestingly, chol-pHPMAlac(43-57) aggregated at 37 °C (DLS measurements; Table 2), while the size of the liposomes remained unchanged after incubation at 37 °C in buffer and FBS when measured with NTA. The chol-pHPMAlac(43-57) becomes hydrophobic above the CP, which results in aggregation of the liposomes. These (weak) interaction forces are reversible and may be disturbed during agitation of the liposomes during sample preparation for NTA, causing the size of the liposomes to remain unchanged after incubation at 37 °C. Since the sample preparation for DLS measurements is technically different, such

agitation effects do not arise during the DLS assays and the chol-pHPMAlac-grafted liposomes aggregate during the measurement. Furthermore, chol-pHPMAlac(43-57)-grafted liposomes exhibited no release of DOX at 37 °C, suggesting that the liposomes remained intact and therefore were not disrupted at this temperature.

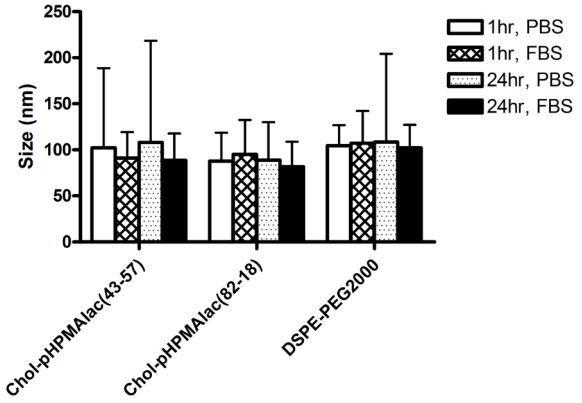

Figure 2. Size of DOPE:EPC:Rho-PE liposomes (70:25:0.1) grafted with 5 mol% polymer after incubation at 37 °C in PBS or FBS for 1 or 24 hours. Size was determined by NTA. *p<0.05.

Association between liposomes and cells

A major challenge for tumor-targeted drug delivery systems after intravenous injection is avoiding the uptake by circulating and resident leukocytes and other non-target cells such as endothelial cells that line the vasculature as well as parenchymal cells of detoxification organs such as the liver. The association between fluorescently labeled chol-pHPMAlac- and DSPE-PEG2000-grafted liposomes and cultured macrophages (RAW 264.7), HUVECs, and hepatocytes (AML-12) was therefore determined. Furthermore, human hepatocellular carcinoma (HepG2) cells were included in the analysis since the liposomes were designed for the treatment of liver cancer. Cationic liposomes containing the cationic lipid DC-cholesterol (DPPC:DC-cholesterol:cholesterol:Rho-PE, 70:25:5:0.1, Ø = 156 nm, PDI = 0.24, ζ potential = 67 ± 9 mV) were used as positive control. Liposomes were incubated with a maximum phospholipid concentration of 150 μM in these assays since this concentration is clinically relevant [37-40]. When these liposomes are loaded with DOX (2.5 mg/ml) and diluted to a phospholipid concentration of 150 μM, the DOX concentration in these assays will exceed the C_{max} of DOX after i.v. administration of Doxil [37-40].
Liposomes grafted with chol-pHPMAlac(43-57), chol-pHPMAlac(82-18), or DSPE-PEG2000 did not associate with cells after 30-minutes incubation (Figure 3). The absence of liposome-cell interactions is most likely attributable to the polymers grafted on the surface of the liposomes, which form a hydrophilic shield around the liposomes below the CP of chol-pHPMAlac, and the composition, small size, and near-neutral zeta potential of the liposomes, which are important determinants of uptake [41]. Contrastingly, DC-cholesterol liposomes associated with all types of cells in a lipid concentration-dependent manner. It has been reported previously that positively charged nanoparticles bind to the negative surface of cell membranes [42,43].

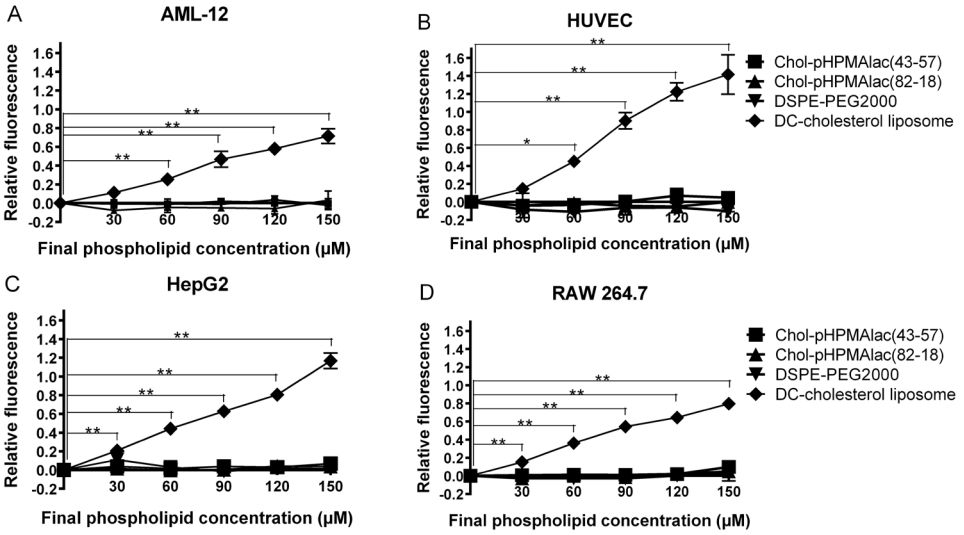

Figure 3. Association between fluorescently labeled DOPE:EPC:Rho-PE liposomes (molar ratio 70:25:0.1) grafted with 5% chol-pHPMAlac(43-47), chol-pHPMAlac(82-18), or DSPE-PEG2000 and DC-cholesterol liposomes by AML-12 (A), HUVECs (B), HepG2 (C) and RAW 264.7 cells (D) after 30-minute incubation at standard culture conditions. The degree of association is proportional to the fluorescence intensity of cells. *p<0.01, **p<0.001.

Liposome-cell interactions were also visualized by fluorescence microscopy, which corroborated that there was no association between cells and liposomes grafted with chol-pHPMAlac and DSPE-PEG2000, while a strong interaction was observed between DC-cholesterol liposomes and all types of cells (Figure 4 and Supplementary Figure 1).

Finally, liposome-cell interactions were determined after 24-hour incubation with liposomes, which is a more relevant time frame because chol-pHPMAlac-grafted liposomes are expected to undergo relatively slow elimination from the circulation (comparable to PEGylated liposomes) and reside in the tumor for an extended period of time. Liposomes grafted with chol-pHPMAlac(43-57), chol-pHPMAlac(82-18), or DSPE-PEG2000 exhibited only a marginal increase in cell association when incubated for 24 hours compared to 30-minute incubation (Figure 5 and Supplementary Figure 2). In contrast, DC-cholesterol liposomes exhibited a profound increase in cell association following 24-hour incubation versus 30-minute incubation (Figure 3). Taken altogether, liposomes grafted with chol-pHPMAlac showed no notable association with macrophages, endothelial cells, hepatocytes, and hepatocellular carcinoma cells. These liposomes are therefore not likely to be taken up directly after intravenous administration, which improves the probability that the liposomes reach the target site (tumor tissue) after systemic administration, where the chemotherapeutic payload can be released locally upon the induction of mild hyperthermia.

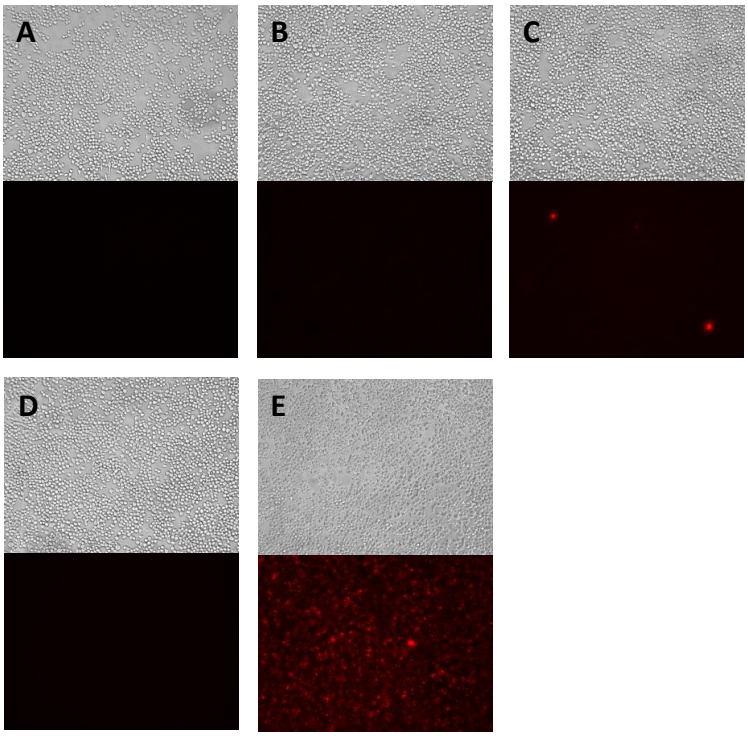

Figure 4. Phase contrast microscopy images (top row) and corresponding fluorescence microscopy images (bottom row) of RAW 264.7 cells incubated for 30 minutes at standard culture conditions without liposomes (A) or with fluorescently labeled liposomes grafted with 5% chol-pHPMAlac(43-57) (B), chol-pHPMAlac(82-18) (C), or DSPE-PEG2000 (D) or DC-cholesterol liposomes (150 μM final lipid concentration). The degree of association is proportional to the fluorescence intensity of cells.

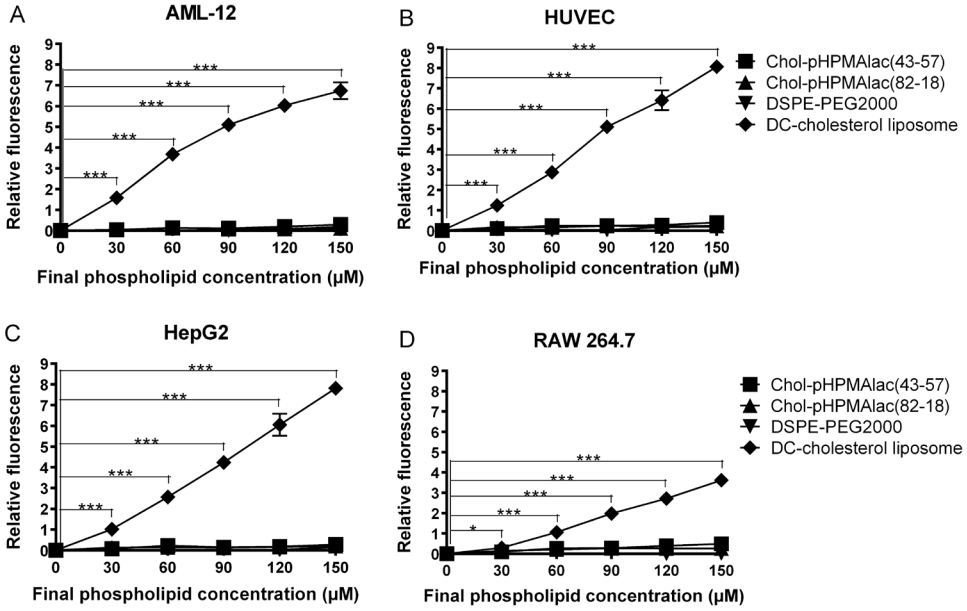

Figure 5. Association between fluorescently labeled DOPE:EPC:Rho-PE liposomes (70:25:0.1) grafted with 5% chol-pHPMAlac(43-47), chol-pHPMAlac(82-18), or DSPE-PEG2000 and DC-cholesterol liposomes and AML-12 (A), HUVEC (B), HepG2 (C), and RAW 264.7 cells (D) after 24-hour incubation at standard culture conditions. The degree of association is proportional to the fluorescence intensity of cells. *p<0.05, **p<0.01, ***p<0.001

Cytotoxicity of liposomal formulations

Chol-pHPMAlac-grafted liposomes are not associated to or taken up by various cell-types, therefore these liposomes most likely do not induce cytotoxicity. To confirm this hypothesis, the cytotoxicity of the liposomal formulations was determined by incubating cells with the different liposomal formulations and assaying viability at 24 hours with the MTS assay. Lipofectamine 2000 was used as control since this liposomal formulation is cytotoxic [44]. The MTS assay revealed that liposomes grafted with chol-pHPMAlac or DSPE-PEG2000 had a minimal-to-negligible effect on cell viability up to a lipid concentration of 150 μM. The cell viability decreased to < 20% when lipofectamine was incubated with the cells at concentrations of ≥ 90 μM. Since the phospholipid concentration will not exceed 150 μM after infusion into patients (based on the DOX concentration loaded into these liposomes and the C_{max} achieved in patients after administration of Doxil [37-40]) it is not expected that these liposomes will induce toxicity after i.v. administration.

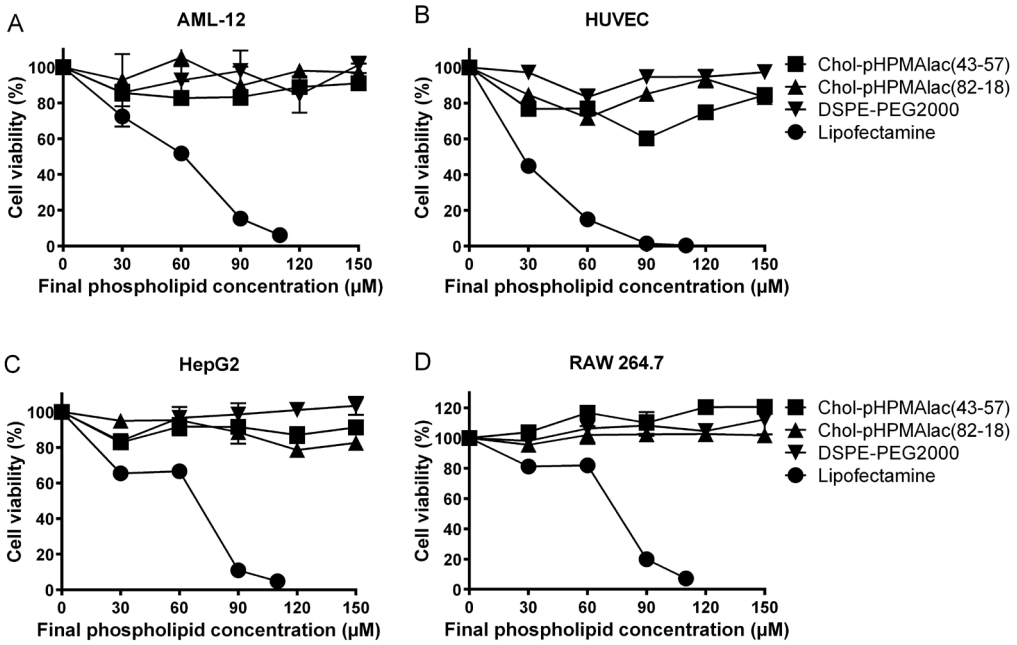

Figure 6. Viability of AML-12 (A), HUVEC (B), HepG2 (C), and RAW264.7 cells (D) after 24-hour incubation with DOPE:EPC liposomes grafted with 5% chol-pHPMAlac(43-57), chol-pHPMAlac(82-18), or DSPE-PEG2000 or lipofectamine.

Platelet activation

Platelets play an important role in hemostasis. Upon vascular injury, platelets become activated and release fibrinogen from the α-granules. The released fibrinogen binds to integrin αIIbβ3 on the activated platelets and forms crosslinks between adjacent platelets, leading to platelet aggregation and fortification of the platelet plug [45-47]. In addition, P-selectin (CD62P) translocates to the membrane outer surface upon activation and stabilizes the interplatelet fibrinogen bridges. Moreover, P-selectin mediates the tethering and accumulation of platelets at the site of injury [48,49]. The density of fibrinogen and P-selectin on the surface of the platelets is a good indicator for platelet activation. Accordingly, platelet activation was assessed in the context of our liposomal formulations to ensure that the liposomes do not induce platelet activation and corollary thromboembolic complications following systemic administration. Thrombin receptor activating peptide (TRAP-6) was used as positive control since TRAP-6 activates αIIbβ3 receptors and induces P-selectin expression. Liposomes grafted with chol-pHPMAlac or DSPE-PEG2000 did not induce the expression of P-selectin and the binding of fibrinogen on isolated platelets after 20-minutes incubation (Figure 7A-B).

Activation of platelets was also determined in whole blood, which better mimics the *in vivo* situation compared to isolated platelets and is therefore more clinically relevant. The extent of fibrinogen binding and P-selectin activation remained unaltered following incubation of whole blood with chol-pHPMAlac- and DSPE-PEG2000-grafted liposomes, confirming that the liposomes do not activate platelets (Fig 7C-D) and therefore pose no threat to the hemostatic checks and balances system as far as primary hemostasis is concerned.

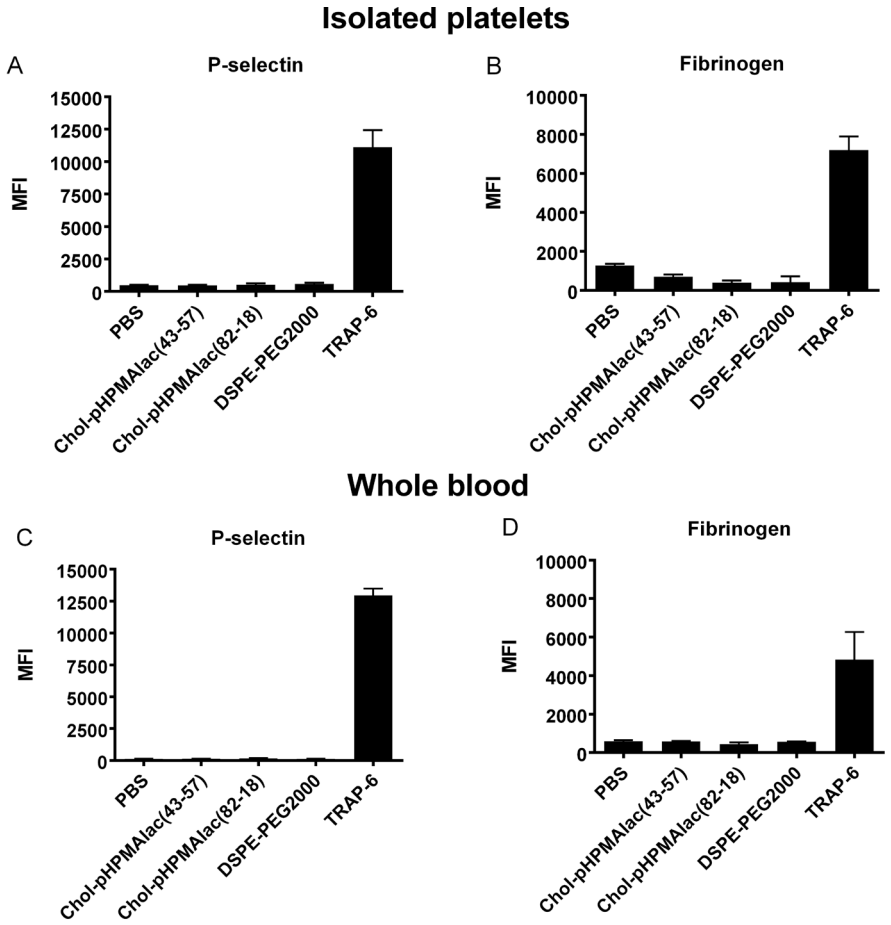

Figure 7. Platelet activation by liposomes grafted with chol-pHPMAlac(43-57), chol-pHPMAlac(82-18), or DSPE-PEG2000 in isolated platelets (A-B) and whole blood (C-D). The mean fluorescence intensity (MFI) is proportional to the degree of P-selectin expression (A+C) and fibrinogen binding (B+D). TRAP-6 was used as positive control and represents complete platelet activation.

Conclusions

The objective of this study was to get insight into the interaction between chol-pHPMAlac-grafted liposomes with blood cells and other cells with which the liposomes may interact after intravenous administration. The chol-pHPMAlac-grafted liposomes exhibited negligible association with macrophages, hepatocytes, and endothelial cells and, as a result, were non-toxic for these cells.

Moreover, chol-pHPMAlac-grafted liposomes did not induce platelet activation. Overall, these results suggest that chol-pHPMAlac-grafted liposomes are not expected to be rapidly cleared from the circulation and most likely do not produce thromboembolic complications after injection. Consequently, liposomes grafted with chol-pHPMAlac constitute a promising drug delivery system for intratumoral DOX delivery and local temperature-triggered release.

Acknowledgements
This research was performed within the framework of CTMM, the Center for Translational Molecular Medicine (www.ctmm.nl), project HIFU-CHEM (grant 030-301). This research was also supported by grants from the Dutch Anti-Cancer Foundation (Stichting Nationaal Fonds Tegen Kanker) in Amsterdam and the Phospholipid Research Center in Heidelberg. Riekelt Houtkooper is kindly acknowledged for providing the AML-12 cells.

References

1. Jemal A, Bray F, Center MM, Ferlay J, Ward E, Forman D. Global cancer statistics. CA Cancer J Clin 2011;61:69-90.
2. Imai N, Ishigami M, Ishizu Y, Kuzuya T, Honda T, Hayashi K, et al. Transarterial chemoembolization for hepatocellular carcinoma: A review of techniques. World J Hepatol 2014;6:844-850.
3. Kamangar F, Dores GM, Anderson WF. Patterns of cancer incidence, mortality, and prevalence across five continents: defining priorities to reduce cancer disparities in different geographic regions of the world. J Clin Oncol 2006;24:2137-2150.
4. Nicolini A, Crespi S, Martinetti L. Drug delivery embolization systems: a physician's perspective. Expert Opin Drug Deliv 2011;8:1071-1084.
5. Liapi E, Lee K, Georgiades CC, Hong K, Geschwind JH. Drug-eluting particles for interventional pharmacology. Tech Vasc Interv Radiol 2007;10:261-269.
6. Barenholz Y. Doxil(R)--the first FDA-approved nano-drug: lessons learned. J Control Release 2012;160:117-134.
7. Maeda H. Tumor-selective delivery of macromolecular drugs via the EPR effect: background and future prospects. Bioconjug Chem 2010;21:797-802.
8. Maeda H, Wu J, Sawa T, Matsumura Y, Hori K. Tumor vascular permeability and the EPR effect in macromolecular therapeutics: a review. J Control Release 2000;65:271-284.
9. Lammers T, Kiessling F, Hennink WE, Storm G. Drug targeting to tumors: principles, pitfalls and (pre-) clinical progress. J Control Release 2012;161:175-187.
10. der Valk FM, van Wijk DF, Lobatto ME, Verberne HJ, Storm G, Willems MC, et al. Prednisolone-containing liposomes accumulate in human atherosclerotic macrophages upon intravenous administration. Nanomedicine 2015.
11. Kastner E, Verma V, Lowry D, Perrie Y. Microfluidic-controlled manufacture of liposomes for the solubilisation of a poorly water soluble drug. Int J Pharm 2015;485:122-130.
12. Grüll H, Langereis S. Hyperthermia-triggered drug delivery from temperature-sensitive liposomes using MRI-guided high intensity focused ultrasound. J Control Release 2012;161:317-327.
13. Landon CD, Park JY, Needham D, Dewhirst MW. Nanoscale drug delivery and hyperthermia: The materials design and preclinical and clinical testing of low temperature-sensitive liposomes used in combination with mild hyperthermia in the treatment of local cancer. Open Nanomed J 2011;3:38-64.
14. Bandak S, Goren D, Horowitz A, Tzemach D, Gabizon A. Pharmacological studies of cisplatin encapsulated in long-circulating liposomes in mouse tumor models. Anticancer Drugs 1999;10:911-920.
15. Gaber MH, Wu NZ, Hong K, Huang SK, Dewhirst MW, Papahadjopoulos D. Thermosensitive liposomes: Extravasation and release of contents in tumor microvascular networks. Int J Radiat Oncol Biol Phys 1996;36:1177-1187.
16. Matteucci ML, Anyarambhatla G, Rosner G, Azuma C, Fisher PE, Dewhirst MW, et al. Hyperthermia increases accumulation of technetium-99m-labeled liposomes in feline sarcomas. Clin Cancer Res 2000;6:3748-3755.

17. Kong G, Braun RD, Dewhirst MW. Characterization of the effect of hyperthermia on nanoparticle extravasation from tumor vasculature. Cancer Res 2001;61:3027-3032.
18. Hahn GM, Braun J, Har-Kedar I. Thermochemotherapy: synergism between hyperthermia (42-43 degrees) and adriamycin (of bleomycin) in mammalian cell inactivation. Proc Natl Acad Sci U S A 1975;72:937-940.
19. Herman TS. Temperature dependence of adriamycin, cis-diamminedichloroplatinum, bleomycin, and 1,3-bis(2-chloroethyl)-1-nitrosourea cytotoxicity in vitro. Cancer Res 1983;43:517-520.
20. Needham D, Anyarambhatla G, Kong G, Dewhirst MW. A new temperature-sensitive liposome for use with mild hyperthermia: characterization and testing in a human tumor xenograft model. Cancer Res 2000;60:1197-1201.
21. Tagami T, May JP, Ernsting MJ, Li S. A thermosensitive liposome prepared with a Cu2+ gradient demonstrates improved pharmacokinetics, drug delivery and antitumor efficacy. J Control Release 2012;161:142-149.
22. Limmer S, Hahn J, Schmidt R, Wachholz K, Zengerle A, Lechner K, et al. Gemcitabine treatment of rat soft tissue sarcoma with phosphatidyldiglycerol-based thermosensitive liposomes. Pharm Res 2014;31:2276-2286.
23. Kong G, Anyarambhatla G, Petros WP, Braun RD, Colvin OM, Needham D, et al. Efficacy of liposomes and hyperthermia in a human tumor xenograft model: importance of triggered drug release. Cancer Res 2000;60:6950-6957.
24. Manzoor AA, Lindner LH, Landon CD, Park J, Simnick AJ, Dreher MR, et al. Overcoming limitations in nanoparticle drug delivery: Triggered, intravascular release to improve drug penetration into tumors. Cancer Res 2012;72:5566-5575.
25. Yarmolenko PS, Zhao Y, Landon C, Spasojevic I, Yuan F, Needham D, et al. Comparative effects of thermosensitive doxorubicin-containing liposomes and hyperthermia in human and murine tumours. Int J Hyperthermia 2010;26:485-498.
26. van Elk M, Deckers R, Oerlemans C, Shi Y, Storm G, Vermonden T, et al. Triggered release of doxorubicin from temperature-sensitive poly(N-(2-hydroxypropyl)-methacrylamide mono/dilactate) grafted liposomes. Biomacromolecules 2014;15:1002-1009.
27. Neradovic D, van Steenbergen MJ, Vansteelant L, Meijer YJ, van Nostrum CF, Hennink WE. Degradation mechanism and kinetics of thermosensitive polyacrylamides containing lactic acid side chains. Macromolecules 2003;36:7491-7498.
28. Paasonen L, Romberg B, Storm G, Yliperttula M, Urtti A, Hennink WE. Temperature-sensitive poly(N-(2-hydroxypropyl)methacrylamide mono/dilactate)-coated liposomes for triggered contents release. Bioconjug Chem 2007;18:2131-2136.
29. Broekgaarden M, de Kroon AL, van Gulik TM, Heger M. Development and in vitro proof-of-concept of interstitially targeted zinc-phthalocyanine liposomes for photodynamic therapy. Curr Med Chem 2014;21:377-391.
30. Korporaal SJ, Van Eck M, Adelmeijer J, Ijsseldijk M, Out R, Lisman T, et al. Platelet activation by oxidized low density lipoprotein is mediated by CD36 and scavenger receptor-A. Arterioscler Thromb Vasc Biol 2007;27:2476-2483.
31. Yousefi A, Lauwers M, Nemes R, van Holten T, Babae N, Roest M, et al. Hemocompatibility assessment of two siRNA nanocarrier formulations. Pharm Res 2014;31:3127-3135.
32.http://avantilipids.com/index.php?option=com_content&view=article&id=565&Itemid=228&catnumber=850725. ;accessed May 2015.
33. Allen TM, Hansen C, Martin F, Redemann C, Yau-Young A. Liposomes containing synthetic lipid derivatives of poly(ethylene glycol) show prolonged circulation half-lives in vivo. Biochim Biophys Acta 1991;1066:29-36.

34. Gabizon A, Catane R, Uziely B, Kaufman B, Safra T, Cohen R, et al. Prolonged circulation time and enhanced accumulation in malignant exudates of doxorubicin encapsulated in polyethylene-glycol coated liposomes. Cancer Res 1994;54:987-992.
35. Torchilin VP, Omelyanenko VG, Papisov MI, Bogdanov Jr. AA, Trubetskoy VS, Herron JN, et al. Poly(ethylene glycol) on the liposome surface: on the mechanism of polymer-coated liposome longevity. Biochim Biophys Acta 1994;1195:11-20.
36. Lasic DD, Martin FJ, Gabizon A, Huang SK, Papahadjopoulos D. Sterically stabilized liposomes: a hypothesis on the molecular origin of the extended circulation times. Biochim Biophys Acta 1991;1070:187-192.
37. Lyass O, Uziely B, Ben-Yosef R, Tzemach D, Heshing NI, Lotem M, et al. Correlation of toxicity with pharmacokinetics of pegylated liposomal doxorubicin (Doxil) in metastatic breast carcinoma. Cancer 2000;89:1037-1047.
38. Gabizon A, Shmeeda H, Barenholz Y. Pharmacokinetics of pegylated liposomal doxorubicin. Clin Pharmacokinet 2003;42:419-436.
39. Mross K, Niemann B, Massing U, Drevs J, Unger C, Bhamra R, et al. Pharmacokinetics of liposomal doxorubicin (TLC-D99; Myocet) in patients with solid tumors: an open-label, single-dose study. Cancer Chemother Pharmacol 2004;54:514-524.
40. Amantea MA, Forrest A, Northfelt DW, Mamelok R. Population pharmacokinetics and pharmacodynamics of pegylated-liposomal doxorubicin in patients with AIDS-related Kaposi's sarcoma. Clin Pharmacol Ther 1997;61:301-311.
41. Dan N. Effect of liposome charge and PEG polymer layer thickness on cell–liposome electrostatic interactions. Biochim Biophys Acta 2002;1564:343-348.
42. Yu B, Zhang Y, Zheng W, Fan C, Chen T. Positive surface charge enhances selective cellular uptake and anticancer efficacy of selenium nanoparticles. Inorg Chem 2012;51:8956-8963.
43. He C, Hu Y, Yin L, Tang C, Yin C. Effects of particle size and surface charge on cellular uptake and biodistribution of polymeric nanoparticles. Biomaterials 2010;31:3657-3666.
44. Jain S, Kumar S, Agrawal AK, Thanki K, Banerjee UC. Enhanced transfection efficiency and reduced cytotoxicity of novel lipid-polymer hybrid nanoplexes. Mol Pharm 2013;10:2416-2425.
45. Broos K, De Meyer SF, Feys HB, Vanhoorelbeke K, Deckmyn H. Blood platelet biochemistry. Thromb Res 2012;129:245-249.
46. Nieswandt B, Varga-Szabo D, Elvers M. Integrins in platelet activation. J Thromb Haemost 2009;7:206-209.
47. Broos K, Feys HB, De Meyer SF, Vanhoorelbeke K, Deckmyn H. Platelets at work in primary hemostasis. Blood Rev 2011;25:155-167.
48. Armstrong PC, Peter K. GPIIb/IIIa inhibitors: from bench to bedside and back to bench again. Thromb Haemost 2012;107:808-814.
49. Merten M, Thiagarajan P. P-selectin expression on platelets determines size and stability of platelet aggregates. Circulation 2000;102:1931-1936.

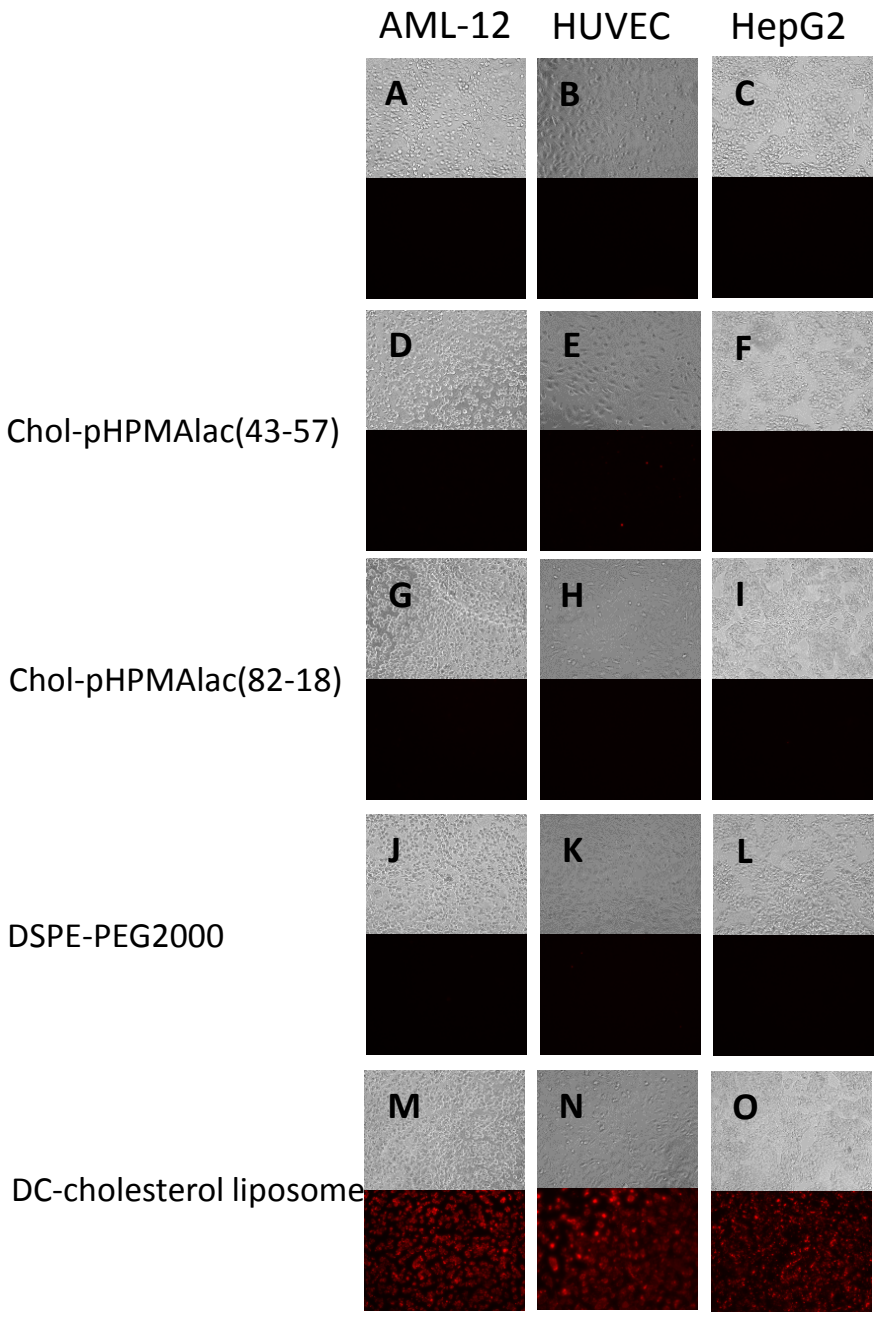

Supplementary Figure 1. Phase contrast microscopy images (top row) and corresponding fluorescence microscopy images (bottom row) of AML-12 (A,D,G,J,M), HUVEC (B,E,HK,N), and HepG2 cells (C,F,I,L,O) incubated with fluorescently labeled DOPE:EPC:Rho-PE liposomes (70:25:0.1) grafted with 5% chol-pHPMAlac(43-47) (D-F), chol-pHPMAlac(82-18) (G-H), or DSPE-PEG2000 (J-L) and DC-cholesterol liposomes (M-O) (150 μM final lipid concentration) for 30 minutes at standard culture conditions. The degree of association is proportional to the fluorescence intensity of cells.

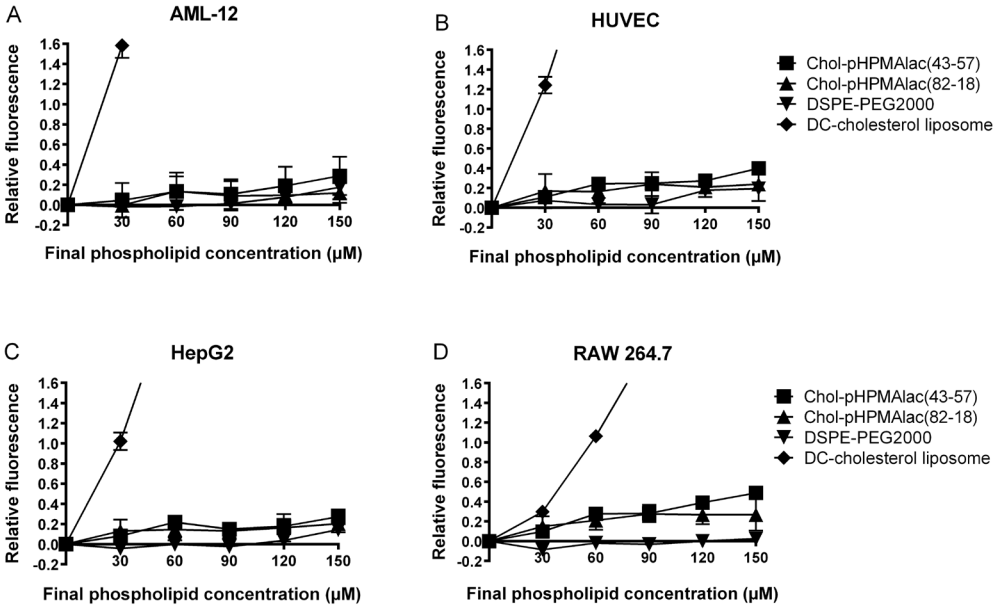

Supplementary Figure 2. Association between fluorescently labeled DOPE:EPC:Rho-PE liposomes (70:25:0.1) grafted with 5% chol-pHPMAlac(43-47), chol-pHPMAlac(82-18), or DSPE-PEG2000 and DC-cholesterol liposomes and AML-12 (A), HUVEC (B), HepG2 (C), and RAW 264.7 cells (D) after 24-hour incubation at standard culture conditions. The degree of association is proportional to the fluorescence intensity of cells.

4

Modulating the stability and drug release characteristics of temperature-sensitive liposomes through PEGylation

Abstract

N-(2-hydroxypropyl)-methacrylamide mono/dilactate polymers display temperature sensitive characteristics and copolymers based on HPMAlac have been investigated as drug delivery systems. In Chapter 2 of this thesis, HPMAlac polymers were attached to the surface of liposomes via a cholesterol anchor (chol-pHPMAlac). Liposomes grafted with chol-pHPMAlac showed a temperature triggered release of doxorubicin (DOX), but meanwhile they aggregated at the necessary elevated temperatures for DOX release. This aggregation is unwanted since circulating aggregates can induce pulmonary embolism and other adverse effects. Therefore, liposomes were grafted with DSPE-PEG10.000 to evaluate whether aggregation of the liposomes could be prevented by this hydrophilic polymer while maintaining the triggered release property. A DSPE-PEG10.000 grafting density of 5% indeed prevented the aggregation of chol-pHPMAlac liposomes above the CP of chol-pHPMAlac. However, no release of DOX from these liposomes was observed at elevated temperatures. Chol-pHPMAlac liposomes with lower PEG-grafting densities kept the triggered release property partially, but the aggregation appeared to occur more severely. Taken together, our strategy to utilize PEG10.000 coating to optimize our novel thermosensitive liposomes was not successful.

Introduction

The success of intravenous administration of chemotherapeutic anticancer drugs is often limited by a low therapeutic index of the drug in question [1,2]. Nanosized drug delivery systems have been developed to improve the therapeutic efficacy and/or to reduce unwanted side effects of chemotherapeutic drugs. Liposomes are the most intensively studied targeted nanoparticle system so far, with several liposomal nanomedicines being approved, but also polymer based systems have entered the clinical evaluation stage [3-7]. Nanoparticulate drug targeting systems can extravasate from the blood vessels when the vasculature is discontinuous, which has been reported to occur in various tumor types and inflamed tissues [8-10]. Circulating nanoparticles invade these pathological areas through such leaky vasculature via the so-called enhanced permeation and retention (EPR) effect [9,11-13].

Nanoparticles like liposomes are opsonized by plasma proteins, like complement factors and immunoglobulins, and are subsequently recognized by the RES macrophages, which causes rapid clearance from the blood circulation [14-17]. The opsonization process can be reduced by PEGylation since poly(ethylene glycol) (PEG) forms a steric barrier around the liposomes opposing protein-liposome interactions and therefore the rate of elimination from the blood circulation by RES macrophages can be reduced substantially [18-21].

Previously, temperature-sensitive liposomes with tunable release characteristics were designed (Chapter 2 of this thesis). These liposomes were grafted with the temperature-sensitive poly(*N*-(2-hydroxypropyl)methacrylamide mono/dilactate having a cholesterol anchor (chol-pHPMAlac). Temperature-sensitive *N*-(2-hydroxypropyl)methacrylamide mono/dilactate polymers show lower critical solution temperature behavior meaning that they are soluble in an aqueous solution at a low temperature but dehydrate and aggregate when the polymers are heated above this temperature (also referred to as the cloud point (CP) of the polymer). Chol-pHPMAlac forms a hydrophilic shield around the liposomes below the CP. Above the CP, chol-pHPMAlac becomes dehydrated and subsequently interacts with the lipid bilayer inducing bilayer destabilization and release of a loaded drug (DOX) from the liposomes. Unfortunately, the release of DOX took only place at a significantly higher temperature than the CP of chol-pHPMAlac (± 20 °C), presumable because the dehydration of the polymer at the CP is insufficient and thus the polymer is not hydrophobic enough to penetrate and permeabilize the liposomal membrane [22]. On the other hand, at the CP aggregation of the liposomes was observed. Likely the polymer is sufficiently hydrophobic to induce aggregation of the liposomes above the CP. As a consequence, a significant drawback related to the use of these thermosensitive liposomes is that they aggregate at body temperature, which limits their clinical application since circulating aggregates could induce pulmonary embolism, stroke and myocardial infarction [23,24].

It is reported that PEG at the surface of liposomes can form a hydrophilic shield opposing aggregation and opsonization. In the present study, liposomes were coated with DSPE-PEG10.000 to evaluate whether liposome aggregation could be prevented at body temperature while maintaining the temperature sensitivity of the system. Therefore, the aim of this study was to develop chol-pHPMAlac grafted liposomes, which release their drug content at mild hyperthermia while preventing liposome aggregation at body temperature.

Material and methods

Materials

Thiocholesterol, *N,N*,-azobisisobutyronitrile (AIBN) and Triton X-100 were purchased from Sigma-Aldrich Chemie BV, Zwijndrecht, the Netherlands. 1,4-Dioxane was obtained from Biosolve Chemie, Valkenswaard, The Netherlands. 1,2-Dioleoyl-*sn*-glycero-3-phosphoethanolamine (DOPE) was purchased from Avanti Polar Lipids, Alabaster, USA. Egg phosphocholine (EPC) was purchased from Lipoid GmbH, Ludwigshafen, Germany and 1,2-distearoyl-*sn*-glycero-3-phosphoethanolamine-*N*-[amino(polyethylene glycol)-10000] (DSPE-PEG10.000) was obtained from Bio-Connect Services BV, Huissen, The Netherlands. Doxorubicin-HCl was purchased from Guanyu bio-technology Co., LTD, Xi'an, China. The PSS (polymer standards service)-kit Poly(ethylene oxide) and PSS-kit Poly(ethylene glycol) were obtained from polymer standards service, Mainz, Germany.

Synthesis of HPMA mono/dilactate polymers with a cholesterol anchor

2-Hydroxypropyl methacrylamide (HPMA), HPMAmono- and dilactate were synthesized as described previously [25]. HPMA mono/dilactate polymers with a cholesterol anchor (chol-pHPMAlac) were synthesized according to a previously reported method [22,26]. In brief, HPMA mono- and dilactate were dissolved in distilled 1,4-dioxane at a concentration of 100 mg/mL with a monomer ratio of 25:75 (HPMA mono/HPMA dilactate, mol/mol). *N,N*-Azobisisobutyronitrile (AIBN) was used as initiator at a ratio of 500:1 (monomer/AIBN, mol/mol). The molar ratio of thiocholesterol (chain transfer agent) was 50:1 (monomer/chain transfer agent). Three nitrogen/vacuum cycles were applied to remove oxygen. The polymerization reaction was performed for 24 hours at 70 °C after removal of oxygen. The polymer was precipitated in diethyl ether and the supernatant was discarded after centrifugation. The precipitated polymer was dried overnight in a vacuum oven and stored in a freezer until further use.

Polymer characterization

The copolymer composition of chol-pHPMAlac was determined by ^{1}H NMR (Gemini 300 MHz spectrometer) in $(CD_3)_2SO$. The ratio of HPMAmonolactate/HPMAdilactate (ML/DL) was determined from the integral of the peak at 5.0 ppm (CO-C*H*(CH_3)-O) divided by the integral of the peaks at 4.1 and 4.2 ppm (CO-C*H*(CH_3)-OH).

The cloud point (CP) of chol-pHPMAlac was determined by light scattering at 650 nm at a polymer concentration of 5 mg/mL in 120 mM ammonium acetate buffer (pH 5.0). The samples were heated from 0 till 70 °C with a rate of 1 °C /min and the CP was taken as the onset of increasing scattering intensity [22].

The number average molecular weight (M_n) and weight average molecular weight (M_w) of chol-pHPMAlac were measured with GPC using a Plgel 5 µm MIXED-D column and PEGs with narrow molecular weights were used as standards. DMF containing 10 mM LiCl was used as eluent at an elution rate of 0.7 mL/min. The column temperature was 40 °C.

Liposome preparation

Temperature-sensitive liposomes (DOPE:EPC:chol-pHPMAlac in molar ratio of 70:25:5) containing varying amounts of DSPE-PEG10.000 were prepared with the lipid film hydration method [22,27]. In short, the phospholipids and chol-pHPMAlac were dissolved in 5 mL chloroform and a lipid film was formed after evaporation of chloroform under reduced pressure, followed by the removal of residual chloroform overnight under a nitrogen flow. The lipid film was subsequently hydrated in 5 mL 240 mM ammonium sulfate buffer (pH 5.4) at a concentration of 6 μmol phospholipid/mL. The liposomal dispersion was subsequently extruded through two 200 nm filters (2 times) and two 100 nm filters (8 times). Next, the extruded liposomes were dialyzed against 20 mM HEPES buffer pH 7.4 also containing 8 g NaCl/L and 292 mg EDTA/L. The liposomes were loaded with 2 mL doxorubicin (DOX, 5mg/mL) for 4 hours at 4 °C [22]. Free DOX and free chol-pHPMAlac were removed by ultracentrifugation (125.000 g for 45 minutes at 4 °C) of the liposome dispersion. The pelleted liposomes were resuspended in 2 mL 20 mM HEPES buffer pH 7.4 (5 mg/mL DOX) and stored at 4 °C.

Liposome characterization

The size of the liposomes and the polydispersity index were measured with dynamic light scattering (DLS, Malvern CGS-3 multiangle goniometer). Intensity correlation functions were measured using a wavelength of 632.8 nm and a scattering angle of 90°. The measurements were performed in 20 mM HEPES buffer pH 7.4 while samples were heated from 15 to 45 °C with a rate of 1 °C/min and measurements were performed every minute to determine the aggregation temperature of the liposomes. The size of the liposomes was also evaluated at 25 °C for 30 minutes using DLS.

The release of DOX was measured by the change in fluorescence intensity of the release medium in time (excitation wavelength 468 nm, emission wavelength 558 nm). DOX-loaded liposomes (1 μL) were added to 2 mL of preheated 20 mM HEPES buffer pH 7.4 of 25, 30, 37, and 42 °C and the fluorescence intensity was measured in time. Triton X-100 (10%, 20 μL) was added at the end of the experiment to destroy remaining liposomes and to determine the total amount of DOX present. The percentage DOX release was calculated using the following equation: $(I_t-I_0)/(I_{TX}-I_0)$ x100 in which I_t is the fluorescence intensity at time t, I_0 the intensity at the start of the experiment and I_{TX} the fluorescence intensity after addition of Triton X-100.

Results and discussion

Polymer synthesis and characterization

Poly(HPMAmono/HPMAdilactate) with a cholesterol anchor (chol-pHPMAlac) was synthesized via free radical polymerization using AIBN as initiator and thiocholesterol as chain transfer agent (CTA) (Fig. 1). The yield was 27%, which is in line with previous findings (chapter 2 of this thesis). The polymers had a M_n of 7.0 kDa and a CP of 16.5 °C. The HPMAmonolactate:dilactate ratio in the polymer was 29:71 according to ^{1}H-NMR, which corresponds to the feed ratio.

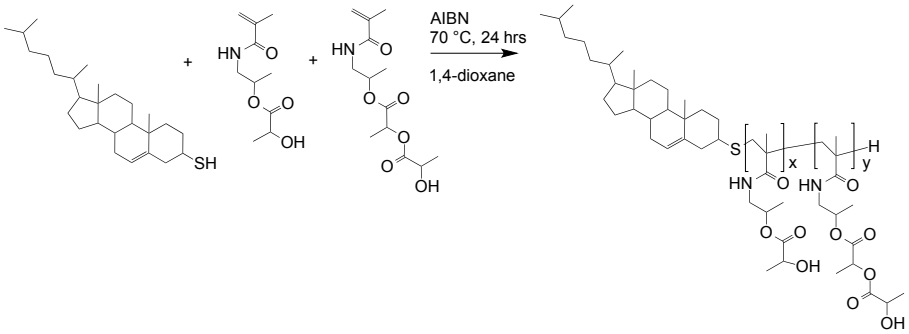

Figure 1. Synthesis of poly(*N*-(2-hydroxypropyl)methacrylamide mono/dilactate having a cholesterol anchor (chol-pHPMAlac).

The characteristics of the synthesized polymer are given in table 1.

Table 1. Characteristics of Chol-pHPMAlac

Monomer feed ratio (monolactate:dilactate) (mol/mol)	CTA:Monomer (mol/mol)	Copolymer composition[a] (monolactate:dilactate) (mol/mol)	Yield (%)	M_n[b] (kDa)	M_w[b] (kDa)	CP[c] (°C)
25:75	1:50	29:71	27	7.0	11.0	16.5

[a] Determined by ^{1}H NMR

[b] Determined by GPC calibrated with narrow molecular weight PEG standards

[c] Determined by light scattering at 650 nm

Liposome characterization

Liposomes grafted with both chol-pHPMAlac (fixed amount) and varying amounts of DSPE-PEG10.000 were prepared by the lipid film hydration method and their characteristics are shown in Table 2. The size of the liposomes varied from 120 to 135 nm with a PDI of ~0.15.

Table 2. Characteristics of temperature sensitive liposomes containing 0-5% DSPE-PEG10.000.

Liposome composition DOPE:EPC:Chol-pHPMAlac:DSPE-PEG10.000 (molar ratio)	Mean diameter (nm ± sd)	PDI
70:25:5:-	128 ± 14	0.20 ±0.01
70:25:5:0.5	130 ± 4	0.17 ± 0.01
70:25:5:1	135 ± 4	0.17 ± 0.01
70:25:5:2.5	121 ± 4	0.09 ± 0.02
70:25:5:5	131 ± 14	0.08 ± 0.02

Stability of chol-pHPMAlac liposomes grafted with 5% DSPE-PEG10.000

Figure 2 shows that liposomes grafted with chol-pHPMAlac were stable < 20 °C as evidenced from a small particle size and low PDI. Above this temperature, the particle size and PDI increased substantially demonstrating particle aggregation. Chol-pHPMAlac dehydrates above the cloud point (CP) of the polymer (16.5 °C) rendering the surface of the liposomes hydrophobic, which in turn results in aggregation of the liposomes. In order to prevent unwanted aggregation of the liposomes above the CP of chol-pHPMAlac, the liposomes were coated with 5% DSPE-PEG10.000. No aggregation of the PEGylated liposomes was observed upon heating to 45 °C indicating that chol-pHPMAlac grafted liposomes coated with DSPE-PEG10.000 remained stable at elevated temperatures (Figure 2).

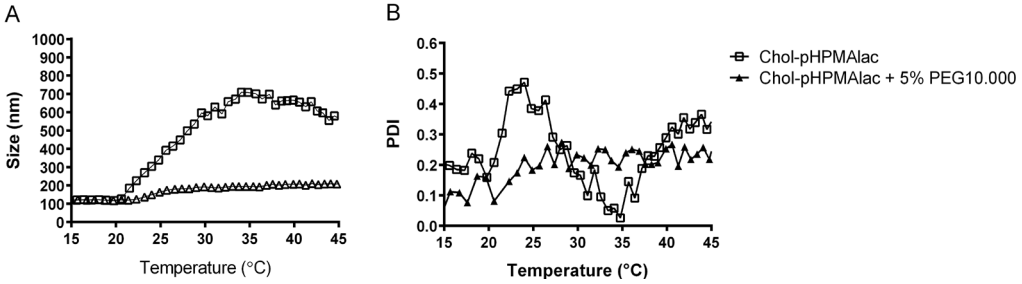

Figure 2. Mean diameter (A) and polydispersity index (PDI) (B) of DOPE:EPC:chol-pHPMAlac liposomes (molar ratio 70:25:5) with or without 5% DSPE-PEG10.000 coating upon incubation from 15 to 45 °C with a heating rate of 1 °C/min.

DOX release from chol-pHPMAlac liposomes grafted with 5% DSPE-PEG10.000

The release of DOX from chol-pHPMAlac liposomes grafted with or without 5% DSPE-PEG10.000 was studied. Figure 3 shows that the liposomes without PEG coating released ~40% of their content after 30 minutes incubation at 30 °C and 55% of the content at 37 °C within 5 minutes, whereas complete release took place within 5 minutes at 42 °C (Figure 3A). Chol-pHPMAlac liposomes grafted with 5% DSPE-PEG10.000 showed a burst release of approximately 20% after incubation at 30, 37, 42 °C and no further release occurred after longer incubation times (Figure 3B). Presumably, PEG forms a dense hydrophilic barrier around the liposomes which prevents the interaction between chol-pHPMAlac and the liposomes. As a consequence, the content release of the liposomes at elevated temperatures is inhibited since chol-pHPMAlac is not able to destabilize the lipid bilayer. Grafting chol-pHPMAlac liposomes with DSPE-

PEG10.000 prevents aggregation of the liposomes (Figure 2) but also inhibits the destabilization of the lipid bilayer at 30, 37 as well as 42 °C (Figure 3B). It was shown in chapter 2 of this thesis that the release of DOX occurred 20 °C above the CP of chol-pHPMAlac while no release of DOX was observed when the chol-pHPMAlac grafted liposomes were incubated at the CP of chol-pHPMAlac. The dehydration of the chol-pHPMAlac is a gradual process that starts at the CP but at this temperature the chol-pHPMAlac is most likely not sufficiently hydrophobic and thereby is not able to penetrate and permeabilize the bilayer inducing liposome destabilization and subsequent release of the drug content. Obviously, chol-pHPMAlac is hydrophobic enough at 20 °C above the CP to induce destabilization of the bilayer.

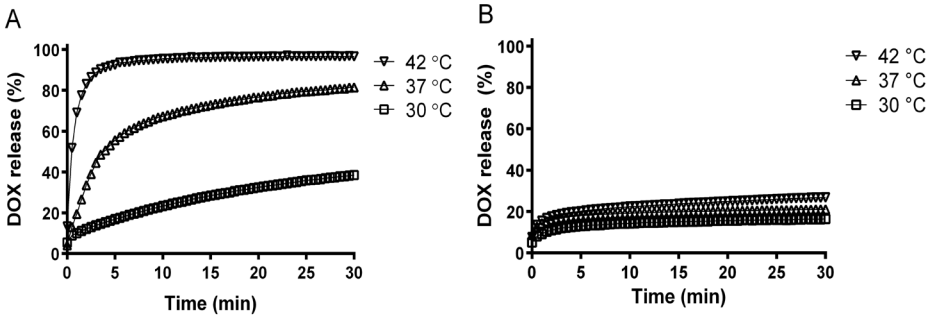

Figure 3. Temperature triggered release of DOX from DOPE:EPC:chol-pHPMAlac liposomes (molar ratio 70:25:5) grafted without (A) or with (B) 5% DSPE-PEG10.000.

Stability of chol-pHPMAlac liposomes with different grafting densities of DSPE-PEG10.000

Chol-pHPMAlac liposomes were grafted with 0.5, 1.0 and 2.5% DSPE-PEG10.000 to explore whether liposomes with a lower density of DSPE-PEG10.000 retained their triggered release pattern without aggregation above the CP of chol-pHPMAlac. Figure 4 shows that liposomes grafted with 2.5% DSPE-PEG10.000 exhibit a small increase in size (from 135 to 200 nm) and PDI (from 0.05 to 0.35) during incubation at 25 °C for 30 minutes. The size of chol-pHPMAlac liposomes grafted with 1.0% DSPE-PEG10.000 increased from 150 nm to 270 nm and the PDI increased from 0.1 to 0.5 whereas a grafting density of 0.5% resulted in liposomes, which aggregated to some extent (size increased from 145 nm to 400 nm) during incubation for 30 minutes at 25 °C. These results demonstrate that prevention of the aggregation of chol-pHPMAlac liposomes depends on the grafting density of DSPE-PEG10.000. A higher grafting density resulted in more stable liposomes which is in line with expectations.

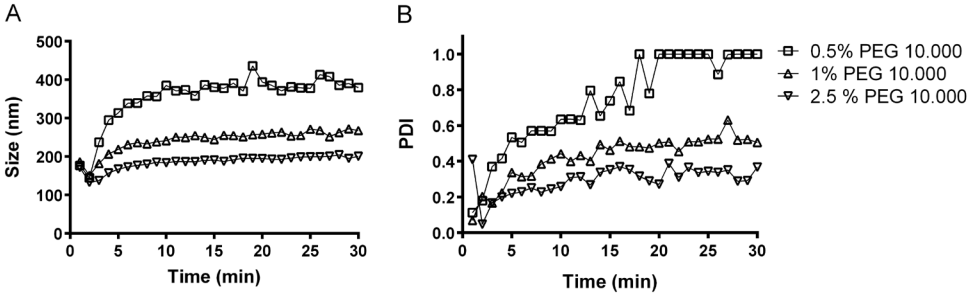

Figure 4. Mean diameter (A) and polydispersity index (PDI) (B) of DOPE:EPC:chol-pHPMAlac liposomes (molar ratio 70:25:5) grafted with 0.5, 1.0 and 2.5% DSPE-PEG10.000 at 25 °C.

DOX release of chol-pHPMAlac liposomes with different grafting densities of DSPE-PEG10.000

The release of DOX from liposomes grafted with 0.5, 1.0 and 2.5% DSPE-PEG10.000 was studied. Figure 5A shows that liposomes grafted with 0.5% DSPE-PEG10.000 retained temperature sensitive release characteristics and their release kinetics was similar to the release of chol-pHPMAlac liposomes without DSPE-PEG10.000 coating (Figure 3A). The DOX release was reduced when liposomes were grafted with 1.0% DSPE-PEG10.000 and incubated at elevated temperatures but still a triggered release profile was observed at 37 and 42 °C (Figure 5B). However, a grafting density of 2.5% inhibited the triggered release almost completely upon incubation at elevated temperatures (Figure 5C).

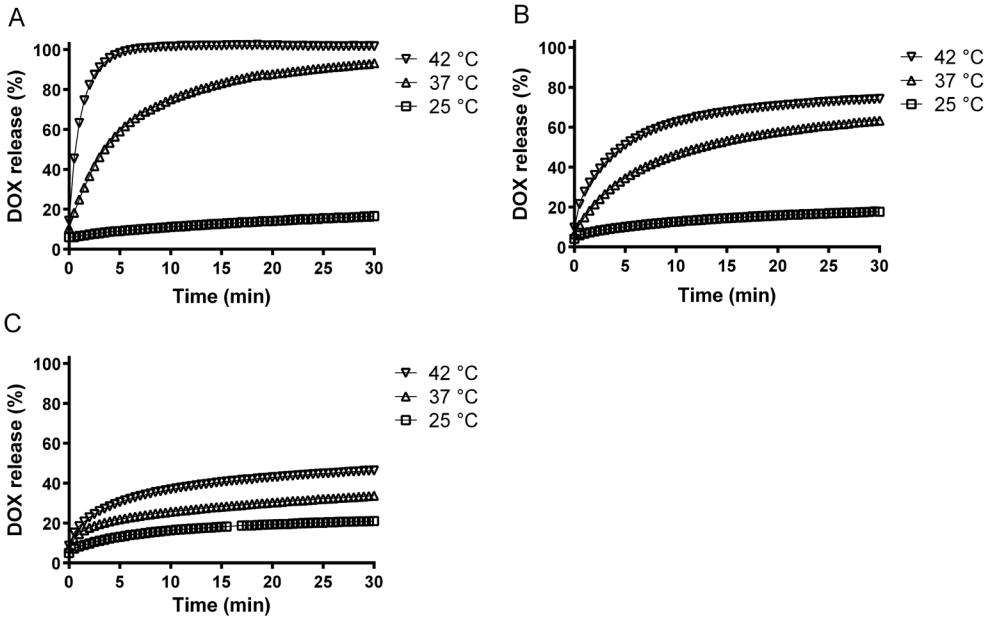

Figure 5. Temperature triggered release of DOX from DOPE:EPC:chol-pHPMAlac liposomes (molar ratio 70:25:5) grafted with 0.5% (A), 1.0% (B) and 2.5% (C) DSPE-PEG10.000.

Conclusion

The results presented in this chapter show that modifying the lipid bilayer of chol-pHPMAlac liposomes with DSPE-PEG10.000 reduces the aggregation of these liposomes above the CP of chol-pHPMAlac. Most likely, the long hydrophilic PEG chains form a hydrophilic shield around the surface of the liposomes, thus preventing liposome aggregation. When this hydrophilic PEG shield is too dense, the temperature increase-triggered interaction between the hydrophobic chol-pHPMAlac and the lipid bilayer is inhibited, preventing the destabilization of the liposomal bilayers and subsequent release of entrapped DOX. Though the triggered DOX release property was maintained by lowering the PEG density, aggregation increased as the shielding capacity was decreased.

The aim of this study was to develop a liposomal formulation that is stable at body temperature but shows a triggered and fast release at mild hyperthermia. Obviously, such a formulation should not aggregate in the circulation since that would block its clinical application. Liposomes grafted with chol-pHPMAlac showed a temperature triggered release profile but the aggregation of this formulation could not be prevented by utilizing the PEG10.000 coating strategy. Therefore, in the next chapters of this thesis, other formulations to realize clinically applicable thermosensitive drug delivery are explored.

References

1. Waterhouse DN, Tardi PG, Mayer LD, Bally MB. A comparison of liposomal formulations of doxorubicin with drug administered in free form: changing toxicity profiles. Drug Saf 2001;24:903-920.
2. Jain RK. Barriers to drug delivery in solid tumors. Sci Am 1994;271:58-65.
3. Torchilin VP. Targeted pharmaceutical nanocarriers for cancer therapy and imaging. AAPS J 2007;9:E128-47.
4. Torchilin VP. Recent advances with liposomes as pharmaceutical carriers. Nat Rev Drug Discov 2005;4:145-160.
5. Svenson S. Clinical translation of nanomedicines. Curr Opin Solid State Mater Sci 2012;16:287-294.
6. Barenholz Y(. Doxil (R) - The first FDA-approved nano-drug: Lessons learned. J Control Release 2012;160:117-134.
7. Allen TM, Cullis PR. Liposomal drug delivery systems: From concept to clinical applications. Adv Drug Deliv Rev 2013;65:36-48.
8. Moghimi SM, Hunter AC, Murray JC. Long-circulating and target-specific nanoparticles: theory to practice. Pharmacol Rev 2001;53:283-318.
9. Maeda H. Tumor-selective delivery of macromolecular drugs via the EPR effect: background and future prospects. Bioconjug Chem 2010;21:797-802.
10. Maeda H, Wu J, Sawa T, Matsumura Y, Hori K. Tumor vascular permeability and the EPR effect in macromolecular therapeutics: a review. J Control Release 2000;65:271-284.
11. Bae YH, Park K. Targeted drug delivery to tumors: Myths, reality and possibility. J Control Release 2011;153:198-205.
12. Lammers T, Kiessling F, Hennink WE, Storm G. Drug targeting to tumors: principles, pitfalls and (pre-) clinical progress. J Control Release 2012;161:175-187.
13. Wang Y, Grainger D. Barriers to advancing nanotechnology to better improve and translate nanomedicines. Front Chem Sci Eng 2014;8:265-275.
14. Yan X, Scherphof GL, Kamps JA. Liposome opsonization. J Liposome Res 2005;15:109-139.
15. Dézsi L, Fülöp T, Mészáros T, Szénási G, Urbanics R, Vázsonyi C, et al. Features of complement activation-related pseudoallergy to liposomes with different surface charge and PEGylation: Comparison of the porcine and rat responses. J Control Release 2014;195:2-10.
16. Bradley AJ, Maurer-Spurej E, Brooks DE, Devine DV. Unusual electrostatic effects on binding of C1q to anionic liposomes: role of anionic phospholipid domains and their line tension. Biochemistry 1999;38:8112-8123.
17. Bradley AJ, Devine DV, Ansell SM, Janzen J, Brooks DE. Inhibition of liposome-induced complement activation by incorporated poly(ethylene glycol)-lipids. Arch Biochem Biophys 1998;357:185-194.
18. Allen TM, Hansen C, Martin F, Redemann C, Yau-Young A. Liposomes containing synthetic lipid derivatives of poly(ethylene glycol) show prolonged circulation half-lives in vivo. Biochim Biophys Acta 1991;1066:29-36.
19. Gabizon A, Catane R, Uziely B, Kaufman B, Safra T, Cohen R, et al. Prolonged circulation time and enhanced accumulation in malignant exudates of doxorubicin encapsulated in polyethylene-glycol coated liposomes. Cancer Res 1994;54:987-992.
20. Torchilin VP, Omelyanenko VG, Papisov MI, Bogdanov Jr. AA, Trubetskoy VS, Herron JN, et al. Poly(ethylene glycol) on the liposome surface: on the mechanism of polymer-coated liposome longevity. Biochim Biophys Acta 1994;1195:11-20.
21. Lasic DD, Martin FJ, Gabizon A, Huang SK, Papahadjopoulos D. Sterically stabilized liposomes: a hypothesis on the molecular origin of the extended circulation times. Biochim Biophys Acta 1991;1070:187-192.

22. van Elk M, Deckers R, Oerlemans C, Shi Y, Storm G, Vermonden T, et al. Triggered release of doxorubicin from temperature-sensitive poly(N-(2-hydroxypropyl)-methacrylamide mono/dilactate) grafted liposomes. Biomacromolecules 2014;15:1002-1009.
23. Faraji AH, Wipf P. Nanoparticles in cellular drug delivery. Bioorg Med Chem 2009;17:2950-2962.
24. Novo L, Rizzo LY, Golombek SK, Dakwar GR, Lou B, Remaut K, et al. Decationized polyplexes as stable and safe carrier systems for improved biodistribution in systemic gene therapy. J Control Release 2014;195:162-175.
25. Neradovic D, van Steenbergen MJ, Vansteelant L, Meijer YJ, van Nostrum CF, Hennink WE. Degradation mechanism and kinetics of thermosensitive polyacrylamides containing lactic acid side chains. Macromolecules 2003;36:7491-7498.
26. Paasonen L, Romberg B, Storm G, Yliperttula M, Urtti A, Hennink WE. Temperature-sensitive poly(N-(2-hydroxypropyl)methacrylamide mono/dilactate)-coated liposomes for triggered contents release. Bioconjug Chem 2007;18:2131-2136.
27. de Smet M, Langereis S, van den Bosch S, Grull H. Temperature-sensitive liposomes for doxorubicin delivery under MRI guidance. J Control Release 2010;143:120-127.

5

Alginate microgels loaded with temperature sensitive liposomes for magnetic resonance imageable drug release and microgel visualization

Merel van Elk, Cyril Lorenzato, Burcin Ozbakir, Chris Oerlemans, Gert Storm, Frank Nijsen, Roel Deckers, Tina Vermonden and Wim E. Hennink

Eur Polym J. 2015; In Press

Abstract

The objective of this study was to prepare and characterize alginate microgels loaded with temperature sensitive liposomes, which release their payload after mild hyperthermia. It is further aimed that by using these microgels both the drug release and the microgel deposition can be visualized by magnetic resonance imaging (MRI) after their administration (e.g. in the vicinity of a tumor). To this end, temperature sensitive (TSL) and non-temperature sensitive liposomes (NTSL) loaded with fluorescein (drug mimicking dye) and a T_1 MRI contrast agent (Prohance®, [Gd(HPDO3A)(H_2O)]) were encapsulated in alginate microgels crosslinked by holmium ions (T_2^* MRI contrast agent). The drug release could be monitored by the release of [Gd(HPDO3A)(H_2O)] while the microgels could be visualized using MRI via the holmium ions in the microgels. The microgels were prepared with a JetCutter and had an average size of 325 μm and contained ~0.6 wt % Ho^{3+}.

Microgels loaded with NTSL (NTSL-Ho-microgels) were stable at 37 and 42 °C with only a minimal release of fluorescein and [Gd(HPDO3A)(H_2O)]. Microgels encapsulating TSL (TSL-Ho-microgels) released fluorescein and [Gd(HPDO3A)(H_2O)] only marginally at 37 °C while, importantly, their payload was co-released within 2 minutes at 42 °C. TSL-Ho-microgels were administered in an *ex vivo* sheep kidney via a catheter. Clusters of TSL-Ho-microgels could be visualized via MRI and were deposited in the interlobular blood vessels. In conclusion, these alginate TSL-Ho-microgels are promising systems for real-time, MR-guided embolization and triggered release of drugs *in vivo*.

Introduction

The success of systemic administration of chemotherapeutic drugs is limited by the unfavorable balance of therapeutic drug concentrations in the tumor and toxic concentrations in healthy tissues. Nanosized drug delivery systems have been developed to improve the therapeutic efficacy and/or to reduce unwanted side effects of chemotherapeutic drugs. These delivery systems can accumulate in the tumor after intravenous injection via the enhanced permeability and retention (EPR) effect [1-5]. Liposomes are the most intensively studied drug delivery systems so far [6-10] and a number of studies showed that encapsulation of doxorubicin (DOX) in liposomes resulted in an increased therapeutic index, particularly due to significantly reduced cardio toxicity and other unwanted side effects. Liposomal DOX showed a significant improvement in response rate from 25 to 46% compared to standard combination chemotherapy for the treatment of kaposi's carcinoma [11]. On the contrary, the anti-tumor efficacy in patients with metastatic breast cancer was not improved by liposomal DOX [12,13]. This variation in antitumor efficacy between tumor types can be explained by the heterogeneous nature of the EPR effect since this phenomenon varies between tumor models, from patient to patient and even varies within one tumor [2,14]. Triggerable liposomal drug release systems can locally release their therapeutic payload in the tumor. Temperature sensitive liposomes have been shown to release their drug content fast at elevated temperatures [15-18] and induce higher peak concentrations at the tumor site after local heat treatment compared to administration of free drug or conventional drug containing liposomes [19-21].

Localized drug delivery of chemotherapeutics can also be achieved via transarterial chemoembolization (TACE). During the TACE procedure, a catheter is positioned in the arterial supply of a tumor via which a chemotherapeutic drug is administered followed by embolic particles [22,23]. These embolic particles occlude the blood vessels preferably in the tumor, leading to a restricted or even loss of blood flow, resulting in ischemia of the tumor. The blockage of the blood vessels by the embolic particles also reduces the washout of the chemotherapeutic drug and therefore minimizes systemic exposure [23,24].

Recently, drug eluting beads (DEB), which consist of embolic particles loaded with a chemotherapeutic drug, have been developed to simplify and standardize the TACE procedure since chemotherapeutic drugs and the embolic particles are delivered simultaneously [23,25,26]. Examples of polymers used for the preparation of DEBs are chitosan [27,28], PLGA (poly(lactide-co-glycolide)) [29] and alginate [30]. Clinically used DEBs are based on polyvinyl alcohol modified with a sulfonic acid group to obtain negatively charged microspheres (DC beads). A high loading of positively charged cytostatics such as DOX and irinotecan can be achieved in these PVA DEBs via an ion exchange mechanism [26,31,32]. Clinical trials have shown that embolization with DEB leads to a significant reduction in peak plasma concentration and area under the curve of DOX [33,34] while increasing the antitumor efficacy compared to conventional TACE [35,36].

A drawback of these clinically used DEBs is however that they lack the ability to be visualized during and after administration. Therefore, it is not possible to monitor whether microspheres are deposited in the tumor or that they are located outside tumor tissue. Also the drug distribution cannot be monitored *in vivo*, making it difficult to predict the efficacy in the tumor. The beads which are currently used for

chemoembolization have a sustained release profile. As a result, the drug is slowly released leading to a relatively low tumor concentration. With our formulation we aim for triggered drug release, resulting in a local high concentration of the antitumor agent. To support this assumption, it was previously shown that high concentrations of DOX in the tumor resulted in a high cellular uptake of this drug [37]. Further, in another study a good correlation was found between the intracellular DOX concentration and the antitumor efficacy [38].

To overcome these challenges, this research aims to prepare microgels that can be visualized in all stadia of treatment. The administration and microgel distribution can be visualized because the used polymer, alginate, is crosslinked with a T_2^* MRI contrast agent (holmium ions) which can be visualized by magnetic resonance imaging (MRI) [39]. The triggered drug release from these alginate microgels by encapsulating temperature sensitive liposomes can be visualized by a T_1 MRI contrast agent ([Gd(HPDO3A)(H_2O)]) which is loaded in the liposomes. In principle, besides monitoring the drug release also the tumor penetration can be visualized (Figure 1). For clinical application of TACE, the diameter of the microgels should be around 300 µm [40].

Alginate was selected for the preparation of microgels since crosslinked microgels can be prepared via a simple procedure [41-43]. The monodisperse alginate microgels can be prepared easily by JetCutting [44,45]. Importantly, mild crosslinking conditions are used, allowing encapsulation of liposomes in alginate microgels [46-48]. Thereby, crosslinking with Ho^{3+} (T_2^* MRI contrast agent) is possible and allows MRI visualization [49]. Finally, alginate microgels have previously been used for arterial embolization. No reopening of the arteries was observed on an angiogram up to 8 weeks after embolization, indicating that alginate microgels are suitable materials for embolization [30,50,51].

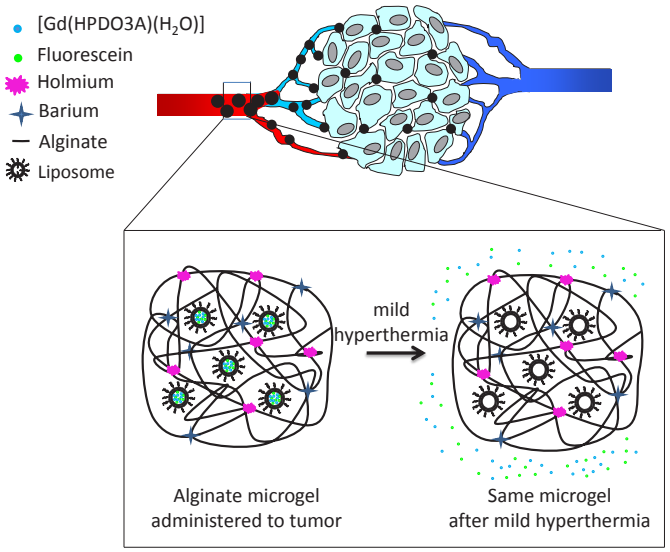

Figure 1. Schematic representation of accumulation of alginate microgels with encapsulated temperature sensitive liposomes in a tumor during embolization. The alginate microgels are crosslinked with holmium ions to allow microgel visualization by magnetic resonance imaging (MRI). Upon mild hyperthermia, the liposomes will release their payload (fluorescein (drug mimicking dye) and [Gd(HPDO3A)(H_2O)] (MRI agent)). This release of [Gd(HPDO3A)(H_2O)] can also be monitored with MRI.

Materials and methods

Materials

1,2-Dipalmitoyl-*sn*-glycero-3-phosphocholine (DPPC), 1,2-distearoyl-*sn*-glycero-3-phosphocholine (DSPC) and 1,2-distearoyl-*sn*-glycero-3-phosphoethanolamine-*N*-[amino(polyethylene glycol)-2000] (DSPE-PEG2000) were purchased from Lipoid GmbH, Ludwigshafen, Germany. 1-Stearoyl-2-hydroxy-*sn*-glycero-3-phosphocholine (MSPC) was obtained from Avanti Polar Lipids, Alabaster, U.S.A. Cholesterol and barium chloride dihydrate were purchased from Sigma-Aldrich Chemie BV, Zwijndrecht, The Netherlands. Holmium chloride hexahydrate was obtained from Metall rare earth limited, Shenzhen, China. Fluorescein disodium for injection was obtained from Fresenius Kabi Nederland BV, 's-Hertogenbosch, The Netherlands. [Gd(HPDO3A)(H_2O)] (Prohance®) was purchased from Bracco Diagnostic Inc., Monroe Township, U.S.A. Sodium alginate (Manucol LKX) was a gift from FMC biopolymer, Philadelphia, U.S.A.

Preparation of empty alginate microgels crosslinked with varying holmium- and barium- ion content

Holmium crosslinked alginate microgels (Ho-microgels) were prepared with a JetCutter (GeniaLab® BioTechnology, Germany) [44,49]. In detail, sodium alginate (3% w/v) was dissolved overnight under magnetic stirring in 20 mM HEPES buffer pH 7.4 also containing 8 g NaCl/L. Air bubbles were removed by sonication. The JetCutter was equipped with a nozzle with a diameter of 150 µm and a cutting tool having 120 wires with a thickness of 100 µm. The rotor speed was 5000 rpm and the alginate flow was set at 0.3 g/s. The alginate droplets were collected in 1 L of 20 mM HEPES buffer pH 7.4 containing different ratios of holmium chloride and barium chloride (0:100 to 100:0) with a total cation concentration of 100 mM. The formed microgels were hardened for 2 hours and subsequently washed three times with 20 mM HEPES buffer pH 7.4 (in total 0.5-1 L) to remove the excess of crosslinking ions.

Preparation of liposomes

Two different liposomal formulations were prepared: non-temperature sensitive liposomes (NTSL) composed of DSPC, cholesterol and DSPE-PEG2000 (in molar ratio of 56:39:5) and temperature sensitive liposomes (TSL) composed of DPPC, MSPC and DSPE-PEG2000 (molar ratio of 86:10:4) [52,53]. A lipid film was formed by dissolving the lipids and cholesterol in 10 mL chloroform (160 µmol total lipids/mL) followed by rotary evaporation of the solvent under reduced pressure in a 100 mL round bottom flask. The resulting lipid film was further dried overnight under a nitrogen flow. The lipid film was hydrated in water for injection (20 mL) containing 0.375 mM [Gd(HPDO3A)(H_2O)] and 25 mg/mL fluorescein at 60 °C. The liposomal dispersion (80 µmol total lipid/mL) was extruded through two 200 nm filters (2 times) and two 100 nm filters (8 times). Liposomes were passed three times through a PD-10 column to remove unencapsulated fluorescein and [Gd(HPDO3A)(H_2O)].

Preparation of alginate microgels loaded with liposomes (NTSL/TSL-Ho-microgels)

NTSL/TSL-Ho-microgels were prepared by mixing a sodium alginate solution (4% w/v in 20 mM HEPES buffer pH 7.4) with NTSL or TSL (80 µmol total lipid/mL) in a 3:1 ratio. The alginate solution was processed by the JetCutter with the same settings as described above. The alginate droplets containing NTSL or TSL were crosslinked with a holmium:barium molar ion ratio of 5:95 to form NTSL/TSL-Ho-microgels. The total cation concentration during crosslinking was 100 mM.

Light microscopy

Morphological examination and size distribution of NTSL/TSL-Ho-microgels were investigated with light microscopy. Microgels were suspended in 20 mM HEPES buffer pH 7.4 (100 mg microgels /mL) and subsequently some droplets were pipetted on a microscopy slide. The size of the microgels was examined using light microscopy with phase contrast (Eclipse E200, Nikon equipped with a DS-Fi1 camera, Nikon and a E plan 10x lens, Nikon). The images were analyzed with NIS-elements D 3.0 software to determine the microgel diameter. The average size of the microgels was calculated by averaging the diameter of 100 microgels.

Analysis of holmium content in microgels

The amount of holmium ions in the microgels was determined via complexometric analysis. Wet microgels (150 mg) were destructed in nitric acid (65%, ± 15 mL) at 100 °C till the solution became transparent (±30 minutes). Hexamine (5 g) was added and the pH of the solution was adjusted with 10 M sodium hydroxide to 5.0-5.5. Next, xylenol-orange (50 mg, 1:100 mixture in potassium nitrate) was added and the solution was titrated with 10 mM ethylenediaminetetraacetic acid (EDTA) till a color shift to yellow was visually observed [45]. The weight percentage of holmium ions present in the microgels was calculated with the following equation: (titer EDTA x mL EDTA) x (molecular weight of Ho (164.93 g/mol)) / mg microgels. The concentration of holmium ions and monomer units in the microgels was calculated to determine the ratio between holmium ions and alginate monomer units. The microgels contain 3 wt% alginate.

Dynamic light scattering

The size of the liposomes and the polydispersity index were measured with dynamic light scattering at 25 °C (DLS; Malvern CGS-3 multiangle goniometer). Intensity correlation functions were measured using a wavelength of 632.8 nm and a scattering angle of 90°. The measurements were performed in 20 mM HEPES buffer pH 7.4.

Determination of fluorescein concentration

The fluorescein concentration in the liposomes was determined after disruption of the liposomes by addition of a small volume of 10% Triton X-100 in water to the liposomal dispersion (final concentration of Triton X-100 was 0.1%) using fluorescence measurements (excitation wavelength 500 nm, emission wavelength 520 nm). The encapsulation efficiency of NTSL and TSL in NTSL-Ho-microgels as well as in TSL-Ho-microgels was determined by measuring the fluorescein concentration in the microgels by disrupting the liposomes in the microgels with Triton X-100.

MR imaging

Magnetic Resonance Imaging (MRI) was used to visualize the holmium crosslinked microgels and to monitor the temperature triggered [Gd(HPDO3A)(H_2O)] release from the liposomes that were entrapped in the microgels. All MRI experiments were performed on a clinical 1.5-Tesla MR scanner (Achieva; Philips Health care). The following MR sequences were used in this study. T_2^*-weighted gradient echo scans were acquired to visualize holmium crosslinked microgels (TR = 570.6 ms, TE = 9.72 ms, FA = 25°, turbo-factor = 32, 32 slices, voxel size = 0.96x0.96x2.0 mm^3). T_1-weighted spin echo scans (TR = 1000 ms, TE = 8 ms, FA = 90°, turbo-factor = 15, 3 slices, voxel size = 0.94x0.94x2.0 mm^3) were acquired and R_1-mapping was performed in order to monitor [Gd(HPDO3A)(H_2O)] release. R_1-maps were obtained by sampling the signal recovery after inversion using a Look-Locker (LL) sequence (TR = 4 s, TE = 2.75 ms, FA = 6°, turbo-factor = 5, 1 slice, voxel size = 0.94×0.94×5 mm^3, 104 timepoints at 29 ms interval).

The images obtained from each LL measurement were automatically fitted with in-house developed Matlab software (7.12, The MathWorks Inc., Natick, MA, USA, 2000). The temporal evolution of the magnitude of the longitudinal magnetization (M) was fitted (Levenberg-Marquardt algorithm) for each pixel with the following equation:

$$M = |A-[(A+B)\bullet e^{-t\bullet R1^*}]| \qquad (1)$$

Where R_1^* is the apparent longitudinal relaxation rate, t is the time after the inversion pulse and A and B are constants. The sample R_1 differs from R_1^* by an offset only dependent on flip angle (α) and delay between 2 consecutive excitation pulses (Δt):

$$R_1=R_1^* + \log(\cos\alpha)/\Delta t \qquad (2)$$

A square ROI (5x5 pixels) was manually selected inside the sample to analyze the R_1 before and after heating.

Fluorescein release

The release of fluorescein from the liposomes and NTSL/TSL-Ho-microgels was measured by the change in fluorescence intensity in time (excitation wavelength 500 nm, emission wavelength 520 nm). Twenty five mL of preheated 20 mM HEPES buffer pH 7.4 (37 or 42 °C, heated in water bath) was added to the liposome suspension (50 µl liposomes with 80 µmol total lipids/ml). Samples (1 mL) were taken at different time points (0, 2, 5, 10, 15, 30, 45 and 60 minutes) and subsequently cooled on ice to prevent further leakage. Triton X-100 (10%, 170 µL) was added at the end of the experiment to destroy remaining liposomes and release entrapped fluorescein. The percentage fluorescein released was calculated using the following equation: $(I_t-I_0)/(I_{TX}-I_0)$ x 100 in which I_t is the fluorescence intensity at time t, I_0 the intensity at the start of the experiment and I_{TX} the fluorescence intensity after addition of Triton X-100.

The release of fluorescein from NTSL/TSL-Ho-microgels was measured at the same wavelengths as described for the liposomes. Fifty mL of preheated buffer was added to the microgels (1.5 gr wet microgels). Microgels were shaken after which the

microgels settled at the bottom due to gravity. Samples (1 mL) were taken at different time points (0, 2, 5, 10, 15, 30, 45 and 60 minutes) and subsequently cooled on ice to prevent further leakage. Triton X-100 (10%, 430 μL) was added to the microgel pellet to disrupt the intact liposomes loaded into the microgels. The percent fluorescein released was calculated as described above.

Fluorescence microscopy

Samples were prepared similarly as for the light microscopy measurements. The release of fluorescein from NTSL/TSL-Ho-microgels was visualized with a fluorescence microscope (BZ-9000, Keyence). A GFP BP filter with an excitation wavelength of 472-30 nm and emission wavelength of 520-35 nm and a Plan Fluor 20x lens (Nikon) was used. The images were analyzed with BZ II Analyzer software. NTSL/TSL-Ho-microgels were imaged in 20 mM HEPES buffer pH 7.4 at room temperature and after incubation at mild hyperthermia for 10 seconds.

***Ex vivo* embolization of a sheep kidney**

The *ex vivo* sheep kidney used as an *ex vivo* model for embolization was derived from a terminated female sheep that was previously used as laboratory animal. A catheter (Abocath 18G, Hospira, U.K.) was inserted into the renal artery and fixed with a suture. The kidney was placed in a plastic bucket fillet with H_2O containing 0.8% NaCl at room temperature. TSL-Ho-microgels crosslinked with 5 mM holmium ions (75 mg wet weight in 1 mL 20 mM HEPES buffer pH 7.4) were administered via the catheter. A T_2^*-weighted MRI scan was made before and after injection of the microgels.

Statistical analysis

Statistical analysis was performed with the software GraphPad Prism 6.01. A 2-way ANOVA was performed followed by a Tukey test for statistical analysis at different temperatures or a Sidak test for statistical analysis of the different microgel formulations.

Results and Discussion

Characterization of empty alginate microgels

Alginate microgels were prepared by crosslinking alginate dissolved in 20 mM HEPES buffer pH 7.4 with di (Ba^{2+}) or trivalent ions (Ho^{3+}) using a JetCutter. Holmium containing particles are paramagnetic contrast agents inducing local magnetic field variations that cause dephasing of the MR signal, which results in local signal voids. Barium based particles do not exhibit these paramagnetic characteristics. Figure 2 shows T_2^*-weighted (wt) and T_1-wt images of microgels that were prepared by crosslinking alginate with different ratios of holmium and barium ions. The microgels contained 0 to 1.35 % of holmium (w/wet weight microgels), which correlates with a holmium ion to alginate monomer ratio of 0 to 0.54 (Table 1). The monomer concentration was calculated assuming that the microgels contain 3% alginate. Microgels crosslinked with solely holmium ions had a holmium ion to alginate monomer ratio of 0.54:1 indicating that one holmium ion crosslinks two monomer units which is in line with previous observations [45]. The diameter of the microgels ranged between 278 and 294 µm which is a clinically relevant size for transarterial chemoembolization of hepatocellular carcinoma [40]. The microgels had a narrow size distribution with a standard deviation of ~ 20 µm (Table 1 and Figure 2). As expected, the microgels crosslinked only with barium ions were not detectable on T_2^*-wt images, whereas microgels crosslinked with increasing amounts of holmium ions showed increasing signal voids on these images. In contrast, on T_1-weighted spin echo images barium as well as holmium ion crosslinked microgels were detectable. Yet, with increasing holmium ion concentrations, the detected MR-signal in these T_1-weighted images decreased due to the pronounced T_2^*-effect. In subsequent experiments, we continued to work with microgels crosslinked with a holmium:barium ratio of 5:95. These microgels were detectable on T_2^*-wt gradient echo images and gave sufficient signal on T_1-wt spin echo images to detect [Gd(HPDO3A)(H_2O)] induced T_1 changes.

Table 1. Characteristics of alginate microgels crosslinked with different holmium:barium ratios with a total cation concentration of 100 mM. Microgels were prepared using a JetCutter.

mM Ho	Ho content [a] (% w/w, wet weight)	Ho:monomer unit (ratio mol/mol)	Mean size [b] (µm)
0	0	0	281 ± 21
2	0.24 ± 0.01	0.10:1	293 ± 20
5	0.30 ± 0.01	0.12:1	294 ± 19
10	0.47 ± 0.01	0.16:1	293 ± 20
25	0.72 ± 0.02	0.29:1	287 ± 19
100	1.35 ± 0.05	0.54:1	278 ± 15

[a] Determined by complexometric titration (standard deviation (sd) of 3 different measurements).

[b] Determined by light microscopy (sd refers to variation in size of microgels with n=100).

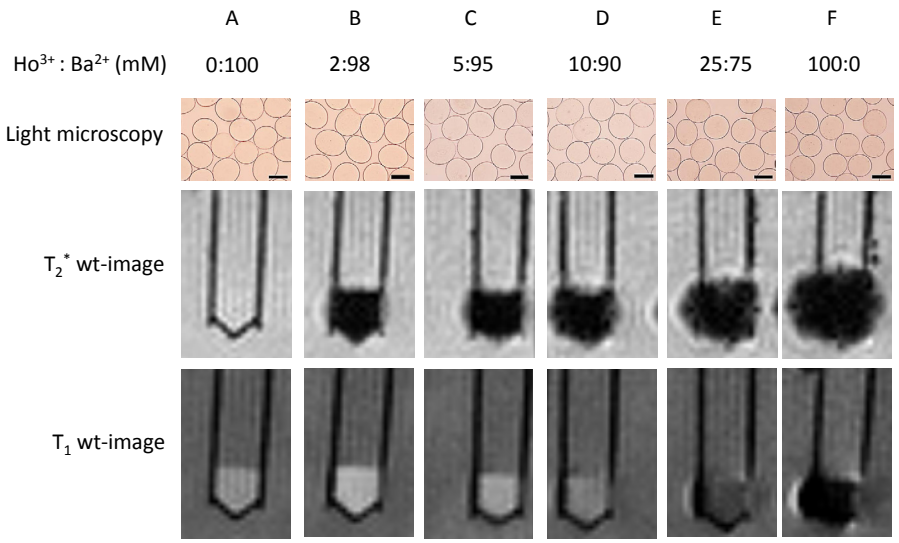

Figure 2. *Top:* Light microscopy images of alginate microgels crosslinked using different holmium and barium ion concentrations. The scale bar represents 200 µm. (mM Ho:Ba in crosslinking solution, A 0:100, B 2:98, C: 5:95, D 10:90, E 25:75 and F 100:0).
Middle: T_2^* wt-image of sedimented alginate microgels crosslinked using different holmium and barium ion concentrations.
Bottom: T_1 wt-image of sedimented alginate microgels crosslinked using different holmium and barium ion concentrations.

Characterization of temperature-sensitive and non-temperature sensitive liposomes encapsulating fluorescein and [Gd(HPDO3A)(H_2O)]

Temperature sensitive liposomes (TSL) containing lysolipids were prepared for encapsulation in alginate microgels. The incorporation of a lysolipid in the bilayer of liposomes enhances the release at mild hyperthermia [15,19,54]. It has been further shown that temperature sensitive liposomes containing 5% mol DSPE-PEG2000 were stable at 37 °C and showed complete content release at 42 °C [55]**.** Non-temperature sensitive liposomes (NTSL) were prepared as control.

Table 2. Characteristics of non-temperature sensitive (NTSL) and temperature sensitive liposomes (TSL) encapsulating fluorescein and [Gd(HPDO3A)(H_2O)]

	NTSL	TSL
Lipid composition	DSPC:Chol:DSPE-PEG2000	DPPC:MSPC:DSPE-PEG2000
Molar ratio lipids (feed ratio)	56:39:5	86:10:4
Mean size (nm)	108 ± 1 nm	133 ± 1 nm
PDI	0.07 ± 0.02	0.09 ± 0.02
Fluorescein encapsulation (%)	7.6	11.2

Liposomes loaded with fluorescein and [Gd(HPDO3A)(H_2O)] (MRI-contrast agent) were prepared via the lipid film hydration method (Table 2). The mean size of NTSL and TSL were 108 and 133 nm, respectively, with a PDI ≤ 0.1. The encapsulation efficiency of fluorescein was about 8% for the NTSL and 11% for the TSL. Such encapsulation efficiencies are expected since fluorescein dissolved in water is passively loaded into liposomes [56]. Likely, the extrusion loss is different for these formulations resulting in a slight difference in encapsulation efficiency.

Figure 3 shows the fluorescence signal and T_1 relaxation rate (R_1) measured by MRI as function of incubation time at 37 and 42 °C for NTSL (A) and TSL (B). Hardly any release of fluorescein as well as [Gd(HPDO3A)(H_2O)] from the NTSL formulation was observed at 37 and 42 °C during 60 minutes, indicating that the NTSL formulation is stable at both 37 and 42 °C. The TSL formulation showed a slow release at 37 °C but released both fluorescein and [Gd(HPDO3A)(H_2O)] completely at the same rate within 2 minutes at 42 °C.

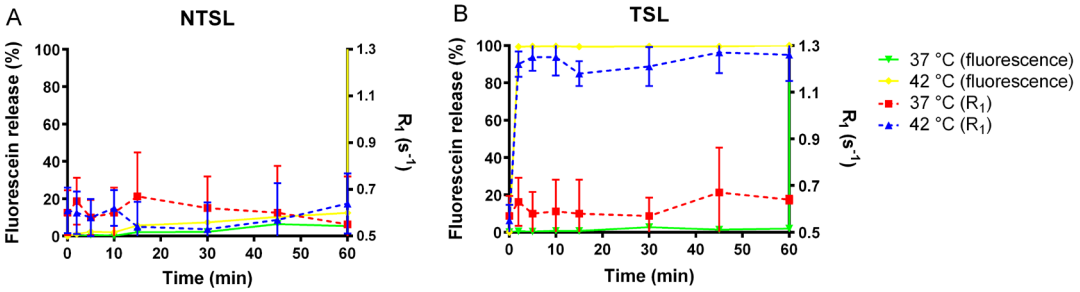

Figure 3. Fluorescence signal and T_1 relaxation rate measured by MRI as function of incubation time at 37 and 42 °C for NTSL (A) and TSL (B). Liposomes were diluted in 20 mM HEPES buffer pH 7.4 to a total lipid concentration of 0.16 µmol/mL.

Preparation of holmium crosslinked alginate microgels containing NTSL or TSL (NTSL-Ho-microgels or TSL-Ho-microgels)

Alginate droplets containing NTSL or TSL were crosslinked by dropping them in a solution of 5 mM Ho^{3+} and 95 mM Ba^{2+} to form microgels (NTSL/TSL-Ho-microgels). Their characteristics are displayed in Table 3.

Table 3. Characteristics of NTSL-Ho-microgels and TSL-Ho-microgels prepared using a JetCutter.

	NTSL-Ho-microgels	TSL-Ho-microgels
Mean size (µm)	325 ± 17	323 ± 18
Ho content (% w/w, wet weight)	0.65 ± 0.03	0.59 ± 0.04
Ho:monomer unit (ratio mol/mol)	0.26:1	0.24:1
Liposome encapsulation (%)	91	97

Both types of microgels had a mean size around 325 µm and displayed a very low size distribution (Table 3 and Figure 4). There was no substantial difference between the diameter of empty alginate microgels (Table 1) and microgels loaded with liposomes (Table 3). Obviously the encapsulation of liposomes did not interfere adversely with the formation of alginate microgels [46,48]. These microgels crosslinked with 5 mM Ho^{3+} and 95 mM Ba^{2+} contained 0.6% holmium^{3+} (w/w, wet weight) corresponding

to a holmium^{3+} to alginate monomer ratio of ~0.25 (mol/mol). Crosslinking alginate microgels with 100 mM holmium ions resulted in a holmium^{3+} to alginate monomer ratio of ~0.54 (Table 1). The relatively high Ho^{3+} ratio of gels prepared at a Ho^{3+}:Ba^{2+} feed ratio of 5:95 suggests that holmium^{3+} has a higher affinity for alginate chains than barium^{2+}. Alginate is a copolymer consisting of β-D-mannuronic acid (M) and α-L-guluronic acid (G) residues. Crosslinking occurs by di or trivalent ions that form bridges between dimers of MM, GG and GM. It has been reported that divalent ions preferably bind to GG dimers while trivalent ions bind to GG as well as to MM dimers [57]. Consequently, trivalent ions like holmium are incorporated into alginate gels to a larger extent than divalent ions such as barium (Table 1). In a phase 1 clinical trial, the safety of holmium-166 microspheres is assed in patients with liver metastases. This clinical trial showed that embolization with holmium microspheres is a safe treatment option and the toxicity observed after administration of 600 mg microspheres was mainly associated with post embolization syndrome [58]. Thereby, the intraperitoneal LD_{50} of holmium salts in mice is 320-560 mg/kg [59,60]. NTSL/TSL-Ho-microgels crosslinked with 5 mM Ho^{3+} and 95 mM Ba^{2+} contain a relatively low concentration of holmium ions (≤ 1% w/w), corresponding with ≤ 6 mg holmium ions per 600 mg microgels. Therefore the toxicity of the microgels is expected to be low. Liposomes were encapsulated nearly quantitatively into the alginate microgels. The presence of fluorescein encapsulated in the liposomes loaded in the microgels could be observed with light microscopy; the NTSL/TSL-Ho-microgels are yellow due to the presence of fluorescein loaded liposomes while empty microgels are transparent (Figures 2 and 4A-B). A modest variation in size and holmium content was observed between the empty and liposome loaded microgels (Table 1 and 3). The differences observed are batch-to-batch variations and are likely due to small variations in the processing variables (e.g. nitrogen pressure and flow rate are all manually set).

Release of fluorescein and [Gd(HPDO3A)(H_2O)] from NTSL-Ho-microgels and TSL-Ho-microgels

The release of [Gd(HPDO3A)(H_2O)] from the alginate microgels was visualized by T_1-wt MR images (Figure 4C-D). During incubation for 1 hour at 37 °C, both NTSL-Ho-microgels and TSL-Ho-microgels sedimented. A slight increase in signal intensity in the supernatant of the TSL-Ho-microgels was observed after incubation at 37 °C while no change in signal intensity was observed when NTSL-Ho-microgels were incubation at 37 °C. This indicates that [Gd(HPDO3A)(H_2O)] was not released from the NTSL-Ho-microgels (supernatant remained gray) and only marginally from the TSL-Ho-microgels after incubation at 37 °C for 1 hour (~5%). However, a significant signal enhancement was observed after mild hyperthermia (42 °C for 5 minutes) in the aqueous medium above the TSL-Ho-microgels (supernatant became white). This increase in signal demonstrates the release of [Gd(HPDO3A)(H_2O)] from TSL-Ho-microgels while under the same conditions no release of [Gd(HPDO3A)(H_2O)] from NTSL-Ho-microgels was detected.

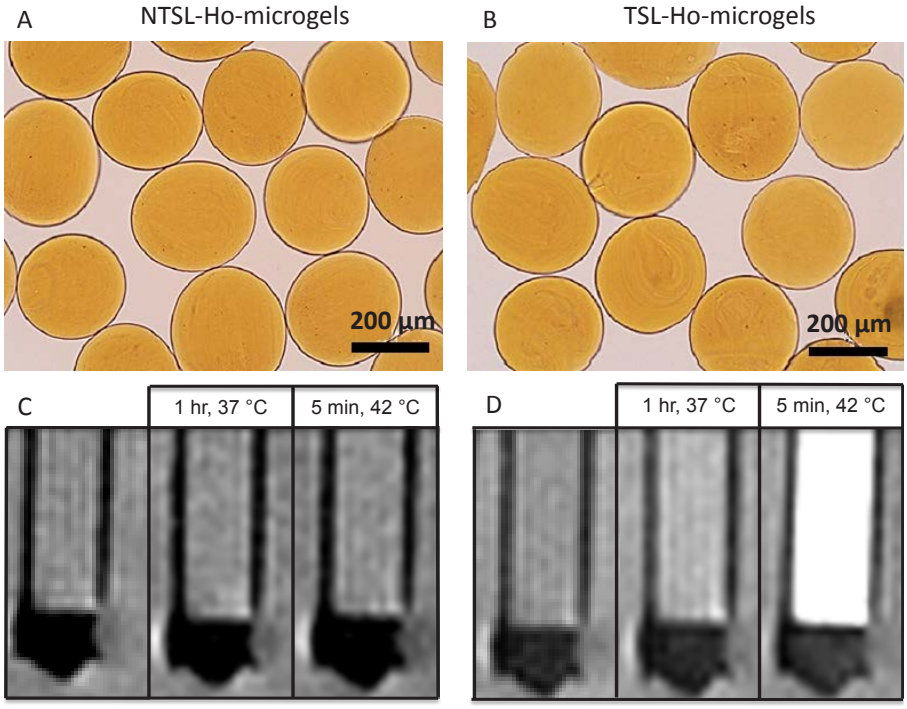

Figure 4. *Top*: Light microscopy image of NTSL-Ho-microgels (A) and TSL-Ho-microgels (B) at room temperature. A black rim is observed around the microgels due to the difference in refractive index of the microgels and the surrounding medium [61].
Bottom: T_1-wt MR images of NTSL-Ho-microgel (C) and TSL-Ho-microgel (D) dispersions at room temperature, after incubation at 37 °C (1 hour) and 42 °C (5 minutes). Signal enhancement/whitening in the supernatant of the TSL-Ho-microgels at 42 °C indicates the release of [Gd(HPDO3A)(H_2O)].

Figure 5 shows the signal intensity in the supernatant as well as in the microgel pellet for NTSL-Ho-microgels and TSL-Ho-microgels before mild hyperthermia, after incubation at 37 °C (1 hour) and 42 °C (5 minutes). In correspondence with Figure 4 no signal enhancement was detected neither in the microgel pellet nor in the supernatant for the NTSL-Ho-microgels at 37 and 42 °C. In contrast, there was a significant signal enhancement observed in the supernatant as well as in the microgel pellet upon incubation of the TSL-Ho-microgels at 42 °C, which indicates the release of [Gd(HPDO3A)(H_2O)]. When the signal intensities between the NTSL-Ho-microgels and the TSL-Ho-microgels are compared, a significantly higher signal is observed in the supernatant and microgel pellet of the TSL-Ho-microgels after incubation at 42 °C. This indicates that the TSL-Ho-microgels released at 42 °C. No significant difference in signal intensity was detected after incubation at 37 °C for 1 hour. Therefore, NTSL-Ho-microgels as well as TSL-Ho-microgels did not release at this temperature.

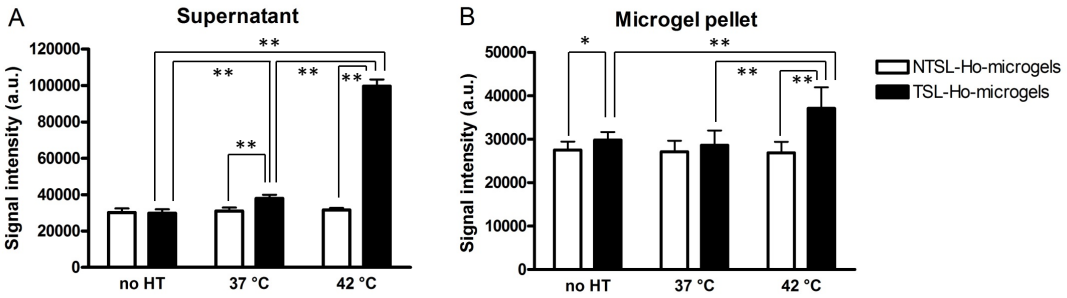

Figure 5. Signal intensity in the supernatant (A) and microgel pellet (B) of NTSL-Ho-microgel and TSL-Ho-microgel dispersions at room temperature (RT) and after incubation at 37 °C (1 hour) and 42 °C (5 minutes). An increase in signal intensity indicates the release of [Gd(HPDO3A)(H_2O)]. * p 0.01 – 0.05, ** p<0.0001

Additionally, the release of fluorescein was examined (Figure 6). Individual NTSL-Ho-microgels and TSL-Ho-microgels were imaged with a fluorescence microscope at room temperature and after mild hyperthermia for 10 seconds. Both types of microgels exhibited a homogeneous distribution of the fluorescein containing liposomes. For both NTSL-Ho-microgels and TSL-Ho-microgels no fluorescence signal was detected outside the microgels at room temperature indicating that all fluorescein remained encapsulated in the liposomes of NTSL/TSL-Ho-microgels. After mild hyperthermia, the fluorescence signal remained restricted to the NTSL-Ho-microgels. This indicates that the NTSL-Ho-microgels are stable during mild hyperthermia with no release of fluorescein. In contrast, after applying mild hyperthermia to TSL-Ho-microgels, the fluorescence signal was not restricted to the microgels only but also detected in the surrounding medium. This observation demonstrates that fluorescein was released from TSL-Ho-microgels.

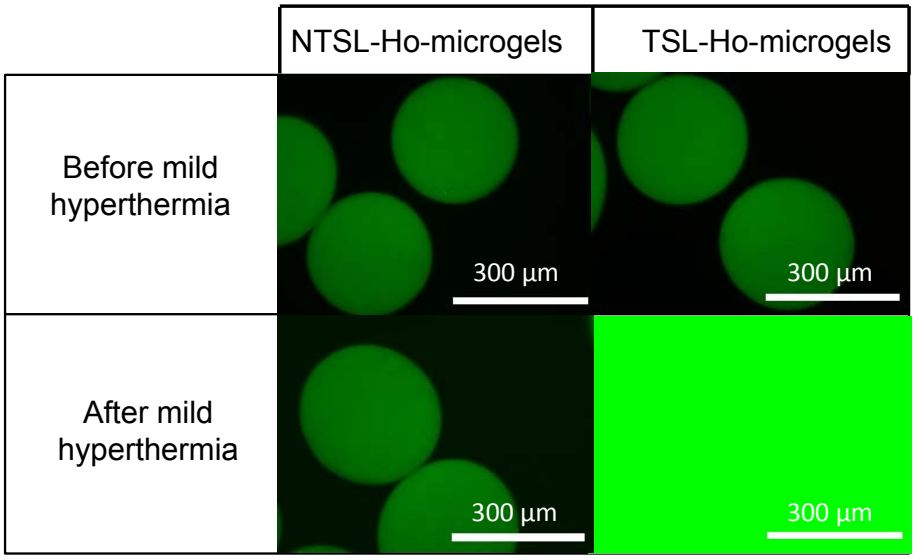

Figure 6. Fluorescence microscopy images of NTSL/TSL-Ho-microgels at room temperature and after incubation at mild hyperthermia for 10 seconds. Fluorescein appears green in these fluorescence images.

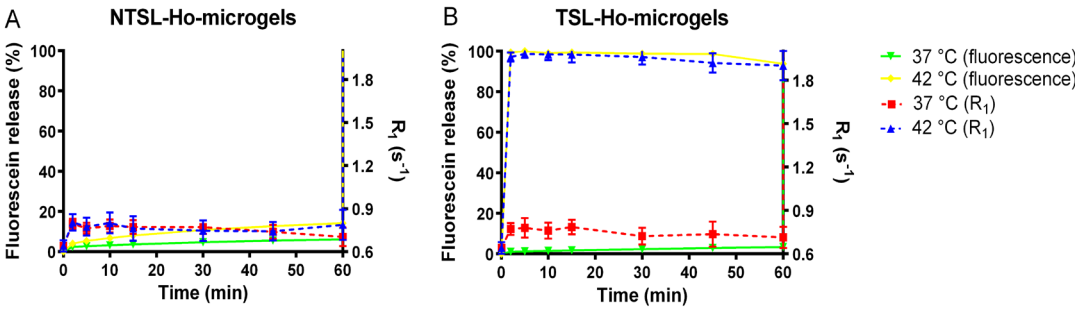

Figure 7. Release of fluorescein and [Gd(HPDO3A)(H_2O)] from NTSL-Ho-microgels (A) and TSL-Ho-microgels (B) at 37 and 42 °C in 20 mM HEPES buffer pH 7.4.

To investigate whether fluorescein and [Gd(HPDO3A)(H_2O)] are released completely and with the same kinetics, the release was monitored at 37 and 42 °C for 60 minutes (Figure 7). NTSL-Ho-microgels displayed hardly any release of fluorescein or [Gd(HPDO3A)(H_2O)] at 37 or 42 °C for 60 minutes, which is in line with the lack of release in case of NTSL only (Figure 4). As can be seen in Figure 7B, TSL-Ho-microgels released fluorescein and [Gd(HPDO3A)(H_2O)] only marginally at 37 °C demonstrating that TSL encapsulated in microgels do not release both markers at this temperature. When increasing the temperature to 42 °C, TSL-Ho-microgels released both fluorescein and [Gd(HPDO3A)(H_2O)] completely within 2 minutes. For both types of microgels (containing NTSL or TSL) the release kinetics matches the kinetics of the liposomes not encapsulated in microgels at the investigated temperatures.

This observation indicates that diffusion of fluorescein and [Gd(HPDO3A)(H_2O)] released after destabilization of the entrapped liposomes through the alginate matrix is fast. Alginate forms an open network after crosslinking and a mesh size between 10-60 nm has been reported after crosslinking a 2% alginate solution [62,63]. In this study, we used a higher alginate concentration (3% w/v), which increases the number of crosslinks resulting in a smaller mesh size. This mesh size is small enough to retain liposomes while small molecules like fluorescein (0.7 nm [64], 332.31 g/mol) and [Gd(HPDO3A)(H_2O)] (558.7 g/mol) can diffuse freely from this matrix. Furthermore, the fast release of fluorescein and [Gd(HPDO3A)(H_2O)] also demonstrates that no strong interactions between fluorescein/[Gd(HPDO3A)(H_2O)] and alginate exist.

Ex vivo embolization of a sheep kidney

The *ex vivo* sheep kidney used as an *ex vivo* model for embolization was derived from a terminated female sheep that was previously used as laboratory animal. A T_2^*-wt MR image of the *ex vivo* kidney before and after administration of TSL-Ho-microgels is shown in Figure 8. Prior to administration, the kidney tissue appeared relatively homogeneously on the MR image. After injection of the TSL-Ho-microgels, black spots appeared in the interlobular blood vessels at the start of the cortex of the kidney indicating the presence of clusters of TSL-Ho-microgels. This shows that TSL-Ho-microgels can be visualized by MRI in tissue as expected.

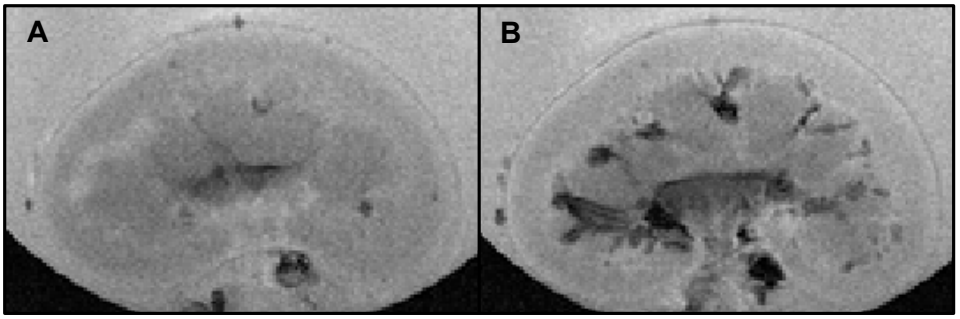

Figure 8. T_2^*-wt MR images of a sheep kidney before (A) and after (B) the administration of TSL-Ho-microgels. The black spots indicate the presence of TSL-Ho-microgels.

In our work, alginate microgels containing temperature sensitive liposomes were exploited for embolization. Several strategies for embolization have been reported previously. Clinically, a chemotherapeutic drug is administered followed by an embolic particle. This embolic particle reduces the wash out of the drug but still a part of the dose ends up in the blood circulation [22,23]. Drug eluting beads (DEB) were developed to simplify the embolization procedure and to reduce the systemic exposure. These DEBs show a sustained release of the loaded drug [23,24]. On the contrary, our TSL-Ho-microgels show complete and very rapid release after a mild hyperthermia pulse. With this strategy, a higher peak concentration of the drug can be reached in the tumor compared to DEBs. Another advantage is that TSL-Ho-microgels can be visualized by MRI during all stadia of the treatment. Importantly, also the drug release from our TSL-Ho-microgels can be monitored after mild hyperthermia using the MRI agent [Gd(HPDO3A)(H_2O)], which is also present in the aqueous core of the liposomes, as tracer.

Conclusion

This paper shows that temperature sensitive MR-imageable microgels that rapidly release their payload upon hyperthermia (42 °C) were successfully developed. The holmium ion content in the microgels was optimized to allow visualization of the microgels by MRI. The temperature triggered release of [Gd(HPDO3A)(H_2O)] was demonstrated with MRI, while fluorescein (a drug mimicking dye) release was visualized with fluorescence microscopy. Fluorescein and [Gd(HPDO3A)(H_2O)] were released at the same rate and extent, indicating that the release of [Gd(HPDO3A)(H_2O)] is expected to be a good indicator for the *in vivo* release of a cytostatic drug encapsulated in the aqueous core of the liposomes. It is concluded that these triggerable microgels are attractive systems for real-time, MR-guided embolization and triggered release of drugs.

Acknowledgement
Ullrich Jahnz from GeniaLab® is kindly acknowledged for his advice concerning the JetCutter system and Frederike Huissoon, FMC Biopolymers and IMCD Benelux B.V. for supplying the Manucol LKX. This research was performed within the framework of CTMM, the Center for Translational Molecular Medicine (www.ctmm.nl), project HIFU-CHEM (grant 030-301).

References

1. Maeda H. Tumor-selective delivery of macromolecular drugs via the EPR effect: background and future prospects. Bioconjug Chem 2010;21:797-802.
2. Bae YH, Park K. Targeted drug delivery to tumors: Myths, reality and possibility. J Control Release 2011;153:198-205.
3. Lammers T, Kiessling F, Hennink WE, Storm G. Drug targeting to tumors: principles, pitfalls and (pre-) clinical progress. J Control Release 2012;161:175-187.
4. Duncan R. Polymer therapeutics: Top 10 selling pharmaceuticals - What next? J Control Release 2014;190:371-80.
5. Wang Y, Grainger D. Barriers to advancing nanotechnology to better improve and translate nanomedicines. Front Chem Sci Eng 2014;8:265-275.
6. Torchilin VP. Targeted pharmaceutical nanocarriers for cancer therapy and imaging. AAPS J 2007;9:E128-47.
7. Torchilin VP. Recent advances with liposomes as pharmaceutical carriers. Nat Rev Drug Discov 2005;4:145-160.
8. Svenson S. Clinical translation of nanomedicines. Curr Opin Solid State Mater Sci 2012;16:287-294.
9. Barenholz Y(. Doxil (R) - The first FDA-approved nano-drug: Lessons learned. J Control Release 2012;160:117-134.
10. Allen TM, Cullis PR. Liposomal drug delivery systems: From concept to clinical applications. Adv Drug Deliv Rev 2013;65:36-48.
11. Northfelt DW, Dezube BJ, Thommes JA, Miller BJ, Fischl MA, Friedman-Kien A, et al. Pegylated-liposomal doxorubicin versus doxorubicin, bleomycin, and vincristine in the treatment of AIDS-related Kaposi's sarcoma: results of a randomized phase III clinical trial. J Clin Oncol 1998;16:2445-2451.
12. O'Brien ME, Wigler N, Inbar M, Rosso R, Grischke E, Santoro A, et al. Reduced cardiotoxicity and comparable efficacy in a phase III trial of pegylated liposomal doxorubicin HCl (CAELYX/Doxil) versus conventional doxorubicin for first-line treatment of metastatic breast cancer. Ann Oncol 2004;15:440-449.
13. Harris L, Batist G, Belt R, Rovira D, Navari R, Azarnia N, et al. Liposome-encapsulated doxorubicin compared with conventional doxorubicin in a randomized multicenter trial as first-line therapy of metastatic breast carcinoma. Cancer 2002;94:25-36.
14. Jain RK, Stylianopoulos T. Delivering nanomedicine to solid tumors. Nat Rev Clin Oncol 2010;7:653-664.
15. Needham D, Anyarambhatla G, Kong G, Dewhirst MW. A new temperature-sensitive liposome for use with mild hyperthermia: characterization and testing in a human tumor xenograft model. Cancer Res 2000;60:1197-1201.
16. van Elk M, Deckers R, Oerlemans C, Shi Y, Storm G, Vermonden T, et al. Triggered release of doxorubicin from temperature-sensitive poly(N-(2-hydroxypropyl)-methacrylamide mono/dilactate) grafted liposomes. Biomacromolecules 2014;15:1002-1009.

17. Tagami T, May JP, Ernsting MJ, Li S. A thermosensitive liposome prepared with a Cu2+ gradient demonstrates improved pharmacokinetics, drug delivery and antitumor efficacy. J Control Release 2012;161:142-149.
18. Limmer S, Hahn J, Schmidt R, Wachholz K, Zengerle A, Lechner K, et al. Gemcitabine treatment of rat soft tissue sarcoma with phosphatidyldiglycerol-based thermosensitive liposomes. Pharm Res 2014;31:2276-2286.
19. Kong G, Anyarambhatla G, Petros WP, Braun RD, Colvin OM, Needham D, et al. Efficacy of liposomes and hyperthermia in a human tumor xenograft model: importance of triggered drug release. Cancer Res 2000;60:6950-6957.
20. Manzoor AA, Lindner LH, Landon CD, Park J, Simnick AJ, Dreher MR, et al. Overcoming limitations in nanoparticle drug delivery: Triggered, intravascular release to improve drug penetration into tumors. Cancer Res 2012;72:5566-5575.
21. Li L, ten Hagen TLM, Haeri A, Soullie T, Scholten C, Seynhaeve ALB, et al. A novel two-step mild hyperthermia for advanced liposomal chemotherapy. J Control Release 2014;174:202-208.
22. Brown DB, Gould JE, Gervais DA, Goldberg SN, Murthy R, Millward SF, et al. Transcatheter therapy for hepatic malignancy: standardization of terminology and reporting criteria. J Vasc Interv Radiol 2009;20:S425-S434.
23. Lewandowski RJ, Geschwind J, Liapi E, Salem R. Transcatheter intraarterial therapies: Rationale and overview. Radiology 2011;259:641-657.
24. Lencioni R. Loco-regional treatment of hepatocellular carcinoma in the era of molecular targeted therapies. Oncology 2010;78:107-112.
25. Hong K, Khwaja A, Liapi E, Torbenson MS, Georgiades CS, Geschwind JFH. New intra-arterial drug delivery system for the treatment of liver cancer: Preclinical assessment in a rabbit model of liver cancer. Clin Cancer Res 2006;12:2563-2567.
26. Lewis AL, Dreher MR. Locoregional drug delivery using image-guided intra-arterial drug eluting bead therapy. J Control Release 2012;161:338-350.
27. Chung E, Kim H, Lee G, Kwak B, Jung J, Kuh H, et al. Design of deformable chitosan microspheres loaded with superparamagnetic iron oxide nanoparticles for embolotherapy detectable by magnetic resonance imaging. Carbohydr Polym 2012;90:1725-1731.
28. Kim JS, Kwak BK, Shim HJ, Lee YC, Baik HW, Lee MJ, et al. Preparation of doxorubicin-containing chitosan microspheres for transcatheter arterial chemoembolization of hepatocellular carcinoma. J Microencapsul 2007;24:408-419.
29. Chen J, Sheu AY, Li W, Zhang Z, Kim D, Lewandowski RJ, et al. Poly(lactide-co-glycolide) microspheres for MRI-monitored transcatheter delivery of sorafenib to liver tumors. J Control Release 2014;184:10-17.
30. Forster REJ, Thuermer F, Wallrapp C, Lloyd AW, Macfarlane W, Phillips GJ, et al. Characterisation of physico-mechanical properties and degradation potential of calcium alginate beads for use in embolisation. J Mater Sci Mater Med 2010;21:2243-2251.
31. Lewis AL, Gonzalez MV, Lloyd AW, Hall B, Tang YQ, Willis SL, et al. DC bead: In vitro characterization of a drug-delivery device for transarterial chemoembolization. J Vasc Interv Radiol 2006;17:335-342.
32. Lewis AL, Holden RR. DC Bead embolic drug-eluting bead: clinical application in the locoregional treatment of tumours. Expert Opin Drug Deliv 2011;8:153-169.
33. Poon RT, Tso WK, Pang RW, Ng KK, Woo R, Tai KS, et al. A phase I/II trial of chemoembolization for hepatocellular carcinoma using a novel intra-arterial drug-eluting bead. Clin Gastroenterol Hepatol 2007;5:1100-1108.
34. Varela M, Real MI, Burrel M, Forner A, Sala M, Brunet M, et al. Chemoembolization of hepatocellular carcinoma with drug eluting beads: efficacy and doxorubicin pharmacokinetics. J Hepatol 2007;46:474-481.

35. Dhanasekaran R, Kooby DA, Staley CA, Kauh JS, Khanna V, Kim HS. Comparison of conventional transarterial chemoembolization (TACE) and chemoembolization with doxorubicin drug eluting beads (DEB) for unresectable hepatocelluar carcinoma (HCC). J Surg Oncol 2010;101:476-480.
36. Nicolini D, Svegliati-Baroni G, Candelari R, Mincarelli C, Mandolesi A, Bearzi I, et al. Doxorubicin-eluting bead vs conventional transcatheter arterial chemoembolization for hepatocellular carcinoma before liver transplantation. World J Gastroenterol 2013;19:5622-5632.
37. Gasselhuber A, Dreher MR, Rattay F, Wood BJ, Haemmerich D. Comparison of conventional chemotherapy, stealth liposomes and temperature-sensitive liposomes in a mathematical model. PLoS One 2012;7.
38. Kerr DJ, Kerr AM, Freshney RI, Kaye SB. Comparative intracellular uptake of adriamycin and 4'-deoxydoxorubicin by nonsmall cell lung tumor cells in culture and its relationship to cell survival. Biochem Pharmacol 1986;35:2817-2823.
39. Oerlemans C, Seevinck PR, Smits ML, Hennink WE, Bakker CJG, van den Bosch MAAJ, et al. Holmium–lipiodol–alginate microspheres for fluoroscopy-guided embolotherapy and multimodality imaging. Int J Pharm 2014.
40. Lencioni R, de Baere T, Burrel M, Caridi JG, Lammer J, Malagari K, et al. Transcatheter treatment of hepatocellular carcinoma with doxorubicin-loaded DC Bead (DEBDOX): Technical recommendations. Cardiovasc Intervent Radiol 2012;35:980-985.
41. Ko JA, Lee YL, Jeong HJ, Park HJ. Preparation of encapsulated alliinase in alginate microparticles. Biotechnol Lett 2012;34:515-518.
42. Park H, Kim P, Hwang T, Kwon O, Park T, Choi S, et al. Fabrication of cross-linked alginate beads using electrospraying for adenovirus delivery. Int J Pharm 2012;427:417-425.
43. Hanus J, Ullrich M, Dohnal J, Singh M, Stepanek F. Remotely Controlled Diffusion from Magnetic Liposome Microgels. Langmuir 2013;29:4381-4387.
44. Prusse U, Dalluhn J, Breford J, Vorlop KD. Production of spherical beads by JetCutting. Chem Eng Technol 2000;23:1105-1110.
45. Oerlemans C, Seevinck PR, van de Maat GH, Boulkhrif H, Bakker CJG, Hennink WE, et al. Alginate-lanthanide microspheres for MRI-guided embolotherapy. Acta Biomater 2013;9:4681-4687.
46. Dai CY, Wang BC, Zhao HW, Li B, Wang H. Preparation and characterization of liposomes-in-alginate (LIA) for protein delivery system. Colloids Surf B Biointerfaces 2006;47:205-210.
47. Cohen R, Kanaan H, Grant GJ, Barenholz Y. Prolonged analgesia from Bupisome and Bupigel formulations: From design and fabrication to improved stability. J Control Release 2012;160:346-352.
48. Ullrich M, Hanus J, Dohnal J, Stepanek F. Encapsulation stability and temperature-dependent release kinetics from hydrogel-immobilised liposomes. J Colloid Interface Sci 2013;394:380-385.
49. Zielhuis SW, Seppenwoolde JH, Bakker CJG, Jahnz U, Zonnenberg BA, van het Schip AD, et al. Characterization of holmium loaded alginate microspheres for multimodality imaging and therapeutic applications. J Biomed Mater Res A 2007;82A:892-898.
50. Li S, Wang X, Zhang X, Yang R, Zhang H, Zhu L, et al. Studies on alginate-chitosan microcapsules and renal arterial embolization in rabbits. J Control Release 2002;84:87-98.
51. Eroglu M, Kursaklioglu H, Misirli Y, Iyisoy A, Acar A, Dogan AI, et al. Chitosan-coated alginate microspheres for embolization and/or chemoembolization: In vivo studies. J Microencapsul 2006;23:367-376.
52. Negussie AH, Yarmolenko PS, Partanen A, Ranjan A, Jacobs G, Woods D, et al. Formulation and characterisation of magnetic resonance imageable thermally sensitive liposomes for use with magnetic resonance-guided high intensity focused ultrasound. Int J Hyperthermia 2011;27:140-155.

53. Ponce AM, Viglianti BL, Yu D, Yarmolenko PS, Michelich CR, Woo J, et al. Magnetic resonance imaging of temperature-sensitive liposome release: Drug dose painting and antitumor effects. J Natl Cancer Inst 2007;99:53-63.
54. Anyarambhatla GR, Needham D. Enhancement of the phase transition permeability of DPPC liposomes by incorporation of MPPC: A new temperature-sensitive liposome for use with mild hyperthermia. J Liposome Res 1999;9:491-506.
55. Li L, ten Hagen TLM, Schipper D, Wijnberg TM, van Rhoon GC, Eggermont AMM, et al. Triggered content release from optimized stealth thermosensitive liposomes using mild hyperthermia. J Control Release 2010;143:274-279.
56. Lindner LH, Eichhorn ME, Eibl H, Teichert N, Schmitt-Sody M, Issels RD, et al. Novel temperature-sensitive liposomes with prolonged circulation time. Clin Cancer Res 2004;10:2168-2178.
57. DeRamos CM, Irwin AE, Nauss JL, Stout BE. C-13 NMR and molecular modeling studies of alginic acid binding with alkaline earth and lanthanide metal ions. Inorg Chim Acta 1997;256:69-75.
58. Smits ML, Nijsen JF, van den Bosch MA, Lam MG, Vente MA, Mali WP, et al. Holmium-166 radioembolisation in patients with unresectable, chemorefractory liver metastases (HEPAR trial): a phase 1, dose-escalation study. Lancet Oncol 2012;13:1025-1034.
59. Bruce DW, Hietbrink BE, DuBois KP. The acute mammalian toxicity of rare earth nitrates and oxides. Toxicol Appl Pharmacol 1963;5:750-759.
60. Haley TJ, Koste L, Komesu N, Efros M, Upham HC. Pharmacology and toxicology of dysprosium, holmium, and erbium chlorides. Toxicol Appl Pharmacol 1966;8:37-43.
61. http://www.microscopyu.com/tutorials/java/phasecontrast/shadeoff/. ;accessed December 2014.
62. Decho AW. Imaging an alginate polymer gel matrix using atomic force microscopy. Carbohydr Res 1999;315:330-333.
63. Turco G, Donati I, Grassi M, Marchioli G, Lapasin R, Paoletti S. Mechanical spectroscopy and relaxometry on alginate hydrogels: A comparative analysis for structural characterization and network mesh size determination. Biomacromolecules 2011;12:1272-1282.
64. Cvetkovic A, Picioreanu C, Straathof A, Krishna R, van der Wielent L. Relation between pore sizes of protein crystals and anisotropic solute diffusivities. J Am Chem Soc 2005;127:875-879.

6

Alginate microspheres containing temperature sensitive liposomes (TSL) for MR-guided embolization and triggered release of doxorubicin

Merel van Elk, Burcin Ozbakir, Angelique D. Barten-Rijbroek, Gert Storm, Frank Nijsen, Wim E. Hennink, Tina Vermonden and Roel Deckers

Submitted for publication

Abstract

The objective of this study was to develop and characterize alginate microspheres suitable for embolization with on-demand triggered doxorubicin (DOX) release and whereby the microspheres as well as the drug releasing process can be visualized *in vivo* using MRI. For this purpose, barium crosslinked alginate microspheres were loaded with temperature sensitive liposomes (TSL/TSL-Ba-ms), which release their payload upon mild hyperthermia. These TSL contained DOX and [Gd(HPDO3A)(H_2O)], a T_1 MRI contrast agent, for real time visualization of the release. Empty alginate microspheres crosslinked with holmium ions (T_2^* MRI contrast agent, Ho-ms) were mixed with TSL-Ba-ms to allow microsphere visualization. TSL-Ba-ms and Ho-ms were prepared with a homemade spray device and sized by sieving.

Encapsulation of TSL in barium crosslinked microspheres changed the triggered release properties only slightly: 95% of the loaded DOX was released from free TSL vs. 86% release for TSL-Ba-ms within 30 seconds in 50% FBS at 42 °C. TSL-Ba-ms (76 ± 41 μm) and Ho-ms (64 ± 29 μm) had a comparable size, which most likely will result in a similar *in vivo* tissue distribution after an i.v. co-injection and therefore Ho-ms can be used as tracer for the TSL-Ba-ms. MR imaging of a TSL-Ba-ms and Ho-ms mixture (ratio 95:5) before and after hyperthermia allowed *in vitro* and *in vivo* visualization of microsphere deposition (T_2^*-weighted images) as well as temperature-triggered release (T_1-weighted images). The [Gd(HPDO3A)(H_2O)] release and clusters of microspheres containing holmium ions were visualized in a VX_2 tumor model in a rabbit using MRI.

In conclusion, these TSL-Ba-ms and Ho-ms are promising systems for real-time, MR-guided embolization and triggered release of drugs *in vivo*.

Introduction

Liver cancer is the fifth most frequently diagnosed cancer in men and the second most frequent cause of cancer death worldwide. Among primary liver cancers, hepatocellular carcinoma (HCC) represents the major histological subtype, accounting for 70 to 85% of the total liver cancer burden worldwide [1]. More than 700.000 cases of this malignant disease are diagnosed yearly with a five year survival of less than 5% [2]. Nowadays, surgical resection is the primary curative therapy for patients with HCC. Unfortunately, only 20-35% of the patients are eligible for partial resection or liver transplantation and the recurrence rate is high [3-5]. Additionally, systemic chemotherapy is mostly ineffective for these patients because only low drug concentrations are reached in the tumor, while the treatment results in severe adverse events and patient morbidity [2,6].

Transarterial chemoembolization (TACE) is a more effective treatment modality than systemic chemotherapy [6,7]. During the TACE procedure, a catheter is positioned in the arterial supply of a tumor via which a chemotherapeutic drug is administered followed by embolic particles [8,9]. These embolic particles block the feeding vessels of the tumor and restrict nutrient and oxygen supply to the tumor cells. In addition, the blockage of the blood vessels by the embolic particles reduces the washout of the chemotherapeutic drug, which results in higher drug concentrations in the tumor area (i.e. increased efficacy) and reduced systemic exposure (i.e. less side effects) [9,10].

Recently, drug eluting beads (DEBs), which consist of embolic particles with sizes ranging from 70-150 μm to 500-700 μm and loaded with a chemotherapeutic drug, have been developed for the TACE procedure [9,11,12], delivering the embolic particles and the chemotherapeutic drugs at once [13-15]. One of the clinically used DEB formulations is based on crosslinked polyvinyl alcohol (PVA) modified with sulfonic acid groups to obtain negatively charged microspheres (DC beads®). A high drug concentration of positively charged cytostatics such as doxorubicin and irinotecan can be achieved in these PVA DEBs via an ion exchange mechanism [12,16,17]. Clinical trials have shown that embolization with DEBs leads to a significant reduction in peak plasma concentrations and area under the curve of doxorubicin [18,19] while increasing the antitumor efficacy compared to conventional TACE [20,21].

A drawback of these clinically used DEBs is, however, that they lack the ability to be visualized both during and after administration. Therefore, it is not possible to monitor the microsphere distribution in the tumor tissue, which is likely a very important factor for the treatment efficacy. Furthermore, the beads which are currently used for chemoembolization display a sustained release profile leading to low drug concentrations in the tumor over long periods of time (weeks) [17,22]. In contrast, it was recently shown by several studies that rapid intravascular release of doxorubicin from temperature sensitive liposomes leads to high intravascular drug concentrations, which subsequently enhances the drug penetration into the tumor [23-25]. This approach may lead to 20-30 times higher total drug deposition in tumor tissue compared to free drug administration and 5 times more than a Doxil-like formulation [26,27] thereby improving antitumor efficacy [26,28].

Therefore, the objective of this study was to develop and characterize microspheres that combine embolization with on-demand triggered drug release and whereby the microspheres as well as the drug releasing process can be visualized. To this end,

we previously encapsulated temperature sensitive liposomes in alginate microspheres [29]. Alginate microspheres have been used for arterial embolization [30,31] and showed to be excellent embolization agents on the short term as well as the long term [28,31,32]. Furthermore, MR imaging agents were incorporated in the microspheres (i.e. holmium ions; T_2^* contrast agent) as well as in the liposomes (i.e [Gd(HPDO3A)(H_2O)]; T_1 contrast agent) allowing the visualization of both the microspheres and the triggered drug release. In this article we take this concept to a next level by encapsulating a cytostatic drug (doxorubicin) and a contrast agent in the liposomes. Unfortunatly, the system described in our previous study [29] is not compatible with doxorubicin release since holmium ions used for crosslinking the alginate microspheres hamper doxorubicin release (see results and discussion section). Here an improved system, consisting of TSL loaded in barium crosslinked alginate microspheres (TSL-Ba-ms) and empty microspheres crosslinked with holmium ions (Ho-ms), is presented and characterized (Fig. 1). Moreover, the applicability of this system was evaluated *in vivo* in a VX_2 tumor in the auricle of a New Zealand White rabbit.

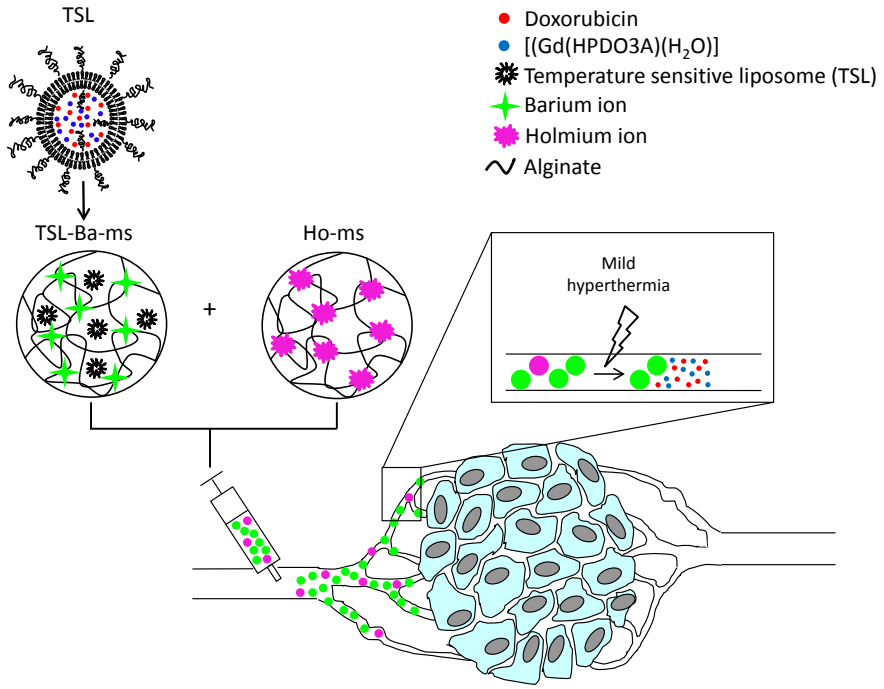

Fig. 1 Schematic representation of temperature sensitive liposomes (TSL) loaded in alginate microspheres crosslinked with barium ions (TSL-Ba-ms). The TSL are loaded with doxorubicin (DOX) and [Gd(HPDO3A)(H_2O)] (T_1 MRI contrast agent). The DOX and [Gd(HPDO3A)(H_2O)] will be released from the TSL-Ba-ms during mild hyperthermia. The release of [Gd(HPDO3A)(H_2O)] can be monitored by MRI. Empty alginate microspheres crosslinked with holmium ions (T_2^* MRI contrast agent, Ho-ms) are co-injected with TSL-Ba-ms to allow microsphere visualization by MRI.

Materials and methods

Materials

The phospholipids 1,2-dipalmitoyl-*sn*-glycero-3-phosphocholine (DPPC), and 1,2-distearoyl-*sn*-glycero-3-phosphoethanolamine-*N*-[amino(polyethylene glycol)-2000] (DSPE-PEG2.000) were purchased from Lipoid GmbH, Ludwigshafen, Germany, and 1-stearoyl-2-hydroxy-*sn*-glycero-3-phosphocholine (MSPC) was obtained from Avanti Polar Lipids, Alabaster, U.S.A. Doxorubicin-HCl was purchased from Guanyu bio-technology Co., LTD, Xi'an, China. [Gd(HPDO3A)(H_2O)] (Prohance®) was acquired from Bracco Diagnostic Inc., Monroe Township, U.S.A. Barium chloride dihydrate, Triton X-100, zinc sulfate heptahydrate, fetal bovine serum and ethylenediaminetetraacetic acid disodium salt dehydrate (EDTA) were purchased from Sigma-Aldrich Chemie BV, Zwijndrecht, The Netherlands. Holmium chloride hexahydrate was obtained from Metall rare earth limited, Shenzhen, China. Sodium alginate (Manucol LKX) was a gift from FMC biopolymer, Philadelphia, U.S.A.

Liposome preparation

Temperature sensitive liposomes (TSL) were prepared via the well-known lipid film hydration method as described previously [33,34]. DPPC, MSPC and DSPE-PEG2.000 were dissolved in chloroform (15 mL) in a molar ratio of 86:10:4. Chloroform was evaporated under reduced pressure to form a lipid film. Residual chloroform was removed overnight under a nitrogen flow. Next, the lipid film was hydrated in 20 mL 120 mM ammonium sulfate (pH 5.4) containing 375 mM [Gd(HPDO3A)(H_2O)] at 60 °C for 15 minutes (80 µmol phospholipids/mL). The liposomal dispersion was extruded through two 200 nm filters (2 times) and two 100 nm filters (8 times). The continuous phase of the liposome dispersion was substituted by 20 mM HEPES buffer pH 7.4 containing 8 g NaCl/L via a PD-10 gel filtration column. The liposomes (15 mL) were remotely loaded with doxorubicin (DOX, 15 mL, 5 mg/mL) at 37 °C for 90 minutes at a pH of 7.4 [35]. Unencapsulated DOX and [Gd(HPDO3A)(H_2O)] were removed by ultracentrifugation (125.000 g for 45 min at 4 °C). The liposomes were resuspended in 20 mM HEPES buffer pH 7.4 (15 mL) at a DOX concentration of 5 mg/mL.

Liposome characterization

Dynamic light scattering (DLS, Malvern ALV CGS-3 system) was used to determine the size of the liposomes and their polydispersity index. Intensity correlation functions were measured using a wavelength of 632.8 nm and a scattering angle of 90°. The measurements were performed in 20 mM HEPES buffer pH 7.4 at 25 °C.

In order to measure the loading efficiency, liposomes were disrupted with Triton X-100 (0.1% final concentration) and the DOX concentration in the samples was determined using fluorescence measurements (excitation wavelength 485 nm, emission wavelength 600 nm FLUOstar Optima, BMG Labtech). A calibration curve of DOX from 0 to 6 µg/mL in 20 mM HEPES buffer pH 7.4 containing 0.1% Triton X-100 was used to determine the DOX concentrations in the samples.

The temperature triggered release of DOX was measured by the change in fluorescence intensity in time (3 hours) at 37 and 42 °C (excitation wavelength 468 nm, emission wavelength 558 nm, Fluorolog connected to a water bath, Horiba scientific). DOX-

loaded liposomes (1 µL) were added to preheated (2 mL) 20 mM HEPES buffer (pH 7.4) or 50% fetal bovine serum (FBS) at 37 or 42 °C. Triton X-100 was added at the end of the experiment to destroy remaining liposomes and thereby release the DOX which was still encapsulated. The percentage DOX release at both temperatures was calculated using the following equation: $(I_t-I_0)/(I_{TX}-I_0)x100$ in which I_t is the fluorescence intensity at time t, I_0 the intensity at the start of the experiment and I_{TX} the fluorescence intensity after addition of Triton X-100.

Alginate microsphere preparation

The experimental setup for the preparation of alginate microspheres consisted of a homemade spraying device connected to a collecting vessel which is schematically displayed in Fig. 2. The spraying devise consisted of a syringe pump connected to a glass nozzle via plastic tubing. Furthermore, a nitrogen flow was connected to the nozzle to induce the formation of droplets.

All types of alginate microspheres used in this study (i.e. barium crosslinked microspheres encapsulating TSL and empty microspheres crosslinked with barium ions or holmium ions) were prepared with the following protocol. An alginate solution (3% w/v in 20 mM HEPES buffer pH 7.4) was passed through the nozzle (1.5 mL/min) simultaneously with nitrogen gas (0.8 Bar) to form alginate droplets. The droplets were hardened in a crosslinking solution containing 100 mM barium chloride or 100 mM holmium chloride. The microspheres were allowed to solidify for 2 hours in the crosslinking solution and subsequently they were sized with a 300 µm sieve to remove large microspheres and aggregates. In a second sieving step, the microspheres were collected on a 50 µm sieve and washed 3 times with 20 mM HEPES buffer pH 7.4 (in total 500 mL).

Microspheres loaded with TSL were prepared by mixing 6% alginate (w/v, in 20 mM HEPES buffer pH 7.4) in a 1:1 (w/w) ratio with TSL (resulting in a final alginate solution of 3% w/v containing 40 µmol phospholipids/mL). The alginate droplets were hardened in 20 mM HEPES buffer containing 100 mM barium chloride to form TSL-Ba-ms. Empty alginate microspheres crosslinked with barium ions (Ba-ms) were prepared by spraying the alginate solution (3% w/v) in 20 mM HEPES buffer pH 7.4 containing 100 mM barium chloride. Alginate microspheres crosslinked with holmium ions (Ho-ms) were prepared by spraying the alginate solution in a crosslinking aqueous solution of 100 mM holmium chloride.

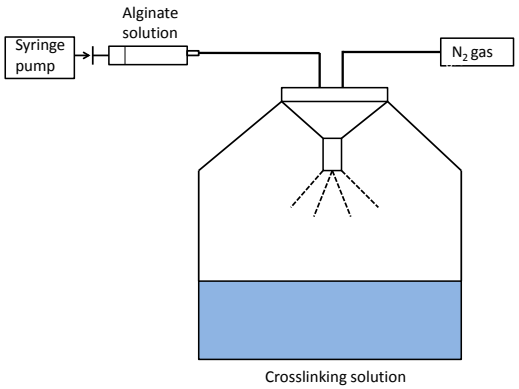

Fig. 2 Experimental setup for the preparation of alginate microspheres.

Microsphere characterization

Morphological examination and size distribution determination of the microspheres before and after sieving were investigated with fluorescence (TSL-Ba-ms) and bright-field (Ho-ms) microscopy (BZ-9000, Keyence equipped with a GFP BP filter with an excitation wavelength of 472-30 nm and an emission wavelength of 520-35 nm and a Plan Fluor 20x lens, Nikon). The images were analyzed with calibrated BZ II Analyzer software to determine the diameter of the microspheres. The average size of the microspheres was based on the measured diameter of 500 microspheres.

In order to determine the DOX concentration in the TSL-Ba-ms, 30 mg of wet TSL-Ba-ms was disrupted in 20 mL ethylenediaminetetraacetic acid (EDTA, 5% w/v in reverse osmosis water) containing 0.1% Triton X-100. Subsequently, the DOX concentration in TSL-Ba-ms was determined by fluorescence measurements as described above.

The DOX release kinetics from TSL-Ba-ms were examined at 37 and 42 °C whereby the DOX concentration in the samples was measured by UPLC. Preheated medium (20 mL, 20 mM HEPES buffer pH 7.4 or 50% FBS) at 37 or 42 °C was added to TSL-Ba-ms (75 mg wet weight) and samples (1.5 mL) were taken in time. Subsequently, the samples were mixed with the same volume of cold (4 °C) 20 mM HEPES buffer pH 7.4 to prevent further leakage of DOX. The samples were divided into two vials; one vial was used to determine the amount DOX released and the second vial was used to determine the total amount of DOX.

Release samples (1 mL) containing FBS were centrifuged (2000 g, 5 min, 4 °C) to sediment the microspheres. Acetonitrile (0.25 mL) and an aqueous solution of $ZnSO_4$ (0.6 gr/mL, 35 µL) were added to the supernatant (0.75 mL) to precipitate proteins [36] and avoid clogging of the UPLC column, followed by another centrifugation step. An aqueous solution of $ZnSO_4$ (0.6 gr/mL, 45 µL), acetonitrile (333 µL) and Triton X-100 (10%, 10 µL) were added to the second vial containing 1 mL sample for the determination of the total amount DOX present in the FBS samples. These samples were also centrifuged prior to UPLC measurements.

Release samples in HEPES buffer were centrifuged and 0.25 mL acetonitrile was added to 0.75 mL supernatant. EDTA (5%, 2 mL) and Triton X-100 (10%, 20 µL) were added to the second vial containing 1 mL sample for the determination of the total amount DOX. Subsequently, the samples were centrifuged and 0.25 mL acetonitrile was added to 0.75 mL supernatant.

DOX concentrations in the TSL-Ba-ms samples were determined by UPLC using a BEH C18 1.7 µm column (Waters) at 50 °C and a fluorescence detector (excitation wavelength 480 nm, emission wavelength 585 nm). The eluent consisted of 1% perchloric acid and 25% acetonitrile in milli-Q water at an elution rate of 0.5 mL/min. The injection volume was 7.5 µL and the chromatographic runtime per sample was 3 minutes.

Magnetic resonance imaging (MRI) was used to visualize the Ho-ms and to monitor the temperature triggered [Gd(HPDO3A)(H_2O)] release from the TSL-Ba-ms. Four different samples were imaged (i.e. TSL-Ba-ms:Ho-ms (95:5 and 100:0), and Ba-ms:Ho-ms (95:5 and 100:0)) before and after mild hyperthermia (15 minutes at 42 °C) using the MRI sequences as described below. This allows distinghuishing of the contribution of each component in this system (i.e. [Gd(HPDO3A)(H_2O)], barium and holmium ions) on the MRI visualization of microspheres and/or [Gd(HPDO3A)(H_2O)] release.

Magnetic resonance imaging

All MRI experiments were performed on a clinical 1.5-Tesla MR scanner (Achieva; Philips Health care) with an 8 elements head coil (*in vitro* experiment) or a 47 mm microscopy coil (*in vivo* experiment).

The following MR sequences were used in this study: T_1-weighted MR images were obtained using a spin echo sequence (TR = 450 ms, TE = 18 ms, FA = 90°, turbo-factor = 3, 16 slices, voxel size = 0.30x0.30x2.0 mm^3). T_2^*-weighted MR images were obtained using a 3D gradient echo sequence (TR = 15.1 ms, TE = 9.20 ms, FA = 30°, 32 slices, voxel size = 0.30x0.30x1.0 mm^3). Furthermore, T_1-maps were obtained by sampling the signal recovery after inversion using a Look-Locker (LL) sequence (TR = 7.44 ms, TE = 3.5 ms, FA = 5°, turbo-factor = 5, 1 slice, voxel size = 0.80×0.80×3mm^3, 50 timepoints at 60 ms interval).

The images obtained from each LL measurement were automatically fitted with in-house developed Matlab software (7.12, The MathWorks Inc., Natick, MA, USA, 2000). The temporal evolution of the magnitude of the longitudinal magnetization (M) was fitted (Levenberg-Marquardt algorithm) for each pixel with the following equation:

$$M = |A-(A+B)\cdot e^{-t/T1^*}| \qquad (1)$$

Where T_1^* is the apparent longitudinal relaxation rate, t is the time after the inversion pulse and A and B are constants. The sample T_1 differs from T_1^* by an offset only dependent on flip angle (α) and delay between 2 consecutive excitation pulses (Δt):

$$1/T_1 = 1/T_1^* + \ln(\cos\alpha)/\Delta t \qquad (2)$$

Finally, T_2^*-maps were obtained by sampling the signal decay using a multi-echo gradient echo sequence (TR = 100 ms, TE = 8 ms, ΔTE = 8 ms, 8 echos, FA = 90°, turbo-factor = 8, 1 slice, voxel size = 0.80×0.80×3 mm^3).

For the *in vitro* experiment (see section 2.5) the samples were placed in a sample holder containing water, which was placed in the middle of the 8 elements head coil for imaging. For the *in vivo* experiment (see section 2.8) the tumor bearing ear was placed in the middle of a 4.7 cm microcoil.

For T_1 and T_2^* quantification one square ROI (5x5 pixels) was manually selected inside the microsphere pellet and supernatant before and after heating.

Animal model

All experimental protocols and procedures were approved by the local experimental animal welfare committee and conform the national and European regulations for animal experimentation. Female New Zealand White rabbits (2.5-3.5 kg) were purchased from Charles River, France. All rabbits were allowed to acclimatize for at least one week before use.

VX_2 tumor cells [37,38] were propagated in both flanks of a New Zealand White rabbit (analgesia with 4 mg/kg Carprofen®). The tumor was removed under analgesia and sedation (Carprofen® 4 mg/kg, Dexdormitor® 0.125 mg/kg and Narketan® 15 mg/kg) when reaching a tumor diameter of ~ 3 cm. A VX_2 cell suspension was generated by dissecting and fragmenting tumor tissue using a cellstrainer (Easystrainer 100 µm, Greiner Bio-One). A tumor in the auricle of a New Zealand White rabbit was induced by injecting 200 µL of the cell suspension ($8.5x10^8$ cells/mL PBS) subcutaneously into the auricle of the rabbit under analgesia and anesthesia (Carprofen® 4 mg/kg, Dexdormitor® 0.125 mg/kg and Narketan® 15 mg/kg).

***In vivo* imaging**

When the tumor in the auricle reached a diameter of ~2 cm after 2 weeks the *in vivo* imaging study was performed. Carprofen® (4 mg/kg, 0.25 mL), Dexdormitor® (0.125 mg/kg, 0.75 mL) and Narketan® (15 mg/kg, 0.45 mL) were administered subcutaneously for analgesia and anesthesia. The rabbit was positioned in the MRI scanner with the tumor bearing auricle in a warm water bath at 37 °C. A mixture of 152 mg TSL-Ba-ms and 8 mg Ho-ms suspended in 1 mL mM HEPES buffer pH 7.4 was injected intratumorally. Next, the water bath in which the tumor was positioned, was heated up to 46 °C (such that the interior of the tumor reached at least 42 °C) for 15 minutes to induce release of [Gd(HPDO3A)(H_2O)]. T_1 and T_2^*-weighted images and T_1 and T_2^* maps were made (as described in section 2.6) prior to the injection of the microspheres and immediately after the intratumoral injection of the microspheres as well as after the incubation at elevated temperatures.

Results and discussion

Preparation and characterization of temperature sensitive liposomes encapsulating doxorubicin (DOX) and [Gd(HPDO3A)(H_2O)]

Temperature sensitive liposomes (TSL) containing lysolipids were prepared via the lipid film hydration method (the characteristics of the TSL are described in table 1) [35,39]. These TSL were passively loaded with [Gd(HPDO3A)(H_2O)] (a T_1 MRI contrast agent) during hydration of the lipid film and subsequently remotely loaded with doxorubicin (DOX). The mean diameter of the liposomes was 134 nm with a PDI ≤ 0.1. The encapsulation efficiency of DOX was nearly quantitative as expected for remotely loaded liposomes [35,40].

Table 1 Characteristics of temperature senstitive liposomes (TSL) loaded with DOX and [Gd(HPDO3A)(H_2O)].

	TSL
Lipid composition	DPPC:MSPC:DSPE-PEG2.000
Molar ratio lipids (feed ratio)	86:10:4
Mean diameter (PDI)	134 nm (0.09 +/- 0.02)
DOX encapsulation (%)	>99%

Fig. 3 shows the release of DOX from TSL before encapsulation in the alginate microspheres as a function of incubation time at 37 and 42 °C in 20 mM HEPES buffer pH 7.4 (Fig. 3A) and in 50% fetal bovine serum (FBS) (Fig. 3B), respectively. TSL released less than 10% of their content after 3 hours incubation in HEPES buffer at 37 °C while at 42 °C complete release took place within 30 seconds. In 50% FBS at 37 °C, the TSL showed a release of ~15% within 5 minutes and reached 30% release after 3 hours. The release rate at 37 °C in 50% FBS was higher than in HEPES buffer (Figure 3 A-B) likely because proteins destabilized the lipid bilayer [41-43]. At 42 °C more than 95% of the loaded DOX was released within 30 seconds in 50% FBS (Figure 3B), which is comparable with the release of DOX in HEPES buffer at the same temperature, indicating that DOX is released nearly quantitatively at 42 °C independent of the presence of proteins in the release medium.

Preparation of barium crosslinked alginate microspheres loaded with TSL (TSL-Ba-ms)

Alginate microspheres containing TSL were prepared with the spraying device shown in Fig. 2. An alginate solution containing TSL was sprayed into 20 mM HEPES buffer pH 7.4 containing 100 mM barium chloride. The mean diameter of the unfractionated TSL-Ba-ms was 30 µm with a standard deviation of 21 µm while the mean diameter was 76 µm with a standard deviation of 41 µm after sieving (Fig. 4C-D). This demonstrates that many microspheres had a size below 50 µm, which were subsequently successfully removed by sieving. The encapsulation efficiency of TSL into the alginate microspheres was 60% based on DOX measurements. This relatively low encapsulation efficiency is based on the instability of TSL in the alginate solution since alginate can be inserted into the lipid bilayer [44] leading to DOX leakage from the TSL before formation of the TSL-Ba-ms. The presence of DOX loaded liposomes in the alginate microspheres could also be qualitatively observed with fluorescence microscopy (Fig. 4A).

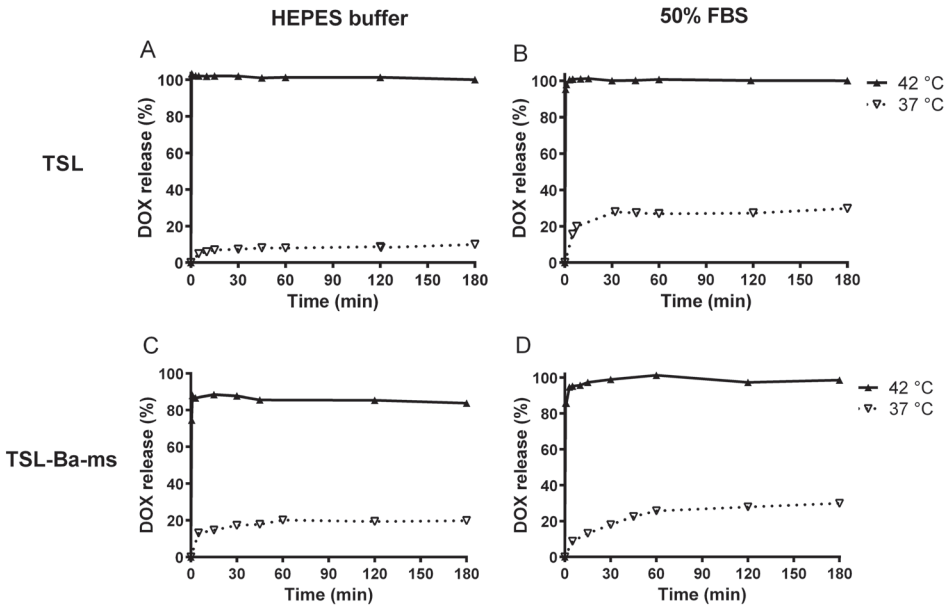

Fig. 3 Temperature triggered release of DOX from TSL (DPPC:MSPC:DSPE-PEG2.000 86:10:4) in 20 mM HEPES buffer pH 7.4 (A) or 50% fetal bovine serum (B) at 37 and 42 °C. Temperature triggered DOX release from TSL-Ba-ms in 20 mM HEPES buffer pH 7.4 (C) and 50% FBS (D) at 37 and 42 °C.

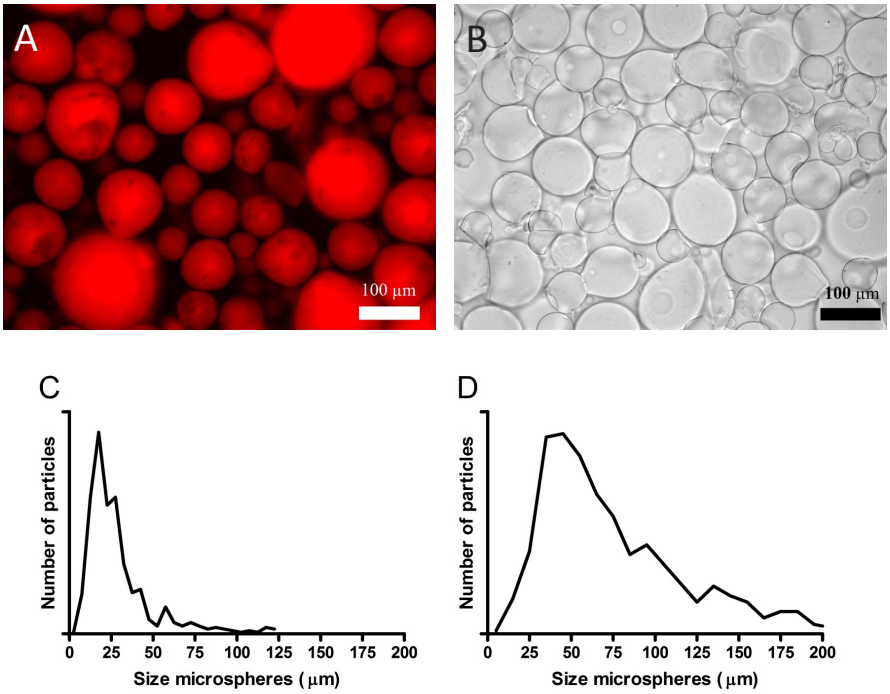

Fig. 4 Fluorescence microscopy image of TSL-Ba-ms (A) and bright-field microscopy image of alginate microspheres crosslinked with holmium ions (Ho-ms) (B) after sieving. The size distribution of TSL-Ba-ms before (C) and after (D) sieving was analyzed with calibrated BZ II Analyzer software.

Characterization of empty alginate microspheres crosslinked with holmium ions
Empty microspheres crosslinked with solely holmium ions (Ho-ms) were prepared and sieved similar to the TSL-Ba-ms described above. This resulted in Ho-ms with a mean diameter of 64 μm and a standard deviation of 29 μm (Fig. 4B), which is similar to the diameter of TSL-Ba-ms (Fig. 4A). Since Ho-ms and TSL-Ba-ms have a comparable size, they most likely have a similar *in vivo* tissue distribution after an i.v. co-injection and therefore Ho-ms can be used as tracer for the TSL-Ba-ms.

Release of doxorubicin (DOX) from TSL-Ba-ms
The release of DOX from TSL-Ba-ms at 37 and 42 °C in 20 mM HEPES buffer pH 7.4 (Fig. 3C) and the same buffer with 50% FBS (Fig. 3D) was evaluated over a time period of 3 hours. At 37 °C, TSL-Ba-ms displayed a marginal release (20%) of DOX after incubation in HEPES buffer for 3 hours. At 42 °C, approximately 75% of DOX was released within 30 seconds while a maximum release of 85% was achieved after 1 minute in HEPES buffer. This incomplete DOX release from TSL-Ba-ms in HEPES buffer (containing 0.8% NaCl) is most likely due to the interaction of positively charged DOX and negatively charged alginate. Addition of Triton X-100 did not lead to extra release of DOX which would be the case if some liposomes remained intact after applying mild hyperthermia. The incomplete release of DOX was also observed visually since TSL-Ba-ms remained slightly pink after incubation at 42 °C.
In 50% FBS, TSL-Ba-ms showed a DOX release of 30% after 3 hours incubation at 37 °C. At 42 °C however, the TSL-Ba-ms released DOX nearly quantitatively within 3 minutes. The difference in DOX release found in HEPES and 50% FBS can be explained by the presence of proteins. Presumably, proteins in the release medium desorb DOX from the negatively charged alginate since it is reported in other studies that DOX can interact with plasma proteins [45,46].
Previously, we prepared microspheres containing liposomes which were crosslinked with barium as well as holmium ions in a molar ratio of 95:5 [29]. When TSL containing DOX were loaded into these microspheres, no release of DOX occurred upon mild hyperthermia. Likely, the released DOX interacted with the holmium ions present in the microspheres since a color shift from red to purple was observed during incubation at 42 °C. This holmium-DOX complexation was reported previously [47,48] and also evidenced by the fact that the purple color of a solution containing DOX and holmium ions returned to red after the addition of EDTA, which captures the holmium ions (data not shown). Thus it was concluded that DOX was released from the liposomes during mild hyperthermia, however the formation of holmium ion-DOX complexes prevented the release of DOX from the microspheres.

Visualization of microspheres and [Gd(HPDO3A)(H_2O)] release by MRI
As mentioned in the introduction holmium ions and [Gd(HPDO3A)(H_2O)] are MRI contrast agents that allow visualization of the microspheres and triggered drug release, respectively. To investigate in more detail the contribution of each component in our system (i.e. barium ions, holmium ions and [Gd(HPDO3A)(H_2O)]) on the MR signal, T_1 and T_2^*-weighted (wt) MR images were obtained of i) TSL-Ba-ms mixed with Ho-ms (ratio 95:5), ii) TSL-Ba-ms only, iii) Ba-ms mixed with Ho-ms (ratio 95:5) and iv) Ba-ms only.

Fig. 5 shows T_2^*-wt and T_1-wt MR images of these four combinations before and after incubation at mild hyperthermia (42 °C for 15 minutes). The microspheres sedimented and the microspheres were therefore present in a pellet at the bottom of the tube. As expected, the holmium containing microspheres were clearly detectable as a black layer on the T_2^*-wt image before and after mild hyperthermia (Fig. 5I, J, M, N), whereas microspheres containing barium only (Ba-ms) were not observed on T_2^*-wt images (Fig. 5O, P). Interestingly, TSL-Ba-ms were also clearly detectable on T_2^*-wt images before hyperthermia because of the T_2^*-effect of [Gd(HPDO3A)(H_2O)] at high concentrations (Fig. 5K). However, upon temperature triggered release and subsequent dilution of [Gd(HPDO3A)(H_2O)], the T_2^*-effect of gadolinium decreased and the TSL-Ba-ms were no longer visible on the T_2^*-wt image (Fig. 5L). The temperature triggered [Gd(HPDO3A)(H_2O)] release was best visualized on T_1-wt images (Fig. 5A-D). These images show a significant increase in signal intensity in the microsphere pellet as well as in the supernatant of the TSL-Ba-ms after applying mild hyperthermia (Fig. 5B, D). This demonstrates that MRI allows the visualization of the microspheres (containing holmium ions) as well as the release of [Gd(HPDO3A)(H_2O)] at the same location in an *in vitro* situation.

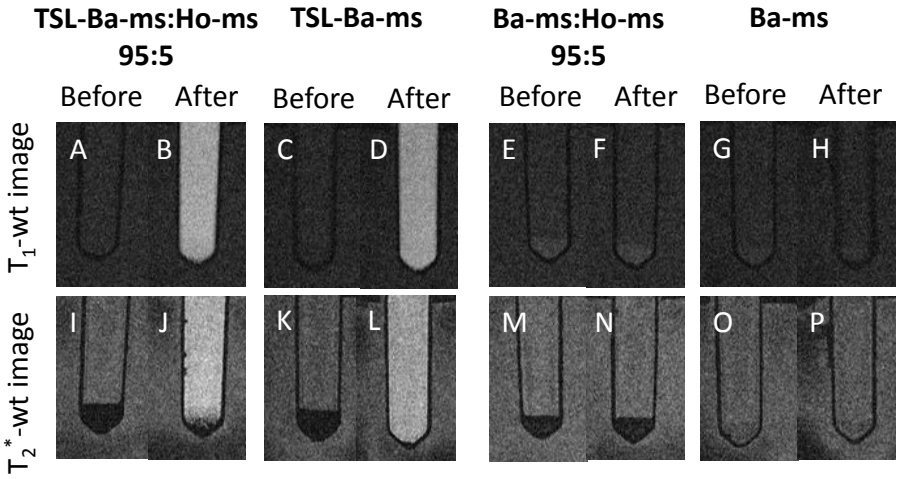

Fig. 5 T_1 and T_2^*-weighted MR images of TSL-Ba-ms or Ba-ms mixed with or without Ho-ms (ratio 95:5) before mild hyperthermia and after incubation at 42 °C for 15 minutes. Signal enhancement in the supernatant after mild hyperthermia indicates release of [Gd(HPDO3A)(H_2O)] in the T_1-wt image. The holmium ions appear hypointense in the T_2^*-wt image due to local distortion of the magnetic field.

Additionally, quantitative T_1 and T_2^*-mapping was performed of the same samples described above (i.e TSL-Ba-ms mixed with Ho-ms (ratio 95:5), TSL-Ba-ms only, Ba-ms mixed with Ho-ms (ratio 95:5) and Ba-ms only) before and after mild hyperthermia (Fig. 6). Furthermore, HEPES and a free [Gd(HPDO3A)(H_2O)] solution, at approximately the same concentration (0.5 mM) as obtained after [Gd(HPDO3A)(H_2O)] release from the TSL-Ba-ms, were included as control samples. Figure 6 shows the mean T_1 and T_2^*-values in a region of interest (ROI) postioned in the microsphere pellet (if present) or the supernatant. The T_2^*-values of the supernatant are not shown because they were too long to be adequately measured with the sequence used. The T_1-value of the samples containing TSL-Ba-ms decreased in the microsphere pellet as well as in the supernatant after mild hyperthermia (Fig. 6A-B). The T_1-values of these samples after heating were the same as the T_1 of free [Gd(HPDO3A)(H_2O)] at the same concentration in the microsphere pellet as well as in the supernatant, indicating quantitative release of [Gd(HPDO3A)(H_2O)] from TSL-Ba-ms after applying hyperthermia. As expected, Ba-ms did not show a change in T_1-value before and after applying mild hyperthermia. The presence of 5% Ho-ms had only a minor effect on the T_1-values of the microsphere pellet and the supernatant and therefore does not interfere with the detection of released [Gd(HPDO3A)(H_2O)]. In contrast, the T_2^*-value of samples containing Ho-ms was, as expected, very short in the presence of Ho-ms before and after mild hyperthermia (Fig. 6C). As explained previously, [Gd(HPDO3A)(H_2O)] exhibits a strong T_2^*-effect at high concentrations (i.e. loaded in TSL). Therefore, the hyperthermia triggered release of [Gd(HPDO3A)(H_2O)] caused an increase of T_2^* in the TSL-Ba-ms pellet, which confirms the necessity of Ho-ms for visualizing the microsphere distribution after applying hyperthermia.

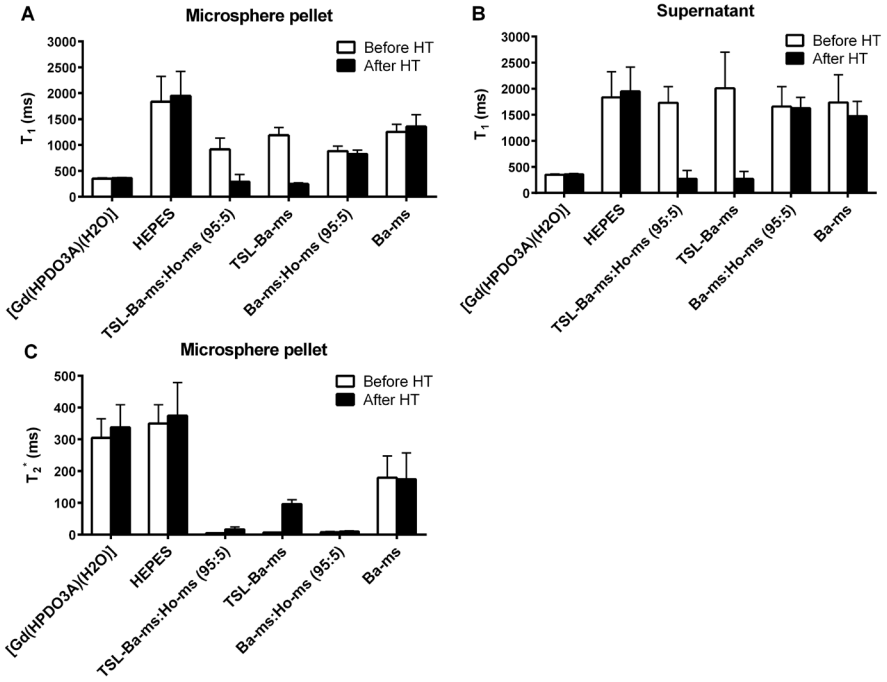

Fig. 6 T_1 in the microsphere pellet (A) and supernatant (B) and T_2^* in the microsphere pellet (C) of alginate microspheres before and after mild hyperthermia (HT; 42 °C for 15 minutes). A region of interested (ROI) was positioned in the microsphere pellet (if present) or the supernatant to determine the T_1 and T_2^*-values (Mean + standard deviation).

***In vivo* visualization of the release of [Gd(HPDO3A)(H_2O)] and the distribution of TSL-Ba-ms and Ho-ms in a VX_2 tumor present in the auricle of a rabbit**

The feasibility of TSL-Ba-ms and Ho-ms (in a ratio of 95:5) to allow *in vivo* monitoring of the microsphere deposition and [Gd(HPDO3A)(H_2O)] release was evaluated in the auricle tumor of a rabbit after intratumoral injection of TSL-Ba-ms and Ho-ms. In addition, the hypothesis that the Ho-ms co-localize with TSL-Ba-ms and therefore can be used as a tracer for TSL-Ba-ms, was investigated. T_1 and T_2^*-wt images and T_1 and T_2^*-maps were made at 3 timepoints: i) before intratumoral injection of the microspheres, ii) immediately after the intratumoral co-injection of TSL-Ba-ms and Ho-ms (95:5 ratio) and iii) shortly after applying mild hyperthermia. The tumor tissue looked relatively homogeneous on the T_2^*-wt image prior to administration (Fig. 7A). Intratumoral co-injection of TSL-Ba-ms and Ho-ms (95:5) caused signal voids on the T_2^*-wt images indicating the presence of microsphere clusters in the tumor (Fig. 7B). These clusters were still visible as signal voids on the T_2^*-wt images after applying mild hyperthermia for 15 minutes (Fig. 7C). The T_2^*-maps showed the same response: intratumoral co-injection of the microspheres caused a significant shortening of the T_2^* in the tumor (Fig. 7D-E), whereas the application of hyperthermia did not influence the T_2^* of the tumor (Fig. 7E-F).

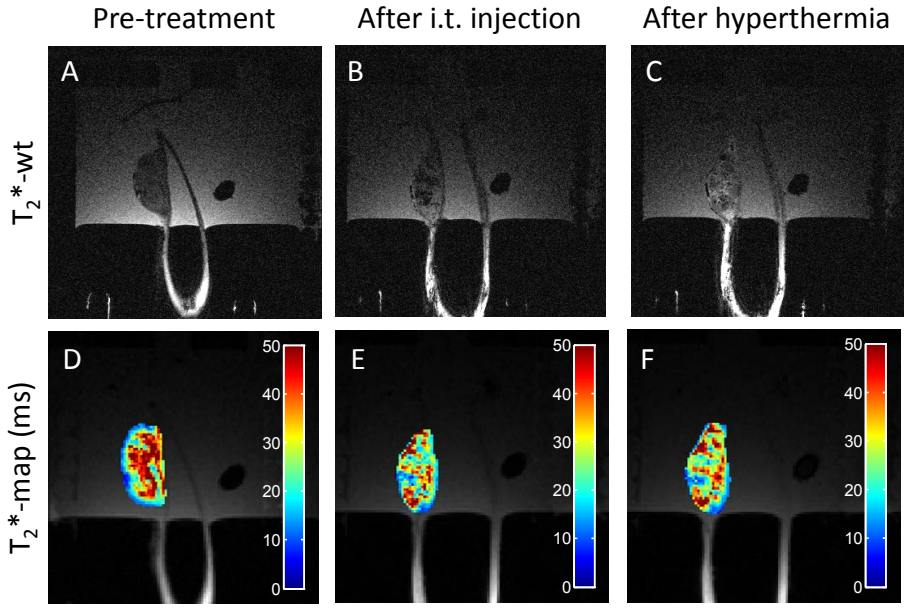

Fig. 7 T_2^*-wt images (A-C) and T_2^*-maps (D-F) of a tumor in the auricle of a New Zealand White rabbit before (A, D) and after (B, E) intratumoral injection of TSL-Ba-ms and Ho-ms. Finally, the tumor was heated in the range between 42 and 46 °C for 15 minutes (C, F).

No significant difference in tumor T_1-values was observed after intratumoral co-injection of the microspheres (Fig. 8A-B). This indicates that [Gd(HPDO3A)(H_2O)] was not released and thus the TSL loaded into the microspheres remained intact during the injection of the microspheres. After the intratumoral co-injection of the microspheres, the tumor was heated in the range between 42 and 46 °C for 15 minutes to trigger the release of [Gd(HPDO3A)(H_2O)] from the liposomes and subsequently from the TSL-Ba-ms. A significant drop in T_1-values was observed in the tumor after applying hyperthermia, indicating release of [Gd(HPDO3A)(H_2O)] from the TSL-Ba-ms (Fig. 8C).
The T_1-wt images showed the same response: the tumor tissue looked relatively homogeneous on the T_1-wt image prior to administration (Fig. 8D), whereas the co-injection of the microspheres followed by applying hyperthermia caused a shortening in T_1 (Fig. 8E).
Furthermore, the location of Ho-ms (i.e. largest change in T_2^*-value) corresponded very closely with the location of the TSL-Ba-ms (i.e. largest change in T_1-value) making Ho-ms a suitable tracer for TSL-Ba-ms.

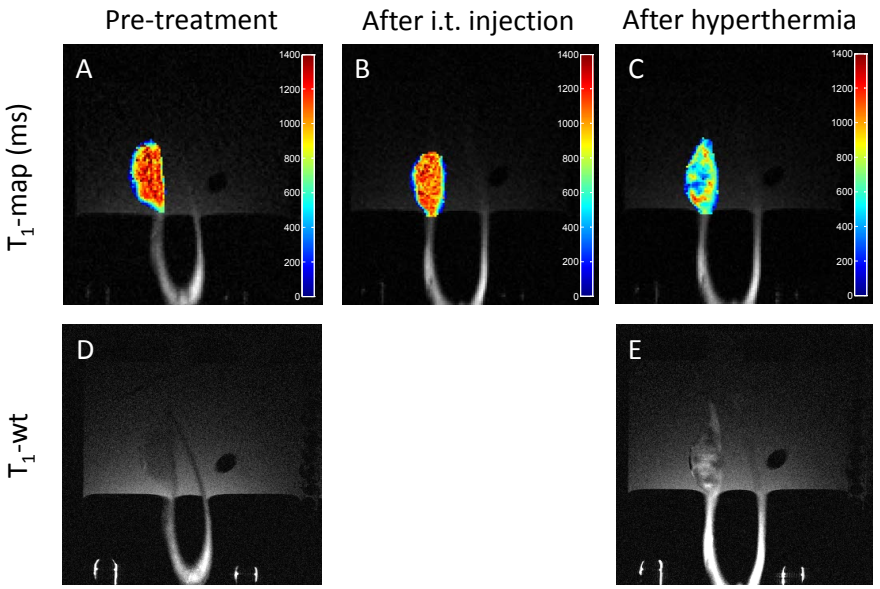

Fig. 8 T_1-maps (A-C) and T_1-wt images (D-E) of a tumor in the auricle of a New Zealand White rabbit before (A,D) and after (B) intratumoral co-injection of TSL-Ba-ms and Ho-ms. Finally, the tumor was heated in the range between 42 and 46 °C for 15 minutes (C,E).

Conclusion

This paper shows that alginate microspheres encapsulating temperature sensitive liposomes containing a T_1 MRI contrast agent ([Gd(HPDO3A)(H_2O)]) and doxorubicin (DOX) (TSL-Ba-ms) were successfully developed. The encapsulation of TSL in Ba-ms changed the triggered release properties only slightly. Also empty holmium (T_2^* MRI contrast agent) crosslinked microspheres (Ho-ms) were prepared. The incorporation of MR imaging agents in the microspheres (i.e. holmium ions in Ho-ms) as well as in the liposomes ([Gd(HPDO3A)(H_2O)] in TSL-Ba-ms) allowed for visualization of both the microspheres and the triggered drug release *in vitro* using MRI. The microsphere deposition and [Gd(HPDO3A)(H_2O)] release after intratumoral co-injection of TSL-Ba-ms and Ho-ms was monitored in the VX_2 tumor model. The deposition of Ho-ms overlapped very closely with the location of the [Gd(HPDO3A)(H_2O)] release from TSL-Ba-ms making Ho-ms a suitable tracer for TSL-Ba-ms. In this study, the microspheres were injected intratumoral but these microspheres are developed for embolization. Therefore, a future study on tumor embolization is needed that also investigates the antitumor efficacy of the proposed system compared to free DOX and standard TACE.
Taken together, these microspheres are attractive systems for real-time, MR-guided embolization and triggered release of drugs.

Acknowledgement
Frederike Huissoon from FMC Biopolymers and IMCD Benelux B.V. is kindly acknowledged for providing Manucol LKX and Dr. Michal Heger from the department of Experimental Surgery, Academic Medical Center, Amsterdam is acknowledged for kindly providing the VX_2 cells. Dr. Clemens Bos is kindly acknowledged for the valuable discussion concerning the MRI experiments. Nico Attevelt, Hester de Bruin, Ingrid van Ark and Thea Leusink-Muis are kindly acknowledged for their assistance during the *in vivo* experiments. This research was performed within the framework of CTMM, the Center for Translational Molecular Medicine (www.ctmm.nl), project HIFU-CHEM (grant 030-301).

References

1. Jemal A, Bray F, Center MM, Ferlay J, Ward E, Forman D. Global cancer statistics. CA Cancer J Clin 2011;61:69-90.
2. Forner A, Llovet JM, Bruix J. Hepatocellular carcinoma. Lancet 2012;379:1245-1255.
3. Kamangar F, Dores GM, Anderson WF. Patterns of cancer incidence, mortality, and prevalence across five continents: defining priorities to reduce cancer disparities in different geographic regions of the world. J Clin Oncol 2006;24:2137-2150.
4. Imai N, Ishigami M, Ishizu Y, Kuzuya T, Honda T, Hayashi K, et al. Transarterial chemoembolization for hepatocellular carcinoma: A review of techniques. World J Hepatol 2014;6:844-850.
5. Nicolini A, Crespi S, Martinetti L. Drug delivery embolization systems: a physician's perspective. Expert Opin Drug Deliv 2011;8:1071-1084.
6. Liapi E, Lee K, Georgiades CC, Hong K, Geschwind JH. Drug-eluting particles for interventional pharmacology. Tech Vasc Interv Radiol 2007;10:261-269.
7. Kettenbach J, Stadler A, Katzler IV, Schernthaner R, Blum M, Lammer J, et al. Drug-loaded microspheres for the treatment of liver cancer: review of current results. Cardiovasc Intervent Radiol 2008;31:468-476.
8. Brown DB, Gould JE, Gervais DA, Goldberg SN, Murthy R, Millward SF, et al. Transcatheter therapy for hepatic malignancy: standardization of terminology and reporting criteria. J Vasc Interv Radiol 2009;20:S425-S434.
9. Lewandowski RJ, Geschwind J, Liapi E, Salem R. Transcatheter intraarterial therapies: Rationale and overview. Radiology 2011;259:641-657.
10. Lencioni R. Loco-regional treatment of hepatocellular carcinoma in the era of molecular targeted therapies. Oncology 2010;78:107-112.
11. Hong K, Khwaja A, Liapi E, Torbenson MS, Georgiades CS, Geschwind JFH. New intra-arterial drug delivery system for the treatment of liver cancer: Preclinical assessment in a rabbit model of liver cancer. Clin Cancer Res 2006;12:2563-2567.
12. Lewis AL, Dreher MR. Locoregional drug delivery using image-guided intra-arterial drug eluting bead therapy. J Control Release 2012;161:338-350.
13. Louguet S, Verret V, Bédouet L, Servais E, Pascale F, Wassef M, et al. Poly(ethylene glycol) methacrylate hydrolyzable microspheres for transient vascular embolization. Acta Biomater 2014;10:1194-1205.
14. Weng L, Rostambeigi N, Zantek ND, Rostamzadeh P, Bravo M, Carey J, et al. An in situ forming biodegradable hydrogel-based embolic agent for interventional therapies. Acta Biomater 2013;9:8182-8191.
15. Weng L, Rostamzadeh P, Nooryshokry N, Le HC, Golzarian J. In vitro and in vivo evaluation of biodegradable embolic microspheres with tunable anticancer drug release. Acta Biomater 2013;9:6823-6833.
16. Lewis AL, Gonzalez MV, Lloyd AW, Hall B, Tang YQ, Willis SL, et al. DC bead: In vitro characterization of a drug-delivery device for transarterial chemoembolization. J Vasc Interv Radiol 2006;17:335-342.
17. Lewis AL, Holden RR. DC Bead embolic drug-eluting bead: clinical application in the locoregional treatment of tumours. Expert Opin Drug Deliv 2011;8:153-169.
18. Poon RT, Tso WK, Pang RW, Ng KK, Woo R, Tai KS, et al. A phase I/II trial of chemoembolization for hepatocellular carcinoma using a novel intra-arterial drug-eluting bead. Clin Gastroenterol Hepatol 2007;5:1100-1108.
19. Varela M, Real MI, Burrel M, Forner A, Sala M, Brunet M, et al. Chemoembolization of hepatocellular carcinoma with drug eluting beads: efficacy and doxorubicin pharmacokinetics. J Hepatol 2007;46:474-481.

20. Dhanasekaran R, Kooby DA, Staley CA, Kauh JS, Khanna V, Kim HS. Comparison of conventional transarterial chemoembolization (TACE) and chemoembolization with doxorubicin drug eluting beads (DEB) for unresectable hepatocelluar carcinoma (HCC). J Surg Oncol 2010;101:476-480.
21. Nicolini D, Svegliati-Baroni G, Candelari R, Mincarelli C, Mandolesi A, Bearzi I, et al. Doxorubicin-eluting bead vs conventional transcatheter arterial chemoembolization for hepatocellular carcinoma before liver transplantation. World J Gastroenterol 2013;19:5622-5632.
22. Namur J, Wassef M, Millot J, Lewis AL, Manfait M, Laurent A. Drug-eluting beads for liver embolization: Concentration of doxorubicin in tissue and in beads in a pig model. J Vasc Interv Radiol 2010;21:259-267.
23. Landon CD, Park JY, Needham D, Dewhirst MW. Nanoscale drug delivery and hyperthermia: The materials design and preclinical and clinical testing of low temperature-sensitive liposomes used in combination with mild hyperthermia in the treatment of local cancer. Open Nanomed J 2011;3:38-64.
24. Needham D, Anyarambhatla G, Kong G, Dewhirst MW. A new temperature-sensitive liposome for use with mild hyperthermia: characterization and testing in a human tumor xenograft model. Cancer Res 2000;60:1197-1201.
25. Grüll H, Langereis S. Hyperthermia-triggered drug delivery from temperature-sensitive liposomes using MRI-guided high intensity focused ultrasound. J Control Release 2012;161:317-327.
26. Yarmolenko PS, Zhao Y, Landon C, Spasojevic I, Yuan F, Needham D, et al. Comparative effects of thermosensitive doxorubicin-containing liposomes and hyperthermia in human and murine tumours. Int J Hyperthermia 2010;26:485-498.
27. Kong G, Anyarambhatla G, Petros WP, Braun RD, Colvin OM, Needham D, et al. Efficacy of liposomes and hyperthermia in a human tumor xenograft model: importance of triggered drug release. Cancer Res 2000;60:6950-6957.
28. Li S, Wang X, Zhang X, Yang R, Zhang H, Zhu L, et al. Studies on alginate-chitosan microcapsules and renal arterial embolization in rabbits. J Control Release 2002;84:87-98.
29. van Elk M, Lorenzato C, Ozbakir B, Oerlemans C, Storm G, Nijsen F, et al. Alginate microgels loaded with temperature sensitive liposomes for magnetic resonance imageable drug release and microgel visualization. Eur Polym J 2015;in press: doi:10.1016/j.eurpolymj.2015.03.013.
30. Oerlemans C, Seevinck PR, van de Maat GH, Boulkhrif H, Bakker CJG, Hennink WE, et al. Alginate-lanthanide microspheres for MRI-guided embolotherapy. Acta Biomater 2013;9:4681-4687.
31. Forster REJ, Thuermer F, Wallrapp C, Lloyd AW, Macfarlane W, Phillips GJ, et al. Characterisation of physico-mechanical properties and degradation potential of calcium alginate beads for use in embolisation. J Mater Sci Mater Med 2010;21:2243-2251.
32. Eroglu M, Kursaklioglu H, Misirli Y, Iyisoy A, Acar A, Dogan AI, et al. Chitosan-coated alginate microspheres for embolization and/or chemoembolization: In vivo studies. J Microencapsul 2006;23:367-376.
33. Negussie AH, Yarmolenko PS, Partanen A, Ranjan A, Jacobs G, Woods D, et al. Formulation and characterisation of magnetic resonance imageable thermally sensitive liposomes for use with magnetic resonance-guided high intensity focused ultrasound. Int J Hyperthermia 2011;27:140-155.
34. Ponce AM, Viglianti BL, Yu D, Yarmolenko PS, Michelich CR, Woo J, et al. Magnetic resonance imaging of temperature-sensitive liposome release: Drug dose painting and antitumor effects. J Natl Cancer Inst 2007;99:53-63.
35. van Elk M, Deckers R, Oerlemans C, Shi Y, Storm G, Vermonden T, et al. Triggered release of doxorubicin from temperature-sensitive poly(N-(2-hydroxypropyl)-methacrylamide mono/dilactate) grafted liposomes. Biomacromolecules 2014;15:1002-1009.

36. Polson C, Sarkar P, Incledon B, Raguvaran V, Grant R. Optimization of protein precipitation based upon effectiveness of protein removal and ionization effect in liquid chromatography–tandem mass spectrometry. J Chromatogr B Analyt Technol Biomed Life Sci 2003;785:263-275.
37. van Es RJJ, Nijsen JFW, Dullens HFJ, Kicken M, van der Bilt A, Hennink WE, et al. Tumour embolization of the Vx2 rabbit head and neck cancer model with Dextran hydrogel and Holmium-poly(L-lactic acid) microspheres: a radionuclide and histological pilot study. J Craniomaxillofac Surg 2001;29:289-297.
38. van Es RJJ, Nijsen JFW, van het Schip AD, Dullens HFJ, Slootweg PJ, Koole R. Intra-arterial embolization of head-and-neck cancer with radioactive holmium-166 poly(L-lactic acid) microspheres: an experimental study in rabbits. Int J Oral Maxillofac Surg 2001;30:407-413.
39. de Smet M, Langereis S, van den Bosch S, Grull H. Temperature-sensitive liposomes for doxorubicin delivery under MRI guidance. J Control Release 2010;143:120-127.
40. Zucker D, Marcus D, Barenholz Y, Goldblum A. Liposome drugs' loading efficiency: A working model based on loading conditions and drug's physicochemical properties. J Control Release 2009;139:73-80.
41. Allen TM, Cleland LG. Serum-induced leakage of liposome contents. Biochim Biophys Acta 1980;597:418-426.
42. Senior J, Gregoriadis G. Is half-life of circulating liposomes determined by changes in their permeability? FEBS Lett 1982;145:109-114.
43. Scherphof G, Roerdink F, Waite M, Parks J. Disintegration of phosphatidylcholine liposomes in plasma as a result of interaction with high-density lipoproteins. Biochim Biophys Acta 1978;542:296-307.
44. Cohen S, Ban MC, Chow M, Langer R. Lipid-alginate interactions render changes in phospholipid bilayer permeability. Biochim Biophys Acta 1991;1063:95-102.
45. Greene RF, Collins JM, Jenkins JF, Speyer JL, Myers CE. Plasma pharmacokinetics of adriamycin and adriamycinol: implications for the design of in vitro experiments and treatment protocols. Cancer Res 1983;43:3417-3421.
46. Liu Y, Ji F, Liu R. The interaction of bovine serum albumin with doxorubicin-loaded superparamagnetic iron oxide nanoparticles: spectroscope and molecular modelling identification. Nanotoxicology 2013;7:97-104.
47. Kooijman H, Nijsen F, Spek AL, van het Schip F. Diaquatris(pentane-2,4-dionato-O,O')holmium(III) monohydrate and diaquatris(pentane-2,4-dionato-O,O')holmium(III) 4-hydroxypentan-2-one solvate dihydrate. Acta Crystallogr C 2000;56:156-158.
48. Wei X, Ming LJ. Comprehensive 2D (1)H NMR studies of paramagnetic lanthanide(III) complexes of anthracycline antitumor antibiotics. Inorg Chem 1998;37:2255-2262.

7

Summary and perspectives

Summary

In the beginning of the 20th century, Paul Ehrlich proposed that drug carrier systems ideally deliver drug molecules specifically to target cells while being harmless for healthy tissues and called this theory the "magic bullet concept" [1]. Drug molecules often lack the selectivity for their target cells and therefore drug carriers are presently under investigation to deliver drugs specifically to aimed tissues and organs. Several carrying systems have been developed to accomplish targeted drug delivery. Liposomes are well-known examples of nanosized drug delivery systems, which can encapsulate e.g. cytostatic drugs [2-4]. Liposomal formulations of cytotoxic drugs have several advantages: i) encapsulated drugs are protected against enzymatic degradation, ii) systemically administered chemotherapeutic drugs often have a short circulation half-life, which can be prolonged by encapsulation into liposomes [5] and iii) long circulating PEGylated liposomes can accumulate into tumors and other inflamed tissues via the enhanced permeation and retention (EPR) effect, providing selective passive targeting to these areas [6-9]. Taken these advantages together, drug encapsulation into liposomes has resulted in increased drug concentrations in tumors while maintaining free drug concentrations low in healthy tissue, resulting in less adverse events [10-12]. Liposomes accumulate in tumors via the EPR effect but this effect is known to be heterogeneous and varies between tumor types, from patient to patient and even varies within one tumor [7,13]. Moreover, the concentration of free drug in the tumor is relatively low due to the slow and uncontrolled release of the drug from the liposomes and as a consequence, cytotoxic free drug concentrations are not always obtained in the tumor [14].
In order to optimize the free drug concentration in the tumor, liposomes have been developed that are capable of releasing drugs at the target site in response to a specific stimulus. As an example, temperature sensitive liposomes release their content during incubation at mild hyperthermia (42 °C) [15,16]. Low temperature sensitive liposomes (LTSL, doxorubicin (DOX) loaded liposomes containing lysolipids) in combination with mild hyperthermia showed a 20-30 times increase in DOX tumor deposition compared to free DOX in nude mice bearing a FaDu human tumor xenograft and a 5 times increased DOX tumor concentration compared to a Doxil-like formulation (non-temperature sensitive liposome encapsulating DOX). Hence, LTSL have shown to improve the antitumor efficacy upon mild hyperthermia treatment compared to free DOX and the Doxil-like formulation [17,18].

The research described in this thesis was performed as part of the HIFU-CHEM project (project of *Center for Translational Molecular Medicine* (CTMM)) that investigated new treatment options for liver and bone malignancies using MRI guided High Intensity Focused Ultrasound (HIFU) in combination with ThermoDox® (temperature sensitive liposome encapsulating DOX). MRI provides anatomical information for planning therapeutic interventions, temperature mapping for local hyperthermia control and the monitoring of drug release. MRI guided HIFU in combination with ThermoDox® is a promising method providing a non-invasive option for the treatment of solid tumors [19].
ThermoDox® is a temperature sensitive liposome, which consists of 1,2-dipalmitoyl-*sn*-glycero-3-phosphocholine (DPPC), 1-stearoyl-2-hydroxy-*sn*-glycero-3-

phosphocholine (MSPC) and 1,2-distearoyl-*sn*-glycero-3-phosphoethanolamine-*N*-[amino(polyethylene glycol)-2000] (DSPE-PEG2.000) encapsulating DOX [15,17]. MSPC, a monochain lysolipid, is incorporated in this formulation since it forms pores in the lipid bilayer at its phase transition temperature, inducing fast release of the content [20-22]. ThermoDox® has an ultrafast release rate with 80% release of entrapped DOX in 20 seconds at 42 °C [15,17]. However, a limitation of this liposomal formulation is that it releases > 20% of DOX at 37 °C within 15 minutes in blood, thereby limiting the amount of DOX delivered to the tumor tissue while exposing healthy tissue to DOX [23,24].
Therefore, as part of the CTMM project, in this thesis alternative temperature sensitive drug delivery systems were explored that release their content in a fast manner at mild hyperthermia while remaining stable at body temperature.

In **Chapter 2**, we describe the development of temperature sensitive liposomes with tunable release characteristics that release their content at elevated temperatures. Temperature-sensitive *N*-(2-hydroxypropyl)methacrylamide mono/dilactate polymers are presently under investigation for the design of drug delivery systems and hydrogel scaffolds for regenerative medicine [25-29]. These polymers were incorporated into liposomes via a cholesterol anchor (chol-pHPMAlac). Polymers with different copolymer compositions and molecular weights (resulting in variation in cloud point (CP)) were synthesized to evaluate their influence on the DOX release from the loaded liposomes. The liposomes had a size between 100 and 150 nm (PDI ~0.1) and a DOX encapsulation efficiency > 95%. All the liposomal formulations showed a triggered release of DOX and the onset-temperature of the DOX release was dependent on the characteristics of the chol-pHPMAlac used. Grafting liposomes with chol-pHPMAlac with a higher percentage HPMAmonolactate, and therefore a higher CP, resulted in an increase in release on-set temperature. It was further shown that an increase in molecular weight of chol-pHPMAlac resulted in a decrease of the release temperature. Liposomes with a chol-pHPMAlac (10.0 kDa and a CP of 19.0 °C) grafting density of 5% were identified as the best performing formulation since they were stable at body temperature while a fast release was obtained at mild hyperthermia (> 90% during 10 min incubation at 47 °C). It was also shown that these liposomes released their DOX content quantitatively upon exposure to HIFU.

Encouraged by these results, we further evaluated the chol-pHPMAlac grafted liposomes with different *in vitro* assays in **Chapter 3** to get insight into the interaction between chol-pHPMAlac grafted liposomes with blood cells and other cells with which the liposomes come in contact after intravenous (i.v.) administration. The size of chol-pHPMAlac (8.5 kDa and a CP of 16 °C) grafted liposomes remained stable after 24 hour incubation at 37 °C in serum, which is important because pulmonary embolism, stroke and myocardial infarction can be induced by aggregated nanoparticles [30,31]. Neither cellular association nor cellular uptake was observed for RAW 264.7 (macrophages), HUVEC (endothelial cells) and AML-12 cells (hepatocytes), which indicates that chol-pHPMAlac grafted liposomes are likely not removed rapidly from the blood circulation by these cells after administration. Furthermore, chol-pHPMAlac liposomes did not show signs of cytotoxicity using the MTS assay even at the highest phospholipid concentration (150 μM) after 24

hour incubation. In general, nanoparticles can activate blood platelets leading to the formation of a thrombus, which can occlude blood vessels resulting in necrosis of the tissue supplied by that vessel [32,33]. The amount of fibrinogen and P-selectin on the surface of platelets is a good indicator for platelet activation [34-38]. However, upon incubation with chol-pHPMAlac liposomes no significant binding of fibrinogen and expression of P-selection was found. Taken these results together, it is expected that chol-pHPMAlac liposomes are not cleared rapidly from the blood circulation after i.v. administration and these liposomes do most likely not generate serious complications e.g. the formation of thrombi after injection.

We show in **Chapter 3** that the size of chol-pHPMAlac grafted liposomes were stable during incubation in serum at 37 °C for 24 hours using nanoparticle tracking analysis (NTA). These liposomes showed a complete DOX release at 47 °C within 10 minutes. Nevertheless, dynamic light scattering measurements (**Chapter 2** and **3**) revealed that liposomes grafted with this chol-pHPMAlac with a CP of ~20 °C aggregated at body temperature (37 °C). Since aggregates can induce pulmonary embolism, stroke and myocardial infarction [30,31], we made an effort to prevent aggregation of the developed liposomal system while retaining the triggered release at elevated temperatures in **Chapter 4**. Poly(ethylene glycol) (PEG) is a hydrophilic polymer, which forms a steric barrier around the liposomes reducing opsonization by proteins and consequently decreases elimination from the blood circulation [39-42]. We hypothesized that PEGylation could reduce the aggregation of the liposomes at body temperature (and above the CP of the polymer) due to the formation of a hydrophilic shield around the liposomes. PEGylation indeed reduced the liposome aggregation but unfortunately simultaneously inhibited the triggered release of DOX from the liposomes and consequently prevented the realization of the goal. Therefore in the next chapters of this thesis, other formulations were explored.

Besides nanoparticles, also micro-sized drug delivery systems are often used for local drug delivery in tumor therapy. Drug eluting beads (DEBs) with sizes ranging from 70-150 µm to 500-700 µm and loaded with cytostatic drugs are used for embolization of tumors [43-45]. These DEBs are administered in the arterial supply of the tumor where they block the feeding vessels of the tumor and restrict nutrient and oxygen supply to the tumor cells. The blockage of the blood vessels reduces the washout of the chemotherapeutic drug and hence increases the drug concentration in the tumor area while minimizing the systemic exposure. In preclinical as well as clinical studies it was shown that DEBs release their content locally in a sustained manner in a tumor after i.a. injection and embolization [46-48]. Further, it was recently shown in several studies that rapid intravascular release of DOX from temperature sensitive liposomes after mild hyperthermia at the tumor site leads to high intravascular drug concentrations, which subsequently enhances the drug penetration into the tumor and therefore improves the anti-tumor efficacy [15,49]. Therefore, the objective of **Chapter 5** was to develop and characterize alginate microspheres that combine embolization with on-demand triggered drug release. For that purpose, alginate microspheres loaded with temperature sensitive liposomes (TSL) were developed, which release their payload after mild hyperthermia. These TSL contained fluorescein (a drug mimicking dye) and [Gd(HPDO3A)(H_2O)], a T_1 MRI contrast agent, for real

time monitoring of the release by MRI. These alginate microspheres were crosslinked with barium ions and holmium ions (T_2^* MRI contrast agent) to allow microsphere visualization (TSL-Ho-microspheres). TSL-Ho-microspheres released fluorescein and [Gd(HPDO3A)(H_2O)] simultaneously and completely within 2 minutes at 42 °C showing that [Gd(HPDO3A)(H_2O)] is a good indicator for the release *in vivo*. Holmium crosslinked microspheres and the release of [Gd(HPDO3A)(H_2O)] were visualized *in vitro* using MRI. In addition, microsphere clusters were observed in an *ex vivo* kidney after injection of TSL-Ho-microspheres. These results show that, as expected, TSL-Ho-microspheres can be visualized by MRI in tissue.

In **Chapter 6**, the concept of combining embolization with on-demand triggered drug release was taken a step further by encapsulating a cytostatic drug (DOX) together with a contrast agent ([Gd(HPDO3A)(H_2O)]) in thermosensitive liposomes. However, when TSL containing DOX were loaded into microspheres crosslinked with barium and holmium ions, no release of DOX occurred at mild hyperthermia likely because holmium-DOX complexes were formed, which hampered the release of DOX. Therefore, alginate microspheres encapsulating TSL were crosslinked with solely barium ions (TSL-Ba-ms) while empty microspheres were crosslinked with solely holmium ions (Ho-ms) to allow MRI visualization of the microspheres. TSL-Ba-ms had a mean diameter of 76 µm and released DOX quantitatively within 3 minutes at 42 °C in 50% serum. Ho-ms had an average diameter of 64 µm and since this size was similar to that of TSL-Ba-ms, they are expected to display a similar *in vivo* tissue distribution after an i.a. co-injection. A mixture of TSL-Ba-ms and Ho-ms in a ratio of 95:5 was visualized on a T_2^* and a T_1-weighted (wt) image before and after incubation at mild hyperthermia (42 °C for 15 minutes) *in vitro*. The holmium containing microspheres were clearly detectable on the T_2^*-wt image before and after mild hyperthermia while [Gd(HPDO3A)(H_2O)] release was only observed after mild hyperthermia in the supernatant as well as in the microsphere pellet on a T_1-wt image. The deposition of the microspheres and [Gd(HPDO3A)(H_2O)] release after co-administration of TSL-Ba-ms and Ho-ms was monitored in the VX_2 tumor model in the auricle of a New Zealand White rabbit. Microsphere clusters appeared on the T_2^*-wt image after the co-administration of TSL-Ba-ms and Ho-ms. These clusters remained visible after applying mild hyperthermia. No change in T_1 was observed after co-administration of the microspheres indicating the presence of intact TSL. A significant drop in T_1-values was observed in the tumor after applying hyperthermia, indicating the release of [Gd(HPDO3A)(H_2O)] from the TSL-Ba-ms. The location of Ho-ms overlapped with the location of [Gd(HPDO3A)(H_2O)] released from TSL-Ba-ms making Ho-ms a suitable marker for TSL-Ba-ms. In conclusion, these microspheres are attractive systems for real-time, MR-guided embolization and triggered release of drugs.

Future perspectives

Optimizing release properties of chol-pHPMAlac grafted liposomes

The research described in this thesis was performed as part of a CTMM project that investigated novel biodegradable temperature-sensitive drug delivery carriers, which release their content fast at mild hyperthermia to achieve high drug concentrations in the tumor. Simultaneously no leakage at 37 °C should occur since premature release of the drug before arrival at the tumor limits the amount of drug delivered to the tumor tissue and induces exposure of healthy tissue to the drug. The best chol-pHPMAlac liposomal formulation described in **Chapter 2** released its content quantitatively at 47 °C in 10 minutes while remaining stable at body temperature (< 10% release at 37 °C in 30 minutes). Unfortunately, our temperature-sensitive system did not completely fulfill our expectations (**Chapter 2**). The release of DOX took place at significantly higher temperatures (± 20 °C) than the CP of chol-pHPMAlac, presumably because the dehydration of the polymer is insufficient at the CP and thus the polymer is not hydrophobic enough to penetrate and permeabilize the liposomal membrane at that temperature. As a consequence, a drawback of these thermosensitive liposomes is that they aggregate at body temperature, which obstructs their clinical application since circulating aggregates could induce pulmonary embolism, stroke and myocardial infarction [30]. Therefore, we made an effort to prevent aggregation of our liposomal system while retaining the triggered release at elevated temperatures by PEGylation in **Chapter 4**. Unfortunately, this strategy to utilize a PEG coating to optimize our novel thermosensitive liposomes was not successful. Therefore, other approaches are proposed to prevent aggregation of the liposomes or to induce the release from the liposomes at the CP of chol-pHPMAlac. One option to prevent aggregation is to couple a hydrophilic block (HPB, e.g. PEG or HPMA) to the chol-pHPMAlac resulting in chol-pHPMAlac-HPB. The cholesterol will facilitate the incorporation into the liposomes, while HPMAlac is the temperature-sensitive moiety and HPB will form a hydrophilic shield around the liposomes. At the CP of chol-pHPMAlac-HPB, the polymer will start to dehydrate but aggregation is most likely prevented by the HPB since PEGylation also prevented the aggregation of chol-pHPMAlac grafted liposomes in **Chapter 4**. In this approach, the release of the content will most likely not be inhibited by the HPB since the hydrophilic shield is formed solely around the liposome and not between the HPMAlac chains.

Another strategy to induce content release at the CP of the polymer would be to vary the position of the lipid anchor on the polymer chain. The chol-pHPMAlac used in this thesis has an anchor group at the terminal end of the polymer chain while polymers with lipid anchors distributed over the polymer chain are less flexible upon grafting on liposomes and might therefore induce permeabilization of the liposomes and release of the loaded drug at temperatures slightly above the CP of the polymer. A final option would be to change the lipid composition of chol-pHPMAlac grafted liposomes since it was reported previously that the release from poly(NIPAM-co-ODA) grafted liposomes composing of DPPC or EPC was incomplete while an enhanced and complete release was observed from DOPE liposomes modified with poly(NIPAM-co-ODA) [50-52].

Optimizing the preparation method of alginate microspheres

The alginate microspheres described in **Chapter 5** are prepared using a Jet Cutter. This technique is ideal for the preparation of monodisperse microspheres but the Jet Cutter is not suitable for the production of microspheres containing toxic components (e.g. DOX) due to the formation of aerosols. Therefore, a homemade spray device is described in **Chapter 6**. The disadvantages of this technique are 1) a low yield because a relatively large percentage of the alginate solution is sprayed onto the vessel wall, 2) difficulties to clean the spraying device since the inside of the collecting vessel and the nozzle are difficult to reach and 3) the fragility of the device since it is fabricated of glass. In literature, several other methods for the preparation of alginate microspheres are described, of which some are more reproducible and safer. Examples are microfluidics [53], electro spraying [54], ink jetting [55] and compressed air spraying [56]. These methods could be explored for the preparation of TSL-Ba-ms.

***In vivo* evaluation of TSL-Ba-ms and Ho-ms**

We report introductory data of the visualization of TSL-Ba-ms and Ho-ms *in vivo* in the VX_2 model in **Chapter 6**. The microsphere deposition and [Gd(HPDO3A)(H_2O)] release after co-administration of TSL-Ba-ms and Ho-ms was visualized in this model. The location of Ho-ms corresponded very closely with the location of [Gd(HPDO3A)(H_2O)] released from TSL-Ba-ms making Ho-ms a suitable marker for TSL-Ba-ms. To explore this formulation further, an additional VX_2 study is needed in which microspheres are evaluated with and without applying mild hyperthermia and with or without the encapsulation of [Gd(HPDO3A)(H_2O)] in the TSL-Ba-ms. Furthermore, the DOX concentration in blood and tumor should be measured to evaluate if high drug concentrations are reached in the tumor (i.e. efficacy) while retaining the systemic exposure low (i.e. side effects).

Up till now, a water bath was used to heat the tumor. This is a very easy and efficient heating method but clinically less applicable since only superficial tumors can be heated and this method is not very convenient for patients. Therefore, in the proposed *in vivo* studies, RFA and HIFU can be considered as more clinical relevant heating modalities.

In conclusion, chol-pHPMAlac grafted liposomes developed in this thesis show promising results for temperature triggered local drug delivery although some modifications of this system are needed. Furthermore, substantial progress has been made in the development of alginate microspheres suitable for embolization with on-demand triggered drug release and whereby the microspheres as well as the drug releasing process can be visualized.

References

1. Strebhardt K, Ullrich A. Paul Ehrlich's magic bullet concept: 100 years of progress. Nat Rev Cancer 2008;8:473-480.
2. Allen TM, Cullis PR. Liposomal drug delivery systems: From concept to clinical applications. Adv Drug Deliv Rev 2013;65:36-48.
3. Mayer LD, Bally MB, Cullis PR. Uptake of adriamycin into large unilamellar vesicles in response to a pH gradient. Biochim Biophys Acta 1986;857:123-126.
4. Madden TD, Harrigan PR, Tai LCL, Bally MB, Mayer LD, Redelmeier TE, et al. The accumulation of drugs within large unilamellar vesicles exhibiting a proton gradient: a survey. Chem Phys Lipids 1990;53:37-46.
5. Li L, ten Hagen TLM, Schipper D, Wijnberg TM, van Rhoon GC, Eggermont AMM, et al. Triggered content release from optimized stealth thermosensitive liposomes using mild hyperthermia. J Control Release 2010;143:274-279.
6. Maeda H. Tumor-selective delivery of macromolecular drugs via the EPR effect: background and future prospects. Bioconjug Chem 2010;21:797-802.
7. Bae YH, Park K. Targeted drug delivery to tumors: Myths, reality and possibility. J Control Release 2011;153:198-205.
8. Lammers T, Kiessling F, Hennink WE, Storm G. Drug targeting to tumors: principles, pitfalls and (pre-) clinical progress. J Control Release 2012;161:175-187.
9. Wang Y, Grainger D. Barriers to advancing nanotechnology to better improve and translate nanomedicines. Front Chem Sci Eng 2014;8:265-275.
10. Harris L, Batist G, Belt R, Rovira D, Navari R, Azarnia N, et al. Liposome-encapsulated doxorubicin compared with conventional doxorubicin in a randomized multicenter trial as first-line therapy of metastatic breast carcinoma. Cancer 2002;94:25-36.
11. Northfelt DW, Dezube BJ, Thommes JA, Miller BJ, Fischl MA, Friedman-Kien A, et al. Pegylated-liposomal doxorubicin versus doxorubicin, bleomycin, and vincristine in the treatment of AIDS-related Kaposi's sarcoma: results of a randomized phase III clinical trial. J Clin Oncol 1998;16:2445-2451.
12. O'Brien ME, Wigler N, Inbar M, Rosso R, Grischke E, Santoro A, et al. Reduced cardiotoxicity and comparable efficacy in a phase III trial of pegylated liposomal doxorubicin HCl (CAELYX/Doxil) versus conventional doxorubicin for first-line treatment of metastatic breast cancer. Ann Oncol 2004;15:440-449.
13. Jain RK, Stylianopoulos T. Delivering nanomedicine to solid tumors. Nat Rev Clin Oncol 2010;7:653-664.
14. Bandak S, Goren D, Horowitz A, Tzemach D, Gabizon A. Pharmacological studies of cisplatin encapsulated in long-circulating liposomes in mouse tumor models. Anticancer Drugs 1999;10:911-920.
15. Needham D, Anyarambhatla G, Kong G, Dewhirst MW. A new temperature-sensitive liposome for use with mild hyperthermia: characterization and testing in a human tumor xenograft model. Cancer Res 2000;60:1197-1201.
16. Lindner LH, Eichhorn ME, Eibl H, Teichert N, Schmitt-Sody M, Issels RD, et al. Novel temperature-sensitive liposomes with prolonged circulation time. Clin Cancer Res 2004;10:2168-2178.
17. Kong G, Anyarambhatla G, Petros WP, Braun RD, Colvin OM, Needham D, et al. Efficacy of liposomes and hyperthermia in a human tumor xenograft model: importance of triggered drug release. Cancer Res 2000;60:6950-6957.
18. Yarmolenko PS, Zhao Y, Landon C, Spasojevic I, Yuan F, Needham D, et al. Comparative effects of thermosensitive doxorubicin-containing liposomes and hyperthermia in human and murine tumours. Int J Hyperthermia 2010;26:485-498.

19. http://www.ctmm.nl/nl/downloadsnl-pdf/volledig-programma-artikel-pdf/full-article-on-project-hifu-chem. ;accessed May 2015.
20. Mills JK, Needham D. Lysolipid incorporation in dipalmitoylphosphatidylcholine bilayer membranes enhances the ion permeability and drug release rates at the membrane phase transition. Biochim Biophys Acta 2005;1716:77-96.
21. Sandstrom MC, Ickenstein LM, Mayer LD, Edwards K. Effects of lipid segregation and lysolipid dissociation on drug release from thermosensitive liposomes. J Control Release 2005;107:131-142.
22. Winter ND, Murphy RK, O'Halloran TV, Schatz GC. Development and modeling of arsenic-trioxide-loaded thermosensitive liposomes for anticancer drug delivery. J Liposome Res 2011;21:106-115.
23. Negussie AH, Yarmolenko PS, Partanen A, Ranjan A, Jacobs G, Woods D, et al. Formulation and characterisation of magnetic resonance imageable thermally sensitive liposomes for use with magnetic resonance-guided high intensity focused ultrasound. Int J Hyperthermia 2011;27:140-155.
24. de Smet M, Langereis S, van den Bosch S, Grull H. Temperature-sensitive liposomes for doxorubicin delivery under MRI guidance. J Control Release 2010;143:120-127.
25. Censi R, Schuurman W, Malda J, Di Dato G, Burgisser PE, Dhert WJ, et al. A printable photopolymerizable thermosensitive p (HPMAm-lactate)-PEG hydrogel for tissue engineering. Adv Funct Mater 2011;21:1833-1842.
26. Censi R, Vermonden T, Deschout H, Braeckmans K, di Martino P, De Smedt SC, et al. Photopolymerized thermosensitive poly(HPMAlactate)-PEG-based hydrogels: effect of network design on mechanical properties, degradation, and release behavior. Biomacromolecules 2010;11:2143-2151.
27. Shi Y, van Steenbergen MJ, Teunissen EA, Novo L, Gradmann S, Baldus M, et al. Pi-Pi stacking increases the stability and loading capacity of thermosensitive polymeric micelles for chemotherapeutic drugs. Biomacromolecules 2013;14:1826-1837.
28. Talelli M, Oliveira S, Rijcken CJ, Pieters EH, Etrych T, Ulbrich K, et al. Intrinsically active nanobody-modified polymeric micelles for tumor-targeted combination therapy. Biomaterials 2013;34:1255-1260.
29. Vermonden T, Jena SS, Barriet D, Censi R, van der Gucht J, Hennink WE, et al. Macromolecular diffusion in self-assembling biodegradable thermosensitive hydrogels. Macromolecules 2010;43:782-789.
30. Faraji AH, Wipf P. Nanoparticles in cellular drug delivery. Bioorg Med Chem 2009;17:2950-2962.
31. Novo L, Rizzo LY, Golombek SK, Dakwar GR, Lou B, Remaut K, et al. Decationized polyplexes as stable and safe carrier systems for improved biodistribution in systemic gene therapy. J Control Release 2014;195:162-175.
32. Strieth S, Nussbaum CF, Eichhorn ME, Fuhrmann M, Teifel M, Michaelis U, et al. Tumor-selective vessel occlusions by platelets after vascular targeting chemotherapy using paclitaxel encapsulated in cationic liposomes. Int J Cancer 2008;122:452-460.
33. Jones CF, Campbell RA, Brooks AE, Assemi S, Tadjiki S, Thiagarajan G, et al. Cationic PAMAM dendrimers aggressively initiate blood clot formation. ACS Nano 2012;6:9900-9910.
34. Broos K, De Meyer SF, Feys HB, Vanhoorelbeke K, Deckmyn H. Blood platelet biochemistry. Thromb Res 2012;129:245-249.
35. Broos K, Feys HB, De Meyer SF, Vanhoorelbeke K, Deckmyn H. Platelets at work in primary hemostasis. Blood Rev 2011;25:155-167.
36. Armstrong PC, Peter K. GPIIb/IIIa inhibitors: from bench to bedside and back to bench again. Thromb Haemost 2012;107:808-814.
37. Merten M, Thiagarajan P. P-selectin expression on platelets determines size and stability of platelet aggregates. Circulation 2000;102:1931-1936.
38. Nieswandt B, Varga-Szabo D, Elvers M. Integrins in platelet activation. J Thromb Haemost 2009;7:206-209.

39. Allen TM, Hansen C, Martin F, Redemann C, Yau-Young A. Liposomes containing synthetic lipid derivatives of poly(ethylene glycol) show prolonged circulation half-lives in vivo. Biochim Biophys Acta 1991;1066:29-36.
40. Gabizon A, Catane R, Uziely B, Kaufman B, Safra T, Cohen R, et al. Prolonged circulation time and enhanced accumulation in malignant exudates of doxorubicin encapsulated in polyethylene-glycol coated liposomes. Cancer Res 1994;54:987-992.
41. Lasic DD, Martin FJ, Gabizon A, Huang SK, Papahadjopoulos D. Sterically stabilized liposomes: a hypothesis on the molecular origin of the extended circulation times. Biochim Biophys Acta 1991;1070:187-192.
42. Torchilin VP, Omelyanenko VG, Papisov MI, Bogdanov Jr. AA, Trubetskoy VS, Herron JN, et al. Poly(ethylene glycol) on the liposome surface: on the mechanism of polymer-coated liposome longevity. Biochim Biophys Acta 1994;1195:11-20.
43. Lewis AL, Gonzalez MV, Lloyd AW, Hall B, Tang YQ, Willis SL, et al. DC bead: In vitro characterization of a drug-delivery device for transarterial chemoembolization. J Vasc Interv Radiol 2006;17:335-342.
44. Lewis AL, Dreher MR. Locoregional drug delivery using image-guided intra-arterial drug eluting bead therapy. J Control Release 2012;161:338-350.
45. Lewis AL, Holden RR. DC Bead embolic drug-eluting bead: clinical application in the locoregional treatment of tumours. Expert Opin Drug Deliv 2011;8:153-169.
46. Gonzalez MV, Tang Y, Phillips GJ, Lloyd AW, Hall B, Stratford PW, et al. Doxorubicin eluting beads-2: methods for evaluating drug elution and in-vitro:in-vivo correlation. J Mater Sci Mater Med 2008;19:767-775.
47. Namur J, Wassef M, Millot J, Lewis AL, Manfait M, Laurent A. Drug-eluting beads for liver embolization: Concentration of doxorubicin in tissue and in beads in a pig model. J Vasc Interv Radiol 2010;21:259-267.
48. Namur J, Citron SJ, Sellers MT, Dupuis MH, Wassef M, Manfait M, et al. Embolization of hepatocellular carcinoma with drug-eluting beads: Doxorubicin tissue concentration and distribution in patient liver explants. J Hepatol 2011;55:1332-1338.
49. Landon CD, Park JY, Needham D, Dewhirst MW. Nanoscale drug delivery and hyperthermia: The materials design and preclinical and clinical testing of low temperature-sensitive liposomes used in combination with mild hyperthermia in the treatment of local cancer. Open Nanomed J 2011;3:38-64.
50. Kono K, Hayashi H, Takagishi T. Temperature-sensitive liposomes: liposomes bearing poly (N-isopropylacrylamide). J Control Release 1994;30:69-75.
51. Kono K, Henmi A, Yamashita H, Hayashi H, Takagishi T. Improvement of temperature-sensitivity of poly (N-isopropylacrylamide)-modified liposomes. J Control Release 1999;59:63-75.
52. Hayashi H, Kono K, Takagishi T. Temperature-controlled release property of phospholipid vesicles bearing a thermo-sensitive polymer. Biochim Biophys Acta 1996;1280:127-134.
53. Kim DH, Choy T, Huang S, Green RM, Omary RA, Larson AC. Microfluidic fabrication of 6-methoxyethylamino numonafide-eluting magnetic microspheres. Acta Biomater 2014;10:742-750.
54. Park H, Kim P, Hwang T, Kwon O, Park T, Choi S, et al. Fabrication of cross-linked alginate beads using electrospraying for adenovirus delivery. Int J Pharm 2012;427:417-425.
55. Hanus J, Ullrich M, Dohnal J, Singh M, Stepanek F. Remotely Controlled Diffusion from Magnetic Liposome Microgels. Langmuir 2013;29:4381-4387.
56. Forster REJ, Thuermer F, Wallrapp C, Lloyd AW, Macfarlane W, Phillips GJ, et al. Characterisation of physico-mechanical properties and degradation potential of calcium alginate beads for use in embolisation. J Mater Sci Mater Med 2010;21:2243-2251.

Appendices

Nederlandse samenvatting
Curriculum Vitae
List of publication
Acknowledgements

Nederlandse samenvatting

Aan het begin van de 20e eeuw beschreef Paul Ehrlich het "magic bullet" ("magische kogel") concept voor het eerst. Volgens dit concept worden farmaca specifiek afgeleverd bij de gewenste cellen terwijl gezonde weefsels niet blootgesteld worden. De meeste farmaca missen deze selectiviteit voor de gewenste cellen en daarom wordt er momenteel onderzoek gedaan naar dragersystemen (de zogenoemde nanomedicijnen) die de farmaca gericht afleveren bij de gewenste weefsels en organen. Liposomen zijn een voorbeeld van veel onderzochte nanomedicijnen, en deze systemen kunnen worden beladen met o.a. cytostatica. Het beladen van liposomen met cytostatica heeft een aantal voordelen: i) cytostatica zijn beschermd tegen enzymatische afbraak, ii) systemisch toegediende cytostatica hebben vaak een korte halfwaardetijd, deze kan verlengd worden door het beladen in liposomen en iii) lang circulerende, gePEGyleerde liposomen accumuleren in tumoren en ontstoken weefsel via het versterkte permeatie en retentie effect (VPR effect). Hierdoor worden hoge farmaconconcentraties bereikt in de tumor terwijl gezonde weefsels blootgesteld worden aan lagere concentraties van de cytostatica. Zoals hierboven genoemd kunnen liposomen in de tumor accumuleren via het VPR effect. Het is bekend dat dit effect zeer heterogeen is en varieert tussen verschillende tumorsoorten, van patiënt tot patiënt en zelfs binnen een tumor. Bovendien is de vrije concentratie van het farmacon in de tumor relatief laag door de langzame en ongecontroleerde afgifte van het farmacon uit de liposomen. Cytotoxische concentraties worden hierdoor niet altijd bereikt in de tumor.
Er zijn verschillende liposomen ontwikkeld die farmaca kunnen vrijgeven in de tumor na een specifieke stimulans zodat er hogere concentraties van het vrije farmacon in de tumor kunnen worden bereikt. Een voorbeeld van liposomen die hun inhoud vrijgeven als gevolg van een specifieke stimulans zijn temperatuurgevoelige liposomen die hun inhoud vrijgeven tijdens een korte blootstelling aan milde hyperthermie (42 °C). Een 20-30 keer hogere doxorubicine (DOX, een cytostaticum) concentratie werd bereikt in tumoren na toediening van temperatuurgevoelige liposomen in combinatie met milde hyperthermie, in vergelijking met de toediening van vrij DOX. Daarnaast is er aangetoond dat temperatuurgevoelige liposomen in combinatie met milde hyperthermie een verbeterde antitumoreffectiviteit hebben in vergelijking met toediening van vrij DOX en niet temperatuurgevoelige liposomen in combinatie met milde hyperthermie.

Het onderzoek beschreven in dit proefschrift maakte deel uit van het HIFU-CHEM project (CTMM) dat nieuwe behandelmethodes voor kwaadaardige lever- en bot tumoren onderzoekt waarbij gebruik gemaakt wordt van MRI gestuurde Hoge Intensiteit Gefocust Ultrageluid (HIGU) in combinatie met ThermoDox.
ThermoDox is een temperatuurgevoelig liposoom dat bestaat uit DPPC, MSPC en DSPE-PEG2000 en is beladen met DOX. MSPC, een lysolipide mono-keten, is opgenomen in deze formulering omdat het poriën vormt in de lipide-bilaag zodra de faseovergangtemperatuur wordt bereikt en hierdoor voor een snelle afgifte van de inhoud van de liposomen zorgt. ThermoDox heeft een zeer snelle afgiftesnelheid met 80% afgifte van DOX in 20 seconden bij 42 °C. Echter, een beperking van deze formulering is dat er meer dan 20% DOX wordt afgegeven binnen 15 minuten in bloed

van 37 °C, waardoor de hoeveelheid DOX, die afgeleverd wordt in het tumorweefsel beperkt is terwijl gezonde weefsels worden blootgesteld aan DOX.

Daarom, als onderdeel van het bovengenoemde CTMM project, worden er in dit proefschrift alternatieve temperatuurgevoelige dragersystemen onderzocht die de inhoud snel afgeven bij verhoogde temperaturen terwijl deze systemen stabiel zijn bij lichaamstemperatuur.

In **Hoofdstuk 2**, beschrijven we de ontwikkeling van temperatuurgevoelige liposomen met stuurbare afgiftekarakteristieken die hun inhoud afgeven bij verhoogde temperaturen. Temperatuurgevoelige *N*-(2-hydroxypropyl)methacrylamide mono/dilactaat polymeren worden momenteel onderzocht als geneesmiddeldragers. Deze polymeren kunnen in liposomen worden ingebouwd door middel van een cholesterol-anker (chol-pHPMAlac). Polymeren met verschillende copolymeercomposities en molecuulgewichten (resulterend in variatie in transitie temperatuur (TT)) zijn gesynthetiseerd om de invloed op het afgiftepatroon van DOX na het inbouwen van deze polymeren in liposomen te onderzoeken. De liposomen hadden een diameter tussen 100 en 150 nm en een DOX beladingseffectiviteit van > 95%. Alle liposomen vertoonden een temperatuur getriggerde afgifte van DOX en de afgiftetemperatuur was afhankelijk van de karakteristieken van het gebruikte chol-pHPMAlac. Het inbouwen van een chol-pHPMAlac met een hoger percentage HPMAmonolactaat, en daardoor een hogere TT, resulteerde in een verhoging van de afgiftetemperatuur. Daarnaast is aangetoond dat het verhogen van het molecuulgewicht resulteerde in een verlaging van de afgiftetemperatuur. Liposomen met 5% chol-pHPMAlac (10 kDa en een TT van 19.0 °C) werden geïdentificeerd als de beste formulering aangezien deze formulering stabiel was bij lichaamstemperatuur terwijl een snelle afgifte plaatsvond tijdens milde hyperthermie (> 90% tijdens 10 minuten incubatie op 47 °C). Daarbij vond er ook een kwantitatieve afgifte van DOX plaats tijdens blootstelling aan HIGU.

Aangemoedigd door deze resultaten, zijn de liposomen met chol-pHPMAlac verder onderzocht *in vitro* in **Hoofdstuk 3** om meer inzicht te krijgen in de interactie tussen de chol-pHPMAlac liposomen en de bloedcellen en andere cellen waarmee de liposomen in contact komen na intraveneuze toediening. De diameter van de liposomen met chol-pHPMAlac (8.5 kDa en een TT van 16 °C) bleef stabiel na een incubatie van 24 uur op 37 °C in serum, wat belangrijk is aangezien een longembolie, beroerte en hartaanval geïnduceerd kunnen worden door geaggregeerde nanomedicijnen. Er vond geen celbinding en celopname plaats in RAW 264.7 cellen (macrofagen), HUVECs (endotheel cellen) en AML-12 cellen (hepatocyten), wat erop duidt dat chol-pHPMAlac liposomen waarschijnlijk niet snel verwijderd worden uit de bloedcirculatie door deze cellen na intraveneuze toediening. Bovendien vertoonden chol-pHPMAlac liposomen geen cytotoxiciteit. In het algemeen gesproken kunnen nanomedicijnen bloedplaatjes activeren, wat kan leiden tot de vorming van een trombus die bloedvaten kan verstoppen, resulterend in necrose van de weefsels die aangevoerd worden door dit vat. De hoeveelheid fibrinogeen en P-selectine op het oppervlak van bloedplaatjes is een goede indicatie voor bloedplaatjesactivering. Echter, er werd geen verhoging in de hoeveelheid fibrinogeen en P-selectine op het oppervlak van bloedplaatjes gevonden na incubatie met chol-pHPMAlac liposomen.

Gezien de behaalde resultaten is het te verwachten dat chol-pHPMAlac liposomen niet snel verwijderd zullen worden uit de bloedcirculatie na intraveneuze toediening en deze liposomen zullen waarschijnlijk geen serieuze complicaties zoals de formatie van een bloedprop genereren na toediening.

Hoofdstuk 3 laat door middel van nanodeeltjesanalyse zien dat de diameter van chol-pHPMAlac liposomen stabiel bleven tijdens incubatie in serum bij 37 °C voor 24 uur. Deze liposomen gaven de inhoud compleet vrij binnen 10 minuten bij 47 °C. Daarentegen lieten dynamische lichtverstrooiingmetingen (**Hoofdstuk 2** en **3**) zien dat liposomen waarin chol-pHPMAlac met een TT van ~20 °C is ingebouwd, aggregeerden op lichaamstemperatuur. Aangezien aggregaten een longembolie, beroerte en hartaanval kunnen induceren, is in **Hoofdstuk 4** geprobeerd de liposomen zo te optimaliseren dat ze niet aggregeren maar nog wel hun inhoud afgeven tijdens milde hyperthermie. Polyethyleenglycol is een hydrofiel polymeer dat een sterische barrière kan vormen om liposomen en daardoor de opsonisatie door eiwitten kan verminderen met als gevolg dat de liposomen minder snel uit de bloedcirculatie worden verwijderd. De hypothese was dat het PEGyleren van chol-pHPMAlac liposomen het aggregeren van de liposomen op lichaamstemperatuur (en dus boven de TT van het polymeer) kan voorkomen door de vorming van een hydrofiele schil om de liposomen. Het PEGyleren van de liposomen zorgde inderdaad voor de vermindering van aggregatie maar tegelijkertijd remde het PEGyleren ook de geactiveerde afgifte van de liposomen tijdens hyperthermie waardoor we ons doel niet konden realiseren. Daarom zijn in de volgende hoofdstukken andere formuleringen onderzocht.

Naast nanomedicijnen worden ook micro-dragersystemen gebruikt voor de lokale afgifte van farmaca in een tumor. Farmacon-eluerende deeltjes (FEDs) met een diameter van 70-150 μm tot 500-700 μm en beladen met een cytostaticum, worden gebruikt voor het emboliseren van tumoren. Deze FEDs worden toegediend in de arteriële bloedvaten van een tumor die daardoor geblokkeerd worden met als gevolg een verminderde toevoer van zuurstof en voedingsstoffen naar de tumorcellen. Door de blokkade van deze bloedvaten wordt er ook minder cytostaticum uit de tumor weggewassen waardoor de cytostaticumconcentratie in de tumor toeneemt, terwijl de systemische blootstelling verminderd wordt. Preklinische en klinische studies hebben aangetoond dat de FEDs hun inhoud erg langzaam vrijgeven na embolisatie. Daarentegen hebben verschillende studies aangetoond dat een snelle intravasculaire afgifte van DOX ervoor zorgt dat er hogere vrije farmaconconcentraties worden bereikt in tumoren. Dit leidt tot een verbeterde antitumoreffectiviteit. Het doel van **Hoofdstuk 5** is daarom om alginaat microsferen te ontwikkelen en karakteriseren die embolisatie combineren met een op "on-demand" getriggerde afgifte van farmaca. Alginaat microsferen werden beladen met temperatuurgevoelige liposomen die hun inhoud afgaven na milde hyperthermie. Deze temperatuurgevoelige liposomen bevatten fluoresceïne (modelstof voor een farmacon) en [Gd(HPDO3A)(H_2O)], een T_1 MRI contrastmiddel, waardoor de afgifte gemonitord kan worden met behulp van MRI. Deze alginaat microsferen werden gecrosslinkt met barium- en holmium-ionen (T_2^* MRI contrastmiddel) zodat de microsferen zelf ook gevisualiseerd kunnen worden met MRI (TSL-Ho-ms). De TSL-Ho-ms gaven de fluoresceïne en [Gd(HPDO3A)(H_2O)] simultaan en kwantitatief vrij binnen 2 minuten bij 42 °C wat

aantoont dat [Gd(HPDO3A)(H_2O)] een goede indicator is voor de afgifte *in vivo*. De holmium gecrosslinkte microsferen en de release van [Gd(HPDO3A)(H_2O)] werden gevisualiseerd *in vitro* met behulp van MRI. Bovendien werden microsfeerclusters waargenomen in een *ex vivo* nier na de toediening van TSL-Ho-ms. Deze resultaten laten zien dat, zoals verwacht, TSL-Ho-ms gevisualiseerd kunnen worden in weefsel met MRI.

In **Hoofdstuk 6** wordt het concept waarin we embolisatie combineren met getriggerde farmaconafgifte verder ontwikkeld door het beladen van de temperatuurgevoelige liposomen met een cytostaticum (DOX) en een contrastmiddel ([Gd(HPDO3A)(H_2O)]). Echter, er vond geen afgifte plaats bij milde hyperthermie wanneer deze DOX beladen temperatuurgevoelige liposomen werden ingebouwd in met barium-holmium ionen gecrosslinkte microsferen. Waarschijnlijk werden er complexen gevormd tussen DOX en holmium ionen waardoor de afgifte van DOX verhinderd werd. Daarom werden de temperatuurgevoelige liposomen beladen in met barium ionen gecrosslinkte microsferen (TSL-Ba-ms) terwijl lege alginaat microsferen werden gecrosslinkt met holmium ionen (Ho-ms) zodat de microsferen toch gevisualiseerd konden worden met MRI. De TSL-Ba-ms hadden een diameter van 76 µm en gaven DOX kwantitatief vrij in 3 minuten bij 42 °C in 50% serum. De Ho-ms hadden een diameter van 64 µm en aangezien deze diameter vergelijkbaar is met de diameter van TSL-Ba-ms, werd eenzelfde weefselverdeling verwacht voor beide microsferen *in vivo* na co-toediening. Een mengsel van TSL-Ba-ms en Ho-ms in een verhouding van 95:5 werd gevisualiseerd op een T_2^* en een T_1 gewogen afbeelding voor en na incubatie bij milde hyperthermie (42 °C voor 15 minuten) *in vitro*. De holmium gecrosslinkte microsferen waren duidelijk zichtbaar op het T_2^* gewogen beeld voor en na milde hyperthermie terwijl de [Gd(HPDO3A)(H_2O)] afgifte alleen zichtbaar was op het T_1 gewogen beeld na milde hyperthermie. De distributie van de microsferen en de afgifte van [Gd(HPDO3A)(H_2O)] na co-toediening van TSL-Ba-ms en Ho-ms werd waargenomen in een VX_2 tumor in het oor van een konijn. Microsfeerclusters verschenen op een T_2^* gewogen beeld na co-toediening van de TSL-Ba-ms en Ho-ms. Deze clusters bleven zichtbaar na het toepassen van milde hyperthermie. Er werd geen verschil in T_1 waargenomen na het co-toedienen van de microsferen wat erop wijst dat de liposomen nog intact zijn. Een significante daling in T_1 waardes werd gemeten in de tumor na milde hyperthermie wat aangeeft dat de TSL-Ba-ms [Gd(HPDO3A)(H_2O)] hebben afgegeven. De locatie van de holmium gecrosslinkte microsferen kwam overeen met de locatie van de [Gd(HPDO3A)(H_2O)] afgifte van de TSL-Ba-ms waardoor de Ho-ms geschikte markers zijn voor de TSL-Ba-ms. Concluderend kan gezegd worden dat, deze microsferen aantrekkelijke systemen zijn voor beeldgestuurde embolisatie en getriggerde afgifte van farmaca.

Curriculum Vitae

Merel van Elk was born on the 1st of June 1986 in Nijmegen, The Netherlands. After graduating from secondary school at Maaswaal College in Wijchen, she started a bachelor's program in Pharmacy at Utrecht University in 2004. Merel began a master's program in Drug Innovation at Utrecht University in 2007, during which she undertook a 9-month research project under the supervision of Dr. Sytze de Roock and Prof. Berent Prakken. This was carried out in the department of Pediatric Immunology at the University Medical Center, Utrecht. Merel then carried on to complete a 6-month research project under the supervision of Lisa Holmdahl and Prof. Herman Vromans in the department of Pharmaceutics at MSD/Organon. Here she developed a solid dispersion for a low molecular weight FSH receptor agonist. In 2010 Merel obtained her master's degree and worked as a researcher in the University Medical Center in Utrecht and the Dutch Vaccine Institute before beginning a PhD project in the department of Pharmaceutics, Utrecht University. This project was supervised by Prof. Wim Hennink, Prof. Gert Storm, Dr. Tina Vermonden and Dr. Frank Nijsen. During her work as a PhD candidate, she developed imageable thermosensitive release systems for local drug delivery. The results of the project are presented in this thesis.

List of publications

M. van Elk, B. Ozbakir, A. Barten-Rijbroek, G. Storm, F. Nijsen, W. E. Hennink, T. Vermonden, R. Deckers. Alginate microspheres containing temperature sensitive liposomes (TSL) for MR-guided embolization and triggered release of doxorubicin. Submitted for publication (2015)

M. van Elk, C. Lorenzato, B. Ozbakir, C. Oerlemans, G. Storm, F. Nijsen, R. Deckers, T. Vermonden, W. E. Hennink. Alginate microgels loaded with temperature sensitive liposomes for magnetic resonance imageable drug release and microgel visualization. Eur Polym J. 2015; In Press

M. van Elk, R. Deckers, C. Oerlemans, Y. Shi, G. Storm, T. Vermonden, W.E. Hennink. Triggered release of doxorubicin from temperature-sensitive poly(*N*-(2-hydroxypropyl)-methacrylamide mono/dilactate) grafted liposomes. Biomacromolecules. 2014;15(3):1002-1009

S. de Roock*, **M. van Elk***, M.O. Hoekstra, B.J. Prakken, G.T. Rijkers, I.M. de Kleer. Gut derived lactic acid bacteria induce strain specific CD4(+) T cell responses in human PBMC.
Clin Nutr. 2011;30(6):845-851
* *These authors contributed equally to this work*

S. de Roock, **M. van Elk**, M.E. van Dijk, H.M. Timmerman, G.T. Rijkers, B.J. Prakken, M.O. Hoekstra, I.M. de Kleer. Lactic acid bacteria differ in their ability to induce functional regulatory T cells in humans.
Clin Exp Allergy. 2010;40(1):103-110

Acknowledgements

No one achieves anything alone and this thesis would not be possible without the contributions that many of you have made. That's why I would like to thank my colleagues, staff and supervisors with whom I spent over four years doing my research. I would like to thank you all for your help and support and for sharing many nice moments with me during this time.

Beste Wim, geachte promotor, bedankt dat je me de mogelijkheid hebt gegeven om bij de afdeling Biofarmacie te promoveren. Ondanks dat het project vele ups en downs heeft gekend, hebben we het samen tot een goed eind kunnen brengen. Bedankt voor de bijdrage die je hebt geleverd aan dit proefschrift en de kritische blik op mijn werk.

Beste Gert, geachte promotor, bedankt voor je vertrouwen en hulp, zonder jou was mijn project niet van de grond gekomen.

Tina, ik zou eigenlijk een bladzijde vol moeten schrijven om je voor alles te bedanken. Zonder jou zou het heel moeilijk zijn geweest om de eindstreep te halen. Ik ben er nog niet achter gekomen hoe het je is gelukt om me altijd weer te motiveren en me een positief gevoel te geven als dingen anders liepen dan gehoopt.

Frank, jij kwam vaak met de goede ideeën als mijn project vast begon te lopen. Daarnaast wist je altijd een positieve draai te geven als het even tegenzat.

Er zijn vele handen geweest die ervoor hebben gezorgd dat hoofdstuk 3 in mijn proefschrift is verschenen. Joep, Michal, Yvonne, Tesse en Jos bedankt voor jullie hulp.

Cyril, I'm very glad you were there, willing to help me with my MRI experiments (sometimes even till very late in the night). Thank you for your patience in explaining me the theory behind MRI.

Angelique, Roel, Thea en Ingrid, jullie hebben me vaak aan het lachen gekregen tijdens de in vivo studie. Wie had dat ooit gedacht! Joep en Roel, bedankt voor het bijspringen als de planning in de soep begon te lopen.

Matthijs en Berend Jan, jullie hebben uren besteed aan het maken van de spraykop, bedankt voor jullie geduld en de passie voor jullie werk.

Jurgen, Nick en Menno bedankt voor de tijd en energie die jullie in mijn project hebben gestoken.

Mies, Ebel, Louis, Barbara en Georgi bedankt voor jullie goede adviezen de afgelopen jaren.

A

Jessica, bedankt voor alle uren die je hebt geholpen met het uitleggen van InDesign. Zonder jou was er letterlijk geen proefschrift geweest. Roy, bedankt voor alle tips met betrekking tot de laatste fase van mijn promotie. Tati, thanks for accidentally designing the cover of my thesis.

One of the best memories of the past years is making friends from all over the world. Even if there are countless histories to tell, I would like to mention a few of those;

Mehrnoush, it was always great to sing Dutch songs with you. Maripaz, I'm very happy that I can visit my own friend now when I go to Mexico. Anastasia, it was so nice to see you in NY, you were the best tour guide. Simatje, it was great sitting behind you for 4 years and to distract you from work for so many hours. Edu and Gracia, I'm very blessed to have such good friends in Ireland and I'm very happy with the chances you are giving me. Filis, we started the master together, did our internship at the same place and met again during our PhD's, I'm sure (and I hope) our paths will cross again. Rachel, I never visited Maastricht so often, let's keep doing that! Andhyk, Luis and Louann, I have great memories of our dinners together. Kristel, het was erg gezellig om je als kamergenoot te hebben. Meriem, we moeten die netwerk gesprekken erin houden, zelfs als we allebei een baan hebben.

Ik ben er de afgelopen jaren achter gekomen dat ik een hele hoop dappere en trouwe vrienden heb die maar bleven vragen hoe het met me ging en die altijd voor me klaar stonden. Lieke, Tessa, Rianne, Viola, Linda, Erik, Inge, Diana, Alex, Nanda, Els en Tessa bedankt voor jullie steun en leuke momenten de afgelopen jaren.

Burcin, darling, we went from dancing and singing in the lab to crying in the lab and back. I think they were right about the fact that we would be way more efficient if we were talking less but I'm happy we didn't listen! I could not wish for a better paranimph.

Pap, mam en Sjoerd, jullie hebben altijd in me geloofd en er vertrouwen in gehad dat ik dit goed kon afronden. Ik kon altijd bij jullie terecht als ik een luisterend oor nodig had.

Gabriel, je stond altijd voor me klaar als ik je nodig had. Ik heb veel mooie herinneringen overgehouden aan de afgelopen jaren en ik hoop dat er nog veel bij zullen komen. Ik ben erg benieuwd wat de toekomst ons zal brengen. Besitos, Love you.

“On Top Of The World”

I’ve had the highest mountain
I’ve had the deepest rivers
You can have it all but life keeps moving

I’ve tried to cut these corners
Try to take the easy way out
I kept on falling short of something

I could gave up then but
Then again I couldn’t have cause
I’ve traveled all this way for something

And I know it’s hard when you’re falling down
And it’s a long way up when you hit the ground
Get up now, get up, get up now.

Take it in but don’t look down

Waiting on this for a while now
I’ve been waiting to smile
Been holding it in for a while
Take you with me if I can
Been dreaming of this since a child
I’m on top of the world.

(Imagine Dragons)